Application of LIBS to study the difference in elemental composition between organic and genetically modified plants

E Moyo

orcid.org/0000-0002-0074-4582

Mini-dissertation accepted in partial fulfilment of the requirements for the degree *Master of Science in Applied Radiation Science and Technology* at the North-West University

Supervisor: Prof M Mathuthu

Graduation: May 2021

Student number: 25266152

Declaration

I, Moyo Elvis, a Masters student at the Center of Applied Radiation Sciences, would like to declare that the dissertation titled; *Application of LIBS to study the difference in elemental composition between organic and genetically modified plants* is my original work and has never been submitted anywhere. I am submitting this dissertation to North-West University

Student signature: 

Student number: 25266152

Acknowledgement

- Firstly, I would like to acknowledge my supervisor Prof Manny Mathuthu for his phenomenal supervision, advises, for being patient with me and pushing me without necessarily putting me under pressure.
- I wish to show my appreciation to the Center of Applied Radiation for granting me the opportunity to enroll my masters at their center, this opportunity enabled me to travel out of the country when I learnt more about my field of study.
- I would like to express my gratitude to Ms M Kakula for her contribution and her big heart especially when it comes to my research logistics.
- I wish to express my appreciation to National Research Foundation (NRF) for their financial assistance, NRF assistance made it possible for me to do my masters and finish in record time without any financial difficulties.
- I would also like to thank Ms D Mokhine for being a wonderful co-supervisor and being there for me anytime when I need her.
- Finally, my special thanks go to God for giving me wonderful friends, my friends played a huge role in my academic life including proof reading my paper before every submission.

Abstract

Genetic modification includes the change in the genetic make-up of a plant in order to meet the requirements for food security, which is in contrast to organic plants that are grown naturally by the use of organic fertilizers and natural manure. The purpose of this research was to study the difference in elemental composition between organic and genetically modified plants. It is believed that change in genetic make-up results in change in elemental composition of a plant. Hence, analyzing and comparing the elemental composition between organic and genetically modified plants can be the key solution to solve the plants related diseases or the environment unfriendliness imposed by genetically modified plants, which can be due to the excess, deficiency or change in elemental expression. Many different techniques can be used for elemental analysis but in this case, laser induced breakdown spectroscopy (LIBS) was used because it is a non-invasive technique that permits concurrent multi-elemental examination in a single measurement, with little or no sample preparation needed. For accuracy, inductively coupled mass spectroscopy (ICP-MS) was used in order to verify and validate LIBS results. Using LIBS technique, one is able to differentiate the two categories according to the signature of their essential and trace elements and determine the effects of GMO to the environment and people. In this study, a solid maize sample was run under LIBS in a dark room to avoid light interference, which resulted in good results as compared to liquid and powder samples. A portion of the same sample was then digested using a Perkin-Elmer microwave digester and then ran under ICP-MS. The obtained results indicated that genetic modification does not add or reduce the expected nutrient elements but it changes the elemental concentration and intensities. LIBS detected six elements, which are Mn I, Fe I, Fe II, Cu II, K I and O I in all organic samples whilst Mn I, Fe I, Fe II, Cu II, K I, O I plus Ca II, C I, N II and CaI were detected in all genetically modified samples. ICP-MS detected all expected seventeen elements in both sample categories. This research thus proved that both techniques (LIBS and ICP-MS) are good when they are both used for the same analysis in order to avoid systematic errors. For future use, it is recommended to run LIBS experiments in the presence of Argon gas to avoid matrix effect and self-absorption.

Keys words: Laser induced breakdown Spectroscopy, inductively coupled mass spectroscopy elemental analysis, organic, genetically modified organisms.

List of abbreviations

CARST	Center of Applied Radiation Science and Technology
LIBS	Laser induce breakdown spectroscopy
LIPS	Laser induced plasma spectroscopy
ICP-MS	Inductively couple mass spectroscopy
GMO	Genetically modified organisms
GMP	Genetically modified plants
AAS	Atomic absorption spectroscopy
FDA	Food and drug administration
DNA	Deoxyribose nucleic acid
XRF	X-ray fluorescence
XRD	X-ray diffraction
FTIR	Fourier transform infrared
SEM	Scanning electron microscopy
PIXE	Proton induced x-ray Emission
UV-Vis	ultra violet visible light
NIST	national institute of standards and technology
TOF	time of flight
USEPA	united state environmental proton agency
MPC	multipoint calibration
CCD	charge-coupled device
NPK	nitrogen, phosphorus and potassium
API	active pharmaceutical ingredient

Table of content

Declaration ii
Acknowledgement iii
Abstract iv
List of abbreviations v
List of figures viii
Table of tables ix
CHAPTER 1: INTRODUCTION AND PROBLEM STATEMENT 1
1.1 Introduction 1
1.1.1 Brief description of ICP-MS 5
1.1.2 Working principles of ICP-MS 6
1.2 Problem statement 7
1.3 Aim 9
1.4 Objectives 9
CHAPTER 2: LITERATURE REVIEW 10
2.1 What is laser induced breakdown spectroscopy (LIBS). 10
2.2 What are the uses of laser induced breakdown spectroscopy? 11
2.3 Pharmaceutical use of LIBS 11
2.4 Application of LIBS in energy 12
2.5 Analysing the archaeology and cultural heritage 13
2.6 Geologic and soil analysis 15
2.7 Forensics 16
2.8 Butter adulteration analysis using LIBS 19
2.10 Determination of ash content of coal using LIBS 19
2.11 Advantages of using LIBS 19
2.12 Challenges of using LIBS 20
CHAPTER 3: METHODS AND MATERIALS 21
3.1 Equipment and samples 21
3.1.1 Genetically modified maize 21
3.1.2 Organic maize 22
3.1.3 Equipment 23
3.2 Methodology 25
3.2.1 Sample preparations ..... **Error! Bookmark not defined.**

3.2.2 LIBS experiment 25
3.3 Experimental design..... **Error! Bookmark not defined.**
3.3.1 Data acquisition setup ..... **Error! Bookmark not defined.**
3.3.2 Data acquisition 26
3.4 ICP-MS experiment 26
3.4.1 Sample preparation 26
3.4.1.1 Reagents used..... 27
CHAPTER 4: RESULTS AND DISCUSSIONS 29
4.1 Organic samples..... 30
4.1.1 ICP-MS data: Golden bantam 31
4.1.2 LIBS data: Golden bantam..... 32
4.1.3 Statistical analysis 36
4.1.4 ICP-MS data: Stowells evergreen 36
4.1.5 LIBS data: Stowells ever-green. 38
4.1.6 Statistical analysis 41
4.2 Genetically modified samples..... 42
4.2.1 ICP-Ms data: CRN 3505 43
4.2.2 LIBS data: CRN 3505 44
4.2.3 Statistical analysis 48
4.2.4 ICP-Ms data: Mon 89..... 49
4.2.5 LIBS data: Mon 89..... 51
4.2.6 Statistical analysis 54
4.2.7 ICP-Ms data: Mon 810..... 55
4.2.8 LIBS data: Mon 810..... 57
4.2.9 Statistical analysis 60
4.3. Discussion 61
4.3.1 ICP-Ms results 61
4.3.2. LIBS results 62
4.3.3 Summary 64
4.4 Conclusion 66
Reference 68
Appendix..... 76

List of figures

Figure 1.1: GMO VS Organic plants [4]. 1
Figure 1.2: Relationships of Fe with plants [7]. 3
Figure 1.3: Schematic diagram for laser induced breakdown spectroscopy..... 26
Figure 1.4: Schematic overview of sample introduction to ICP-MS [29]. 6
Figure 2.1: The Ecce Homo painting [62]. 13
Figure 2.2: Protocol sampling and analysis of stub [84]. 16
Figure 2.3: Glass discrimination and multivariant analysis [82]. 18
Figure 2.4: Determination of ash content of coal [101]..... **Error! Bookmark not defined.**
Figure 3.2.1: Polymix (PX-MCF 90 D). 23
Figure 3.2.2: Laser induced breakdown spectroscopy (LIBS). 23
Figure 3.2.3: Titan microwave digester - Perkin Elmer 24
Figure 3.2.4: Inductively coupled plasma mass spectrometry (ICP-MS). 24
Figure 4.1: The graph of concentration means with nitrogen. 31
Figure 4.2: Emission spectra of sample Golden Bantam 1st trial..... 33
Figure 4.3: Emission spectra of sample Golden Bantam 2nd trial..... 34
Figure 4.5: Emission spectra of sample Golden Bantam 3rd trial. 35
Figure 4.6: The graph of intensity means with standard errors. 36
Figure 4.7: The plot of concentration means with nitrogen. 37
Figure 4.8: Emission spectra of sample stowells ever-green 1st trial..... 38
Figure 4.9: Emission spectra of sample Stowells ever-green 2nd trial. 39
Figure 4.10: Emission spectra of sample Stowells ever-green 3rd trial. 40
Figure 4.11: The plot of intensity means of different elements. 42
Figure 4.12: The plot of concentration means with nitrogen. 43
Figure 4.13: Emission spectra of sample CRN 3505 1st trial. 44
Figure 4.14: Emission spectra of sample CRN 3505 2nd trial. 46
Figure 4.15: Emission spectra of sample CRN 3505 3rd trial. 47
Figure 4.16: The graph of intensity means. 49
Figure 4.17: The plot of concentration means with nitrogen. 49
Figure 4.18: Emission spectra of sample Mon 89 1st trial. 51
Figure 4.19: Emission spectra of sample Mon 89 2nd trial. 52
Figure 4.20: Emission spectra of sample Mon 89 3rd trial. 53
Figure 4.21: The graph of intensity means. 54
Figure 4.22: The plot of concentration means with nitrogen. 56
Figure 4.23: Emission spectra of sample Mon 810 1st trial. 57
Figure 4.24: Emission spectra of sample Mon 810 2nd trial. 58
Figure 4.25: Emission spectra of sample Mon 810 3rd trial. 59
Figure 4.26: The graph of intensity means. 60
Figure 4.27: The graph of all sample concentration means without nitrogen. 62
Figure 4.28: Neil Bohr's Model [135]..... 63

Table of tables

Table 3.1: Mon810 specifications (ISAAA, 2020). 21
Table 3.2: MON89 specifications [111]. 22
Table 4.1: All elements found in organic (natural) grain of corn. 30
Table 4.2: Golden Bantam 1st trial peak information. 33
Table 4.3: Golden Bantam 2nd trial peak information. 34
Table 4.4: Golden Bantam 3rd trial peak information. 35
Table 4.5: Stowells 1st trial peak information. 39
Table 4.6: Stowells 2nd trial peak information. 40
Table 4.7: Stowells 3rd trial peak information. 41
Table 4.8: CRN 3505 1st trial peak information. ..... **Error! Bookmark not defined.**
Table 4.9: CRN 3505 2nd trial peak information. 46
Table 4.10 CRN 3505 3rd trial peak information. 47
Table 4.11: Mon 89 1st trial peak information. 52
Table 4.12: Mon 89 2nd trial peak information. 53
Table 4.13: Mon 89 3rd trial peak information. 53
Table 4.14: Mon 810 1st trial peak information. 57
Table 4.15: Mon 810 2nd trial peak information. 58
Table 4.16: Mon 810 3rd trial peak information. 59
Table 4.17: ICP-MS, Golden Bantam sample concentration (ppb). 78
Table 4.18: Calculated mean, standard deviation and error. 78
Table 4.19: ICP-MS, Stowells evergreen sample concentration (ppb). 79
Table 4.20: LIBS, Stowells ever-green sample Intensity (counts). 79
Table 4.21: ICP-Ms, CRN 3505 sample concentration (ppb). 80
Table 4.22: Calculated mean, standard deviation and error. 80
Table 4.23: ICP-MS, Mon 89 sample concentration (ppb). 81
Table 4.24: Calculated mean, standard deviation and error. 81
Table 4.25: ICP-MS, Mon 810 sample concentration (ppb). 82
Table 4.26: Calculated mean, standard deviation and error. 82
Table 4.27: All samples concentration means. 83

CHAPTER 1: INTRODUCTION AND PROBLEM STATEMENT

1.1 Introduction

Organic plants are those that are planted naturally and grows using natural/ organic fertilizers (manure) without an alteration in the genetic sequence of the plant (Goded et al., 2019). Genetically modified plants are plants that are synthesized in the laboratory and their genetic sequence is engineered and modified by scientists. Genetic modification is a process that is often performed for the sole purpose to meet the population demand and to get the desired tracts. Plant breeders selectively choose plants with desirable characteristics by customary breeding strategies that can take up to 15 years by rehashed sexual crossing over various eras (Nawaz et al., 2018). The aim can be to increase shelf life, adaptability, good taste, high yield enhanced plants/ fruits ability to withstand hash environment and even to increase the plant's nutritional value. Due to their desirable phenotypic tracts, these crop developments have contributed to securing sufficient food. In any case, in future, there will be a worldwide food deficiency as a result of the continuation in climate change and fast increment in population (Satoh and Teshima, 2016).

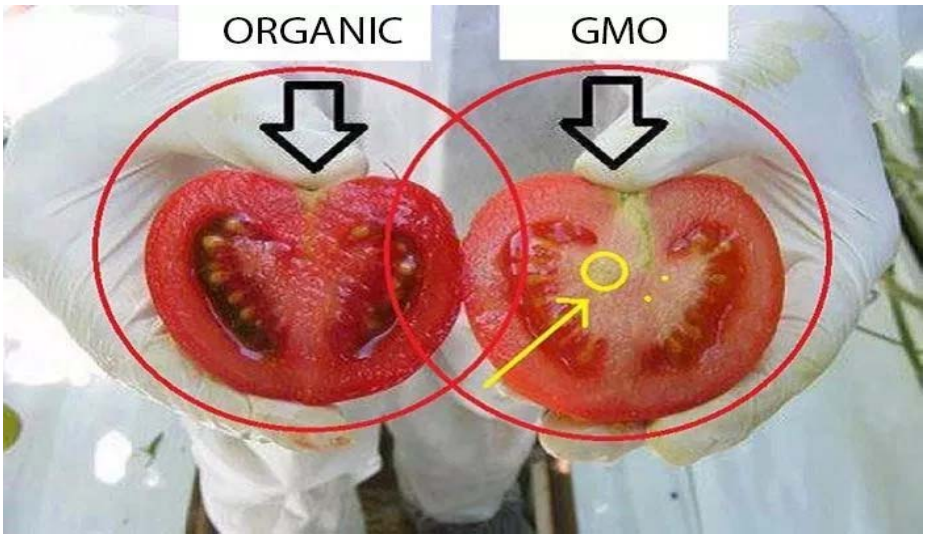

Figure 1.1: GMO VS Organic plants (Egline J., 2016).

Organic plants have either short or normal life span depending on the type of the plant within natural nutritional value as indicated in figure 1.1. In most cases, organic foods are believed to be healthy due to the fact that there are no alterations in the genetic sequence of the plant. Organic plants are considered to be always fresh, no preservatives. Organic plants depend on nature for

pest control (birds and insect). Most notably, pesticides, synthetic fertilizers and genetic modification is prohibited in organic farming. Consuming organic plants/crops does not accommodate everyone since they are sold at expensive shops like Woolworths. Organic farming is often considered as environmentally friendly but recent studies has discovered that, there is a possible accumulation of heavy metal absorbed through animal manure (Bain and Selfa, 2017). Food from organic farming has been demonstrated as healthy and very beneficial but there is no study that proves that organic has better nutritional values as compared to the one grown conventionally. The debate between importation, growing and selling of GMOs has recently been more political than scientific (Forman and Silverstein, 2012).

Elements like zinc (Zn), Iron (Fe), potassium (K), calcium (Ca) manganese (Mn), copper (Cu), nitrogen (N) etc. are essential for both plants' growth and animals, for example:

- Different cellular processes such as chlorophyll biosynthesis, respiration and photosynthesis require Fe, which also serves as a cofactor for enzymes included in oxygen or electron transfer (Kobayashi et al., 2019).
- Zinc is one of the eight essential elements in plants and animal that can be counted as both a metal and an enzyme, but only a small percentage of it. Zinc is responsible for enhancing plants nutritional quality and crop productivity (Sharma et al., 2013).
- Potassium is the most important and abundant nutrient in plants, it is responsible for plant's ability to withstand against abiotic stress (such as salinity, waterlogging and drought) and biotic stress such as insects and pathogens, but it is particularly known for its role in plant's metabolism and growth (Wang et al., 2013).
- Calcium is responsible for plant's defense mechanism; it enhances the creation of advanced mechanisms to perceive the aggressor and change that discernment into signals that trigger a necessary defense reaction which enables the plant's response to stress (Furio et al., 2020).
- Magnesium is amongst the most common abundant elements on earth and the plants highest abundant cation (Mg^{2+}), about 90 to 98%. It is the most important nutrient responsible for plants growth and most importantly for synthesis of nucleic acid, photosynthesis and enzyme activation (Tang and Luan, 2017). Tempering with the production of magnesium in plants inhibits the plants growth and development hence it is

important to maintain the plant's magnesium up-take and transport system (Chen et al., 2018).

- In plant, nitrogen is the fourth abundant element, contributing 78% of earth's air. It plays a very imperative role in plants production and yield enhancement. Insufficient amount of nitrogen in soil (due to low content of inorganic matter in soil) can lead to 100% nitrogen deficiency which (Jahan et al., 2016).

This is not all elements found in the plants, it is estimated that almost half of the elements on the periodic table can be found on plants as either micro or macro nutrients (Rizwan et al., 2019). The deficiency of any of the above-mentioned plants may result in a plant suffering from certain plant diseases, hence fertilizers are applied on the plant and soil to balance the plants nutritional content.

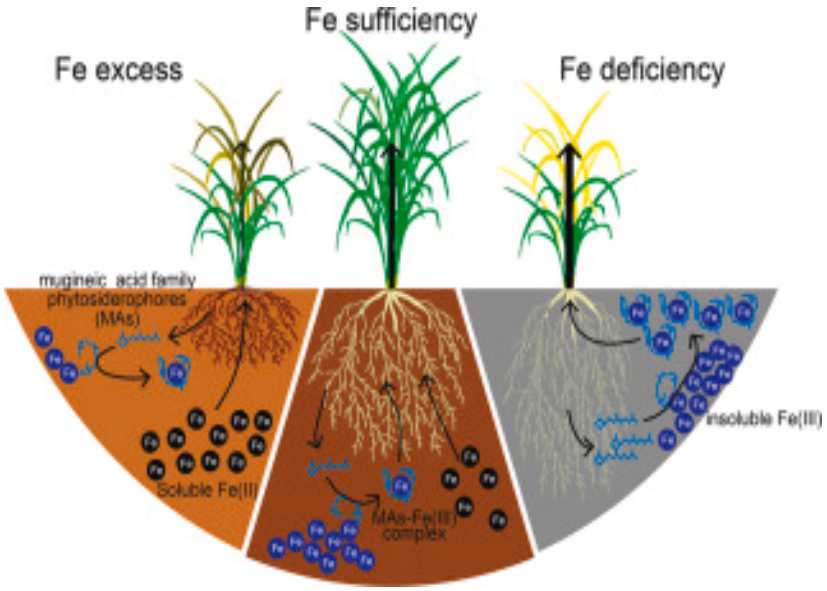

Figure 1.2: Relationships of Fe with plants (Kobayashi et al., 2019).

Figure 1,2 shows what has already been discussed in this work. Genetic engineering can lead to excess of elements or element deficiency of which both affect the plant and animals that depends on a particular plant. The right hand side of figure 2 is iron deficiency which is normally due to lower bioavailability of iron despite high iron content in soil, on the other hand, iron excess leads to plant loss hence homeostasis is maintained in plants (Mai and Bauer, 2016).

Comparing the elemental composition between organic and genetically modified plants can be an effective way for analysis and differentiate between genetically modified plants (GMP) and

Organic plants, which indirectly leads to the difference in their genetic make-up/sequence without going through biochemical processes like: DNA sequencing which is the bases reading process in the molecular DNA (Wasfi et al., 2018).

There are many techniques that can be used to analyze and compare the elemental composition like the atomic Absorption Spectroscopy (AAS), which starts with the digestion of samples in acids after crushing and solubilizing then spectrophotometry (Kobayashi et al., 2019), inductively coupled plasma-mass spectroscopy (ICP-MS), which suffers from the ions interfering the spectra (Arı et al., 2020), X-ray fluorescents. These methods are really accurate but mostly affected by their time-consuming aspects due to too much preparation processes prior to the actual sample analysis. However, Laser Induced Breakdown spectroscopy (LIBS) also known as laser-induced plasma spectroscopy (LIPS), does not need rigorous sample preparation. LIBS is a new spectrometric method used for qualitative and quantitative elemental analysis of a metal or a sample (Lin et al., 2019). It is based on focusing a laser beam with excessive power on the sample surface for plasma production and accumulation of emitting radiation in order to determine the concentration of elements contained in the sample (Yin et al., 2018a).

This technique has numerous industrial applications like in environmental monitoring, medicine, imaging, nuclear forensic, engineering and material sciences food sciences, agriculture study of archeological artifacts to the archaeologist, where it is very meaningful and valuable to study the origin, raw material and manufacturing techniques of the ancient artifacts. For example, in order to determine the origin or a particular source for researchers to gain more enlightening information about the trade, communication and corporate with other sites. Thus, the common aim of the archeologists is to determine and analyse the chemical properties of the archeological artifacts (Machado et al., 2019). Recently, techniques like, X-ray fluorescence (XRF), Raman spectroscopy, Fourier transform infrared (FTIR), thin section petrography, X-ray diffraction (XRD), energy-dispersive X-ray spectroscopy (EDX), scanning electron microscope (SEM), proton-induced X-ray emission (PIXE), (ICP-MS), and (LIBS), are most commonly utilized by the archeologists for chemical analysis and determination (Khedr and Harith, 2013). For LIBS quantitative breakdown, there is a development and a range of methods for data processing in practical application of which free calibration is well-known and widely utilized (Zhang et al., 2019a).

The laser is released from the source to the sample, as the high energy laser strikes the sample, plasma is produced which is composed of different elements. These elements are excited from the plasma at different excitation rate and this allow them to be identified when they de-excite back to ground state- that is, they fluoresce.

Normally, this process is performed under the vacuum to prevent the interference of the plasma with oxygen and nitrogen. In the vacuum, Argon gas is used to provide a transparent media for spectroscopy. As different elements are excited at different excitation rates, they are collected by the collector (fiber optic) and converted from the optical signal to the digital signal that can be read by the computer and be displayed on the monitor as the peaks of different wavelength and energy. The full sample elemental composition is recorded by the LIBS spectrometer, since in a periodic table, an element can have different emission lines between 200 – 900 nm which is the UV-vis light region (Harmon et al., 2018). This is due to the fact that different elements absorb light at different energies. The spectrum displayed on the computer screen allows users to analyze different elements on a sample, and the sample can be liquid, gas or solid. According to different description, LIBS utilizes the following system: Focusing the laser on a target, spectrometer and detector choice. In most cases, the intensity of the analyzed emission lines is largely determined by the laser energy factor, signal-to-noise ratio and subsequent analysis accuracy (Hahn and Omenetto, 2010). Ablation time can be extended to enhance the recording of atomic emission lines and continuum background radiation (Tognoni and Cristoforetti, 2016).

1.1.1 Brief description of ICP-MS

After using LIBS, ICP-MS is another selected technique that was used to verify/validate LIBS results. ICP-MS is a well-known detection technique for quantification of elements and metals (Šebestová et al., 2019). ICP-MS is an analytical technique that is particularly used in biological fluids for the measurement of elements at their trace level (Wilschefski and Baxter, 2019). Even though some laboratories still utilize some detection techniques like atomic emission and atomic absorption, in the last decade, there has been some few developments that resulted in a shift toward ICP-MS. Clinical scientists should be alert to ICP-MS' analytical aspects as this shift is likely to continue, and also to non-spectroscopic obstructions, and methodologies that can be utilized to dispose of these issues (Wilschefski and Baxter, 2019).

Unlike LIBS, ICP-MS requires sample preparation, which involves the digestion of solid sample into liquid. To analyze solid samples, electrothermal vaporization or laser-ablation can be used, in any case both methods are routinely utilized in clinical organic chemistry and research facilities and are thus exterior the scope of this study (Vanhaecke et al., 2002). ICP-MS involves the combination of an ICP with a mass spectrometer. It is capable of doing a multi-element analyses, a long linear dynamic range, good precision, low detection limits, simple spectra, and rapid isotopic analysis capability (Beauchemin, 2017). ICP-MS is widely applied to analyse a variety of samples because of the mentioned advantages, including food and water, as well as environmental, biological and geochemical samples. However, the concentration of the dissolved samples has to be kept low to minimize clogging which is a problem and results to ICP-MS having a number of limitations of which matrix effects being one of them. However, all these limitations can be minimized by appropriate sample preparation and pretreatment which involves calibrations to allow analyses of samples of any type (Beauchemin, 2017).

1.1.2 Working principles of ICP-MS

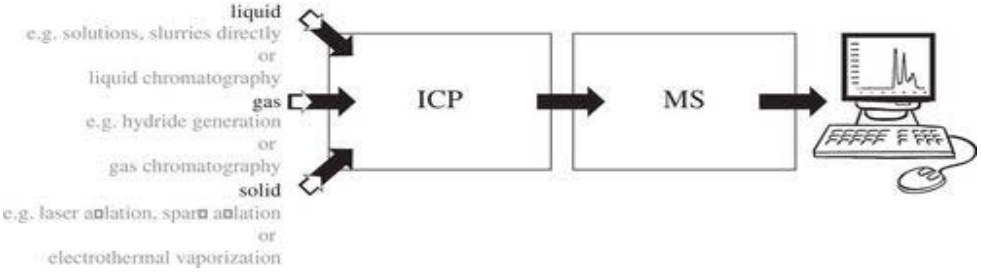

Figure 1.3: Schematic overview of sample introduction to ICP-MS (Bulska and Wagner, 2016).

Figure 1.3 is a schematic diagram of ICP-MS, it involve (a) sample (liquid or solid) conversion into gas or introduction of gaseous sample directly, (b) gas transportation into plasma, (c) introduced compounds are being atomized, then ionization of the atomized compounds in the hot plasma confinement, (d) transferring of the ions generated from the hot plasma environment commissioned at atmospheric pressure to the mass analyzer which operates under extreme vacuum, involving the extraction of ions via ion optics, (e) ions are then separated according to their mass to charge ratios (m/z), and (f). The detector then detects the separated ions, and creates electronic signal (cps) through the conversion of the created ion flux intensity (Bulska and Wagner, 2016).

1.2 Problem statement

Despite the fact that food is modified to meet our desire, there are some disadvantages. Later claims of agreement over the security on genetically altered plants (GMP) appear to be a counterfeit and misinformed propagated construct. There are some conflicting evidences distributed amid the last three decades, which lead scientific community to reconsider the studies as the debate on this subject is not 'over' yet (Hilbeck et al., 2015). The debate was on the impact of GMP/GMO on the environmental and there were some questions such as: what are the possible dangers of the GMO to the environment? (Tsatsakis et al., 2017) and how possibly will the GMO impart unfavorable effects on other species? For the most part, the impact of subsistence, natural or intensive cultivation on the environment is clear and the implications of genetically modified crops on the environment is strongly illustrated (Tsatsakis et al., 2017). The development is modern agricultural science that allows farmers to produce and grow plants that does exist not naturally triggers the skepticisms in the use of GMO (Peter et al., 2011). In contrast to GMP, organic plants are believed to contain the nutrients in their natural and optimum content. It is highly recommended for one to eat organic plants/food since they are considered healthy, traditionally natural plants can be used as remedy since they do not possess only phyto-potentials for reproduction and growth but can also be used to treat several diseases (de la Cámara et al., 2013). Organic agriculture fail to meet popular demands since there are biotic factor that depend on plants for their survival, this is a major disadvantage of depending on organic plants/food (Shaaya et al., 2016).

It is believed that even though GMOs are designed to meet our demands, there has to be a difference in the genetic make-up of the GMO as compared to organic. In this case, GMO can either gain some elements or lose some of the essential elements during the process of modification. The gained or lost elements can be the contributing factor to environmental unfriendliness. In the past decades, analytical chemistry has been focusing on elemental analysis especially on harmful and toxic heavy metals. It is very essential in the fields of food analysis, drugs and environmental analysis (Yang et al., 2020). Approximately 99% of the human body mass is composed of Mg (0.1%), Cl (0.2%), Na (0.2%), S (0.3%), K (0.4%), P (1%), C (1.5%), N (3.2%), H (9.5%), C (18.5%) and O (65%) (Lohman et al., 2005). There are other elements that are found in human body, apart from the most essential ones and mostly present in trace amounts. According to the Food and Drug Administration federal agency (FDA), the recommended macro-

nutrient metals daily intake should be as follows: 1000–1200 mg of calcium per day, 1500 mg of sodium per day, 4700 mg of potassium per day, 400–420 mg of magnesium per day, 700 mg of phosphorus per day, and 1800–2300 mg of chloride per day (Soetan et al., 2010), of which, there should be a daily micronutrient intake of less than 100 ppm of metals such as Al, Ti, Zn, etc. (Song et al., 2013). According to FDA, failure to balance the intake of these elements can be very toxic and even lead to some diseases (Song et al., 2013).

Organic and genetically modified plants have been believed to have the same nutritional value for decades. Yet there are some negative impacts imposed by genetically modified plants on the environment and on people. Despite the fact that food is modified to meet our desire, there are more disadvantages as compared to the known advantages. Genetically modified plants can lead to gene flow, allergies and mutation (Nawaz et al., 2018). The impact of Gene flow in the environment is the decrease of differentiation between populations as well as diversity increment between individuals inside a population including genetic diversity structure as one of the gene flow consequences. (Tsatsakis et al., 2017). Gene flow can also lead to mutation as a result of uncontrolled cross breeding. These genetically Modified Plants can destroy the environmental balance through contamination of other organisms or cross contamination (Gurău and Ranchhod, 2016). Countries like Algeria have already launched a regulatory system that prohibits the importation, production and use of GMOs except for study purposes (Brara et al., 2020). This research was motivated by the fact that the regulations on GMOs is not universal, Most countries like Pakistan, United States of America, Australia and other Asian countries are not strict on the consumption of GMOs as long as there is a proper labelling on the product (Nawaz et al., 2019).

Different techniques can be used to analyse the elemental compositions for both type of plants but in this case a chosen technique has to be simple, accurate and reliable. The best technique and most suitable is laser induced breakdown spectroscopy due to the fact that no sample preparation is needed and in field operations, it can be utilized for quick real-time analysis and by utilizing ordinary (single-element) or multivariate calibration quantitative analytical results can be obtained from LIBS (Wong et al., 2017). As an elemental analysis device, LIBS is progressively becoming more popular due to the fact that it is moderately cheap, fast, non-invasive technique that permits a concurrent multi-element examination in a single measurement (Markiewicz-Keszycka et al., 2019). This technique has been proven to be the promising component investigation procedure due

to its special advantages such as on-line checking and quick in-situ analysis of materials in different forms (Lin et al., 2019). According to (Harmon et al., 2018), LIBS technology has properties that make it much more valuable and exceedingly flexible method for the examination of geological materials within the field. Therefore, analyzing the elemental composition in plants can be very important in diagnosing and preventing most plant and animal related diseases. At the end of this project, one will be able to distinguish the pros and cons in the differences between organic and genetically modified plants in terms of elements contained, healthy and their impact to the environment. In this project, genetically modified and organic maize was analyzed. This is because of the fact that maize is a type of plant that is mostly and widely used in the country and Africa as a whole.

Though LIBS is the technique that this project is mainly focused on, ICP-MS was utilized as a complementary technique. This technique is based on ion interference and has the ability to analyse elements in biological fluid, tissues, trace and ultra-trace level (Amais et al., 2020). Both these techniques are capable of multi-elemental, on-line checking and analysis and the results can be obtained within 24 hours. The motive behind using both these techniques is to make sure that all elements are detected and identified regardless of the detection range.

1.3 Aim

The purpose of this research was to study the differences in elemental composition between organic and genetically modified plants.

1.4 Objectives

The objectives were to:

- Investigate the elemental composition of organic and genetically modified plants using LIBS and ICP-MS.
- Differentiate the two categories and two techniques according to the signature of their essential and trace elements.
- Determine the effects of GMOs to the environment and the people.
- Make a recommendation to the farmers.

CHAPTER 2: LITERATURE REVIEW

In recent studies, LIBS is one of the newest techniques utilized for qualitative and quantitative elemental analysis. This chapter gives more information about LIBS' advantages and disadvantages from different studies. In this research, LIBS was used to analyse the elemental composition in maize grains, since this technique is known for its user friendliness. This chapter talks about how LIBS was used in other sciences branches like; pharmaceuticals, medicine, energy, etc. Other articles may agree and disagree on curtain features of the technique under this section. One will also learn how this technique can be improved just by studying how it has been used in other experiments and also which other techniques work better than LIBS.

2.1 What is laser induced breakdown spectroscopy (LIBS).

According to (Rehse, 2019), LIBS is an effective and adaptable illuminating instrument for the quick examination and characterization of a specimen's natural composition. In many cases, it is frequently used to perform quick elemental analysis on numerous targets of interest (Rehse, 2019). The procedure of LIBS is a new analytical way to study the material composition (Meng et al., 2017). LIBS is a spectrometry technology that deals with the analysis of components of a material by measuring high power laser pulse induced by nuclear emission. Focusing of a high energy laser beam on to the surface of a sample, is the fundamental guideline for the creation of plasma and collection of emitting radiation (Guo et al., 2012). Jingjun Lin further added, that the information obtained can be used for qualitative and quantitative analysis of the elemental composition of the target.

According to Junjuri, LIBS is an emanation based spectroscopic method which utilizes a strongly pulsed laser source to form the plasma of the given analyte (Junjuri et al., 2019). He added that the plasma portion represents the sample composition and by spectrally examining the radiation transmitted from the plasma, one can interpret the elemental data of the sample of interest (LIBS) is a nuclear excitation (sometimes molecular excitation) technique based on focusing a pulsed laser light to the sample producing high energy plasma. The produced plasma consists of ion and electrons that emit radiation when cooling, the radiation is then collected via the optic fiber for further analysis (Myakalwar et al., 2011).

2.2 What are the uses of laser induced breakdown spectroscopy?

LIBS is one of the optical spectroscopic methods that are mostly used because of its flexibility and experimental straightforwardness (Williamson and Kiefer, 2018), it can be used for different purposes at different places. This section reviews different uses of the LIBS. LIBS feature in wide applications in a lot of areas, such as environmental monitoring, biomedicine, material science and industrial engineering etc. The technique is mainly used for qualitative and quantitative analysis (Zhang et al., 2019a). Samples of any physical form can be distinguished using LIBS at a high speed e.g. solid, liquid, powder and gas (Lin et al., 2019). In the last decade, analysis of organic samples has been carried out using LIBS, where elements such has K, Mg, P and Na are referred to as spectral markers for organic samples (Andersen et al., 2016).

2.2.1 Pharmaceutical use of LIBS

Pharmaceutical industry is a big industry. In this case, LIBS can be used a lot and in different ways, this subheading is going to look at the different pharmaceutical uses of LIBS. Amongst LIBS several advantages, high specificity and its capability for sample transfer complements its application in the pharmaceutical field. Nowadays, in the pharmaceutical industry, the technique has been exclusively applied as quantitating active pharmaceutical ingredient (API) to analyze forms of dosage in solids. LIBS was used for analysis of the active agents in the tablet (Nisar et al., 2019). The analysis is based on API specific elements such as chlorine, bromine, fluorine or sulfur. In this case, the elements present in a pharmaceutical tablet (calcium-based tablet) were determined using LIBS and then compared to that of National institute of standards and technology database (NIST) which is a standard reference data program. The same analytical principle can be applied to liquid solutions, however, there have not been any reported scheme of using LIBS in pharmaceutical solutions (Nisar et al., 2019).

Recently, LIBS was chosen as the novel accurate technique to analyse the toxicity in some antibiotic brands of tablets in Pakistan (Ahmed et al., 2020). For these tablets' qualitative and quantitative analysis, LIBS was combined with LA-TOF-MS, which is laser ablation time-of-Flight technique Mass Spectrometry. (Lewen, 2011) agreed with Ahmed on the use of LIBS in drug analysis since it is believed that the Chinese emperor died due to the presence of mercury in drugs, however LIBS made it possible for the quantitative detection of specific elements from trace

to heavy elements (Lewen, 2011). Further, Myakalwar et al. (2011) used LIBS to classify tablets into their functional groups based on ratio metric and chemometric approach

For the first time, LIBS technique was introduced to examine the nanoparticle's penetration depth used in biocidal treatments of archeological artifacts, due to its unique advantage that it is a nondestructive technique that does require little or no sample preparation or pretreatment of the sample and its capability to perform an on-site analysis (Mateo et al., 2019). In order to evaluate the effectiveness of the nanomaterials for protective purposes, this technique enabled the researcher to carry out the silver nanoparticles characterization and analyze its depth (Mateo et al., 2019).

2.2.2 Application of LIBS in energy

In recent years, there has been a tremendous development in the energy fields like batteries and solar cells due to the introduction of LIBS. The application of LIBS allows the most significant alteration, spatial and depth determination throughout sampling in order to resolve features at length scales that corresponds to that of the original materials being studied. Furthermore, in energy research, LIBS exclusive analyzing ability is often utilized particularly in advanced manufacturing for quality control (Zorba et al., 2017). In photovoltaic-grade silicon production, Nanosecond LIBS has been utilized for the most important steps like: Dopant and impurity mapping in silicon, quantification, detection. Thin-film compounds absorption layers' analysis has also been utilizing LIBS in semiconductor solar cells. The technique enabled the appropriate tailoring of the absorber film bandgap through proper management of the chemical composition (Zorba et al., 2017).

Nowadays, tungsten is a metal that is often used in tokamaks diverter for plasma focusing because of its lower sputtering rate and high melting point (Tolias et al., 2020). Tokamaks like FTU and TEXTOR, tested and used tungsten and molybdenum as limiter materials (Vertkov et al., 2017). Both of these metals proved to be suitable and feasible to be applied as limiters, at the same time, molybdenum experimentally appeared to have several times high deposition rate as compared to that tungsten under the same condition (Vertkov et al., 2017). Cooling due to mediated radiation losses can be caused by low rate of sputtering through plasma degradation even though the used materials have successfully proved their suitability for both the diverters and the limiter walls (Krasheninnikov et al., 2016). Detection and removal of the deposits is very important in

tokamaks, since the wall weakening due to sputtering caused by the interaction of the plasma and diverter wall leads to micro-crack formation which further exposes trapped tritium fuel. The deposited mixed layer thickness can be controlled and mapped used molybdenum which can either be part of the wall or background material (Bisson et al., 2015). In this case, there will be material migration which will possibly cause impurities and fuel retaining in the tokamak, therefore, LIBS is required for its suitable non-invasive detection capability in order to perform surface analysis of the deposited impurities, multi-layered sample depth analysis and fuel retention in situ characterization (Miškovičová et al., 2020).

2.2.3 Analysing the archaeology and cultural heritage

To the archaeologist, it is very meaningful and valuable to study the origin, of raw material and manufacturing techniques of the ancient artifacts like the ecce home painting. Thus, the common aim of the archeologists is to determine and analyze the chemical properties of the archeological artifacts (Singh et al., 2018). Recently, techniques like, Raman spectroscopy, fourier transform infrared (FTIR), thin section petrography, proton-induced x-ray emission (PIXE), ICP-MS, and LIBS, are most commonly utilized by the archeologists for chemical analysis and determination (Khedr and Harith, 2013).

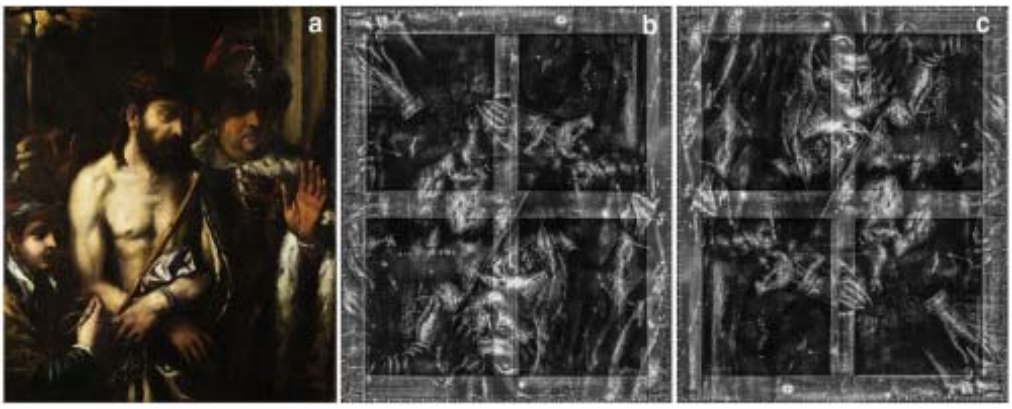

Figure 2.1: The Ecce Homo painting (de Castro and Jurado-López, 2019).

Relevant information about the archeological coins can be reached by elemental analysis, the harvested information is really vital for the archeologists to study the metals used in the coins and determined the techniques involved in the minting of the coins (Awasthi et al., 2016). In this case, using laser based analytical technique is very important. These methods allow one to study the artifacts internal content without destructing the object. There are numerous published articles that agrees with the success of LIBS in the study of ancient artifact, e.g. sculptural art objects, cultural

heritage material ink and pigments, painting, ancient coins, metal artifacts (Bai et al., 2020), geological samples (Díaz Pace et al., 2011), pottery, glass (Singh et al., 2018) and zoo-archaeology (Rusak et al., 2011).

Characterization of submersed artifacts and cultural heritage due to accidents is very important in the field of archeology. Chemical analysis is very essential for the analyses of materials found submerged due to accidents and can be vital the determine to origin especially by analyzing the raw materials (López-Claros et al., 2018). Recently, archeologists have pointed out LIBS as the potential technique in their field due to its combined features such as, real time analysis, no sample preparation, unlimited range of material capability and multi-elemental analysis. The feature qualifies it for under water analysis. In 2020, Bhatt and his colleagues carried out an investigation on the use of LIBS in liquid analysis (Bhatt et al., 2020). The experiment had its drawbacks due to the explosive increase and gas bubble formation due to the continuous heat generated as the laser is focused on to the liquid during the interaction of laser and water. This results in the formation of a short-lived plasma forming a weak signal in a single pulse LIBS analysis (Maurya et al., 2020). In the past few years, double pulse methodology was implemented to improve the technique (Somekawa et al., 2020). In this new technique, gas bubbles are created by the first pulse of laser, then followed by the sample ablation by the second laser pulse that further causes excitation to the plasma in the bubble. This improved technique has been utilized for qualitative and quantitative analyses of underwater solid sediments (Fabre, 2020). Recently, it has been proven that LIBS is capable of carrying a wide range of underwater analysis of metallic like bronze and iron and non-metallic materials wood and rocks (Guirado et al., 2012).

LIBS can still be used to accurately identify, the elemental composition, appearance, colors and pigments present in the paints. Despite all the advantages, the technique does not provide a clear analysis on pigments that contain the same elements, for example, Fe-based elements in red iron oxide (Fe_2O_3) and yellow ochre (FeO(OH)), the emission of iron from both pigments results in the similar LIBS spectra. As a logical choice to overcome this, LIBS have to be coupled with diffuse reflectance spectroscopy. In this diffuse reflectance technique, the surface of the paint is illuminated by a broadband beam of white light, the light will then be absorbed, transmitted and then scattered throughout the composite paint material. Diffuse reflection will then only occur due to back scattering caused by an unabsorbed paint fraction. To provide the correct spectra reliable

for materials, even a low-resolution spectrometer and a source of a broadband light can be utilized to implement the reflectance setup (Siozos et al., 2017).

According to history, a variety of metallic alloys with different compositions, uses and properties has appeared in different metal ages (Tn in the mid Bronze Age), followed by Tn–Pd alloys in the Final Bronze Age and Fe in the Iron Age. Since the evolution of used metal alloy with time, the classification of the metallic constituents and the period of manufacturing can be easily achieved through quantitative analysis of the sample's elemental composition. For example, in the Early Bronze Age, the bronze-based alloys had huge amount of arsenic content as compared to the present days (Snoeck et al., 2020). For the past Metal Ages, archeologists used LIBS for the characterization of archeological metal objects. The technique has enabled the cataloging and analysis of approximately 37 objects of different shapes and sizes. The archeological criteria used for dating strongly correlates with the archeological bronze Chrono cultural sorting based on the cluster analysis and sample arsenic content (Snoeck et al., 2020).

2.2.4 Geologic and soil analysis

Since LIBS emerged in the 80s, Los Alamos National Lab had a major contribution on the LIBS technique before its first application in the early 90s (Ytsma and Dyar, 2018). The first LIBS application was on sulfide minerals for the Yucca Mountain repository performance and licensing. In this experiment, powder rock pellets were used as standards for iron ore quantitative elemental analysis and to establish univariate calibration, they used Fe as internal standard (Fabre, 2020).

400 mg L^{-1} of lead (Pb) in the soil is considered the safe level according to the united states environmental protection Agency (USEPA), whilst in correspondence, 32-100 mg L^{-1} is considered as safe lead level in Europe (Rehan et al., 2018). For Pb quantification, numerous techniques like, XRF, AAS, and ICP-MS were utilized to analyze the level of lead in the soil (Orellana et al., 2013). The crucial technique for these analyses is LIBS since the above-mentioned techniques require rigorous sample preparation and generally led the waste of chemicals, in this case, sample preparation has to be minimized or avoided. Lead contaminated soil is very lethal to both humans and animals and can lead to blindness, central nervous system disorders, convulsions and ataxia (Contessi et al., 2020). In Pakistan, optimized LIBS system is widely used to detect and assess soil contaminated with lead from the oil drilling areas. The method of applying standard calibration curve and the other method based on analyzing the strongest peak of interest are the

two mechanisms that are usually performed for quantitative analysis of lead content in soil sample (Fabre, 2020).

The human settlement, Ny-Aalesund, Svalbard, located at the far north of the world, had a coal mine, which was under operation from the year 1916 to 1963 (Kim et al., 2017). The soil in Aalesund may still be affected by heavy metals from the coal mine waste. To understand the Arctic anthropogenic pollution, it is vital to determine heavy metals in aerosols. Soil LIBS and aerosols LIBS are two techniques performed in this case to determine heavy metals contaminating the Ny-Aalesund, Svalbard soil and aerosols. The effect of local sources on soils in Ny-Aalesund is determined using elemental spatial distribution. A comparison was then between the distribution, soil samples from Korea abandoned mine and urban areas, furthermore, aerosol LIBS determined elements from arctic aerosols that will then be compared to the ones in arctic soils (Kim et al., 2017).

2.2.5 Forensics

In forensic field, broken glass or glass fragments can strengthen the forensic investigation by providing strong evidence that can either favor the defendant or the prosecutor proposition in a specific set of case circumstances (El-Deftar et al., 2014). Recently, LIBS has been widely utilized in forensics to detect trace elements in glass sample for its atomic emission ability on solid samples especially for forensic purposes (El-Deftar et al., 2014). Also, LIBS was used to determine ten glass fragments to obtain their elemental composition from seven automobile glass samples (Rinke-Kneapler and Sigman, 2014). Normally, spectral mask, rank correlation and linear coefficients methods are incorporated with LIBS for discrimination potential of the technique.

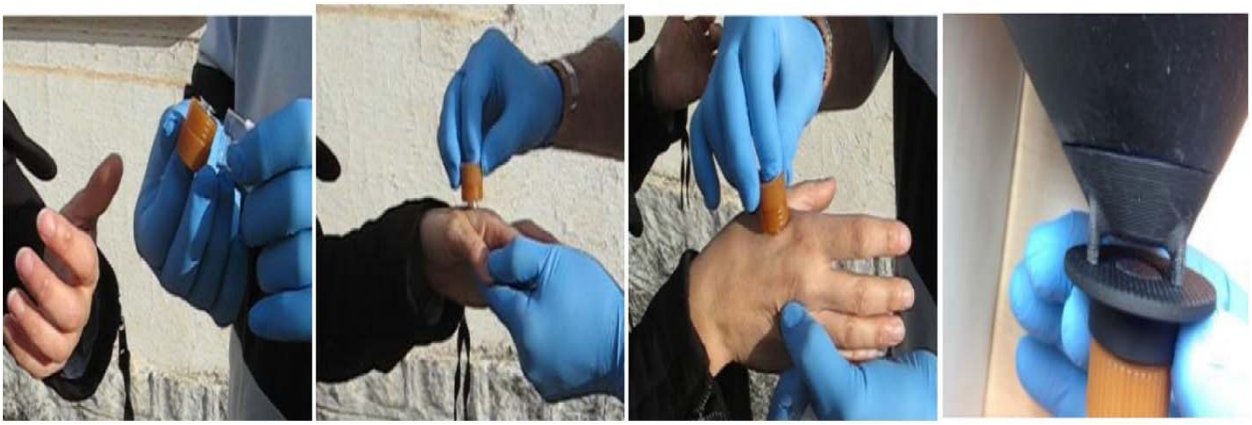

Figure 2.2: Protocol sampling and analysis of stub (Doña-Fernández et al., 2018).

Figure 2.2 shows a forensic scientist detecting the gunshot residue from the suspect. In cases that involve firearms, cartridge cases, bullets, projectile fragments residues from firearm discharge are collected in most cases during investigation of a crime scene. To provide valuable investigative evidence related to gunshot residues (GSR), forensics expert take the collected evidence to their laboratories for analysis in order to determine the firing distance, to differentiate between an accidental shooting, suicide or homicide in order to capture the potential shooter (Stoney and Stoney, 2015). One of the problems faced by scientists during evidence collection is that, after primer percussion, there can be a random projection of gunshot residual in any direction (French and Morgan, 2015). Samples are widely collected from clothing, hands and faces, regarding individual suspects. Random sample collection, which is usually called blind sampling is performed by forensic scientists when dealing with scenarios like; multiple suspects, vehicles and rooms as long as the area is considered to be appropriate (Blakey et al., 2018). A great volume of evidence is harvested using this technique, materials can be wasted and time is consumed amid the analysis, the rational significance is for the investigation and judicial processes to be delayed.

iForenLIBS is a LIBS based equipment that was developed by Indra systems to solve the above-mentioned problem. The aim of this LIBS based equipment is to regulate samples collection at numerous crime scenes (Noll, 2012). This technique allows forensics to do a direct identification and quantification of elements in any physical form (liquid, solid or gas) because of its low limit of detection ability, samples can be analyzed directly at any surface with little or no sample preparation needed (Chen et al., 2020b). Because of its advantages, this technology has been proposed in recent decades as a reliable technique recommended for the analysis of trace elements in environmental and forensic applications, detection of explosives, metallurgy, plastic analysis, etc. (Lucena et al., 2011). Furthermore, metallic nanoparticles has been featured in this technique to enhance detection limits, influenced by the medium and material-elements interaction in the process of ablation (Dell'Aglio et al., 2018).

Syvilay et al. (2019) designed an experiment using standard reference glass material (NIST 1831) to compare the difference in experimental accuracy between LIBS inter-day and intra-day variation, which is the measurements run the same day and those run on a different day or at a later stage (Syvilay et al., 2019). This was done to verify the claim that inter-day variation produces a

more reliable spectrum. Understanding the difference in the two variations has a vital consequence for forensic practitioners (Gupta et al., 2017).

In this experiment, a glass was used since it is easily found in scenes like; burglaries, hit-and-run and not difficult to recover from a crime scene. It is very vital for forensic scientists to be very accurate and precise when measuring glass's physical characteristics like elemental characteristics and refractive index and understanding what could be the limits of other analyzing techniques (Sánchez-Aké et al., 2018). On a study that was done by Orellana et al, NIST SRM 610 AND 1831 was used and showed that consistent results could be produced when LIBS experiment is carried out the same day (Orellana et al., 2013). There was a percentage relative standard deviation (%RSD) variation of 0.8% to 15.0% ratio for each peak from the experiment that was carried out hourly from the same sample on the same day (Bridge et al., 2006). A set of 11 emission line ratios was measured in another experiment to measure the percentage relative standard deviation (%RSD), a standard NIST SRM 610 was utilized for the period of 3 days to measure the same peak ratios of glass sample and the following results were obtained: %RSD of 6.5±1.4% same day, %RSD of 24.5±29.2% for 3 days. The results prove that, conducting the LIBS experiment on the same day is more advantageous (El-Deftar et al., 2014).

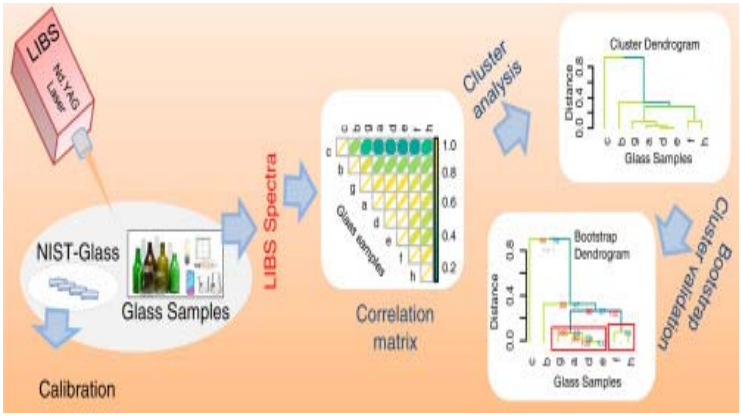

Figure 2.3: Glass discrimination and multivariant analysis (El-Deftar et al., 2014).

Figure 2.3 describes that glass elemental finger printing by utilizing laser induced breakdown spectroscopy (LIBS) has been identified as valuable for coordinating and distinguishing glass as proof to support criminal and lawful procedures (El-Deftar et al., 2014).

2.2.6 Butter adulteration analysis using LIBS

Blending of butter with a much cheaper margarine is now a well-practiced technique for butter adulteration (Deelstra et al., 2014). Butter adulteration has been examined in a few studies; in any case, there's still a need for a fast, easy and non-destructive detection technique. For the detection of the presence of vegetable fats in butter, gas chromatography has been used especially to analyze the composition of fatty acids in oil sample of which at present it requires triglycerides analysis first (Temiz et al., 2018). Although gas chromatography was regarded as an accredited technique, it was still time-consuming, vigorous chemical were needed to be used and that requires well-trained personnel, that eventually make the technique expensive. In this case, the applicability and the effectiveness of LIBS was tested in the detection of butter adulteration with margarine. LIBS produced two spectra with different elemental composition indicating that butter and margarine are different and for the confirmation the results were further evaluated using chemometric methods (Temiz et al., 2018).

2.2.7 Determination of ash content of coal using LIBS

There are many standard chemical approaches that can be used for the coal compositional analysis; however, there is a new proposed technique for accurate and fast detection of chlorine substances in coal. The current studies show that this technique is very simple as compared to others (Zhang et al., 2019b), nowadays power plants need the technique that involves fast response of which the ones used does not meet the requirements anymore (Legnaioli et al., 2019). On the other hand, exceptionally few methods can ensure the on-line coal analysis, energy before it would be burned to generate electricity. For analyzing coal moving on a conveyor belt, before burning ,the only technique capable of fast and precise analysis is LIBS (Legnaioli et al., 2019).

2.3 Advantages of using LIBS

As an elemental analysis device, LIBS is progressively becoming more popular due to the fact that it is moderately cheap, fast, non-destructive technique that permits a concurrent multi-element examination in a single measurement (Hussain Shah et al., 2020). This technique has been proven to be the promising component investigation procedure due to its special advantages such as on-line checking and quick in-situ analysis of materials in different forms (Lin et al., 2019). According to Harmon et al., (2018), LIBS technology has properties that make it much more valuable and exceedingly flexible method for the examination of geological materials within the field. For in-situ and real time analysis, LIBS is the best, by both stand-off or close-in approaches it can also

be used for elemental identification or abundance quantification (Zhang and Yang, 2020). Raman and XRF spectroscopy, no sample preparation is needed in order to use LIBS (Harmon et al., 2018).

LIBS highly depend on calibration accuracy for quantitative analysis and some widely used conventional LIBS methods such as; internal standardization, classical calibration, multipoint calibration (MPC) and multivariate calibration (Yuan et al., 2019). Even though there are a number of accurate techniques, these techniques can be very sophisticated and requires various solutions to dissolve the sample (sample preparation) prior actual experimentation. Due to these measures, a precious sample can be physically destroyed in the process (Awasthi et al., 2016). LIBS can perform some measurements at a range of approximately 130 m, making this technique capable of characterizing objects remotely (Kubitza et al., 2020).

2.4 Challenges of using LIBS

Exploring ways to improve the quality of plasma emission, there has been some challenges in the process of extending LIBS efficiency as the field of application extends and widens with an increase in studies aiming to improve the technique (Goueguel et al., 2010). This technique is considered as the breakthrough because of its countless advantages like analyzing samples of any phase, which is not always the case especially when it comes to analyzing liquid and powder samples. Using the technique in powder samples requires one to go for pretreatment processes that leads to matrix interference effect and this complicates spectral analysis and the impurities compromises detection sensitivity and emission intensity and self-absorption of certain emission peaks.

CHAPTER 3: MATERIALS AND METHODS

This chapter is the most important part of this research, the two techniques (LIBS and ICP-MS) are described in details and how the actual practical work was carried out. All instruments used are properties of the North-West University but from different Departments, of which; the Polymix (PX-MCF 90 D), Titan Microwave digester Perkin Elmer and ICP-MS were from the Center of Applied Radiation Science and Technology (CARST) whilst LIBS was from the Chemistry Department, under the Material Science Research labs.

Genetically modified samples, which are: MON 810, MON 89 and CRN3505 were bought and shipped from Monsanto USA by Prof Johnnie Van Den Berg (NWU Potchefstroom campus). Organic plants seeds: Stowell evergreen and Golden Bantam, from organic seeds, Rosemary Hills, Pretorial east. The methods used in the chapter were carefully created and amended specifically for this project under strict supervision of Ms ND Mokhine (co-supervisor).

3.1 Sample collection

In this project maize used was imported from Monsanto USA since it was not easy to get them in South Africa, the ones sold here are not labeled in details, especially for research purpose.

3.1.1 Genetically modified maize

- **MON810:** This is a recombinant trait introduced into various number of maize, which contains a derived gene called *Bacillus thuringiensis* (*Bt*), which is modified to express truncated *cry*1Ab gene that encodes for δ-endotoxin, an insecticidal protein that manages the *Ostrinia nubilalis* which are some of the lepidopteran pest insects (Hubert et al., 2008). This gene trait allows the plant to combat against moths during maize grain storage period (Ricroch et al., 2010). The sample (Mon810) specifications are displayed in table 3.1 below.

Table 3.1: Mon810 specifications (ISAAA, 2020).

Developer:	Monsanto (both fully and partly owned companies)
Method of trait introduction	Microparticle bombardment of tissue or plant cells
GM traits	Lepidopteran insect resistance, antibiotic resistance and glyphosate herbicide tolerance
Commercial trait	Insect resistance

- **MON89:** this is a transgenic trait introgressed into numerous maize plants, it consists of bacillus thuringiensis subsp. Kumamotoensis is a gene modified to express Cry2Ab and Cry1A.105 protein comprising of Cry1Ab, Cry1Ac and Cry1F proteins, delta that encodes endotoxin. It is responsible for lepidopteran insects' resistance particularly by selectively destroying their mesenteron lining (ISAAA, 2020)**.** Table 3.2 indicated the sample (Mon89) specifications.

Table 3.2: MON89 specifications (ISAAA, 2020).

Developer:	Monsanto Company (both fully and partly owned companies)
Method of trait introduction	mediated plant transformation- *Agrobacterium tumefaciens*
GM traits	Lepidopteran insect resistance
Commercial trait	Insect resistance

- **CRN3505:** this is a newly Monsanto produced dual trait structure version of *Bacillus thuringiensis* that combines two transgenes Cry1A.105 and Cry2Ab which are responsible for toxin-production, this process is known as pyramiding which is a way of replacing a single ineffectual transgene. This results in high yield and drought tolerance (Schnurr, 2019).

3.1.2 Organic maize

- **Golden Bantam:** Since the beginning of the 20th century, yellow corn has been favored by the home gardeners hence it is known as old standard yellow corn. Golden Bantam corn has a great sweet flavor taste that is fantastic for fresh eating or freezing. Very sweet adaptable, and reliable for an open pollinated heirloom corn. It can grow from 150 cm to 180 cm tall and produces 14-18 cm ears, full of golden yellow kernels each in 77 to 80 days (Heirloom, 2012).
- **Stowell ever green:** It is the most delicious white sweet corn, named, the "King of All White Sweet Corn Varieties". For more than 162 years, it has been popularly known by market growers and home gardeners (Heirloom, 2012). A special variety for late season, the maturation of Stowell evergreen is very slow and can occur over a very long period of time, usually elongates harvest and produces 1-2 ears per stalk, sweet white kernels, 0.2 m long with 16 to 20 rows of plump. It is considered one of the best heirloom variety for table food due to

the fact that, it keeps longer than most which makes freezing and canning possible for 80-100 days (Heirloom, 2012).

3.2 Equipment

Figure 3.2.1 is a Polymix (PX-MCF 90D), this equipment is used for sample grinding. It can be using for samples like; maize and even soil. This instrument is very easy to operate, no instruction or guidance is needed.

Figure 3.2.1: Polymix (PX-MCF 90 D).

Figure 3.2.2 is LIBS; this is where all the sample ablation takes place. This instrument uses high energy laser to excite the elements within the sample in order to study the elemental composition of a particular sample.

Figure 3.2.2: Laser induced breakdown spectroscopy (LIBS).

Figure 3.2.3 shows the Titan microwave digester-Perkin Elmer. All the sample digestions were carried out by this instrument. It has the ability to run multiple samples at ones.

Figure 3.2.3: Titan microwave digester - Perkin Elmer

Figure 3.2.4 is the ICP-MS, this instrument is used for elemental analysis and identification. At CARST, the instrument is operated under a direct supervision from Ms ND Mokhine since it is complicated and requires a trained expect to operate.

Figure 3.2.4: Inductively coupled plasma mass spectrometry (ICP-MS).

Figure 3.3.1, 3.3.2 and 3.3.2 and all CARST equipment whilst on figure 3.3.3 is the LIBS from chemistry department.

3.3 Methodology

Although LIBS require little or no sample preparation, all samples: MON810, MON80, CRN3505, Stowell evergreen and Golden Bantam were ground in small portions using Polymix (**PX-MCF 90 D**) at 6000 rpm (maximum revolutions) and 230 V. Samples were ground in their raw form in order to create single phase powder sample to reduce interference and easy to run via LIBS. The sieve and the grinding blades were cleaned after every sample to avoid contamination. The powder samples were then put in different plastics and labelled.

3.3.1 LIBS experiment

This LIBS experimental setup is shown in Fig. 3.3.3 It consists:

- **Laser source** (NT342 series) is the widely tunable system range of 192 – 2600 nm and produces high pulse energy (up to 50 mJ) that permits one to study extensively a range of materials up to 18 micrometres, it is customized to possibly enable the studies of infrared radiation vibrations between molecules.
- **Focusing lens:** 30 mm length plano-convex for bending the laser to the focal point.
- **Fiber optics** (for light collection): silica-clad and silica-core fibers optimized for wavelength ranges: VIS-NIR (450–2200 nm), SR (190–1100 nm) or UV-VIS (300–1100 nm). 2 m standard length of fiber assembly and diameters ranging from 4 μm to 1500 μm (MacArthur et al., 2014).
- **Spectrometer:** Ocean HDX spectrometer utilizes strong optical bench plan, optimized components that are accurately designed to increase optical resolution, maximize throughput, decrease light strays and keep the internal thermal temperature constant for integrated, research and industrial applications (MacArthur et al., 2014).
- **Sample stage:** This is a handmade stage, which is an adjustable stand with a watch glass clamped on it. This was self-designed to allow rotation and vertical adjustment during ablation.

Before running the sample, a dark spectrum was taken whilst the light path was blocked and the reference spectrum was taken with the light path open and using the blank sample. Both the dark and reference spectrum were then saved on the folder created on desktop. On the data acquisition console, the integration time was set to 100 milliseconds so that the detector can have a longer photon monitoring time. Scan average was set to 8 for a better signal-to-noise ratio (S:N). Box

width was set to 4, this value was set higher in order to acquire smoother data and greater signal-to-noise-ratio. Strobe/lamp enable and electric dark correction options were both unchecked.

3.3.2 Data acquisition

This experiment was carried out at night to avoid light and reduced light interference. The ground sample was ablated by an exciting laser pulse from the NT342 series laser with 474 nm laser wavelength. The pulse energy was exactly 10 mJ and a laser pulse duration of 3.6 ns, and the rate of repetition was tuned to 10 Hz. The sample was compressed and horizontally mounted on a flexible *xyz* rotating sample stage so that the laser can always heat a fresh region of the sample during ablation and analysis. The laser pulse was focused to the surface of the sample by a 30 mm length plano-convex, the ablation causes the sample to be excited, exposing different elements on the sample surface. The emitted signal from the excited plasma was collected through a fiber optic coupled into spectrometer through an optic fiber cable. A built-in charge-coupled device (CCD) camera in the spectrometer recorded the spectra. Several pulses from the ablation laser were then allowed to accumulate on the detector for the generation of a single spectral signal. Each sample was measured three times, excluding the outliers.

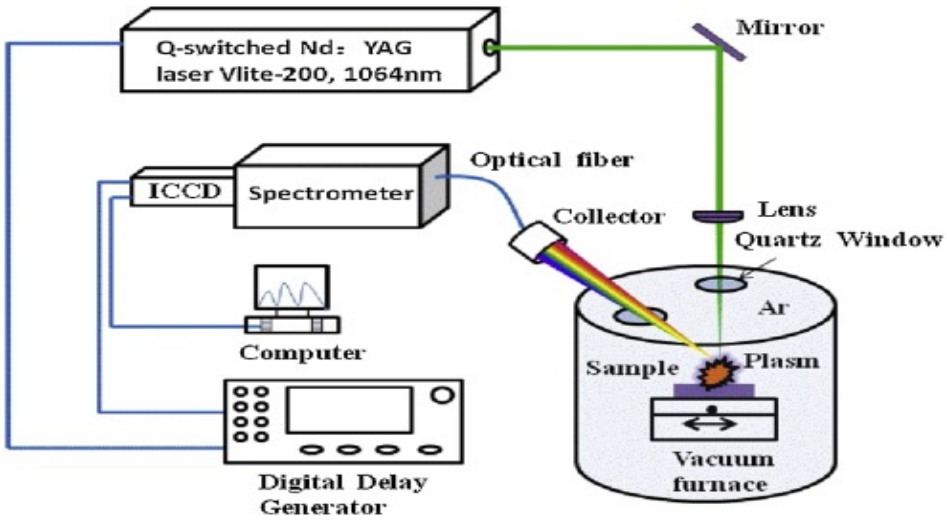

Figure 3.3.1: Schematic diagram for laser induced breakdown spectroscopy.

3.4 ICP-MS experiment

3.4.1 Sample preparation

For ICP-MS, the ground sample has to be digested into 3 replicates of liquid as follows:

3.4.1.1 Reagents used:

- 8ml of 70% high-purity nitric acid (HNO_3)
- 2ml of 30% hydrogen peroxide

0.250 g of the powder sample was accurately weighed and transferred into the digestion vessels. The reagents were then added slowly into the digestion vessels and rinsed so that they get to the bottom of the vessel. The mixture was gently swirled and allowed to set for approximately 10 minutes and the vessels were then sealed and tightly closed. The vessels were then taken to the PerkinElmer Titan MPS system for digestion. The sample digestion took about 30-45 minutes, after digestion, the vessels were allowed to cool enough before being touched to avoid sample loss and forming. After cooling, the sample was then transferred into the sample tube and finally taken to ICP-MS and LIBS for analysis.

Figure 3.4.1, figure 3.4.2 and figure 3.4.3 are the maize samples in different for forms as mentioned previously.

Figure 3.4.1: Solid samples

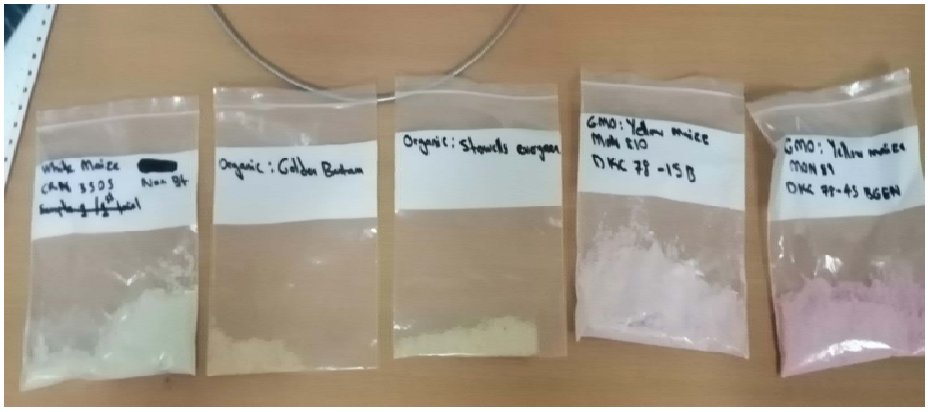

Figure 3.4.2: Powder samples

Figure 3.4.3: Liquid samples

CHAPTER 4: RESULTS AND DISCUSSIONS

This chapter describes the results of LIBS and ICP-MS analysis of GMO and organic seeds. It is divided into results for organic seeds, results for GMO seed then discussions and conclusions.

There are seventeen elements in an organic corn, which can be categorized into four groups, elements from air and water, elements from fertilizer and manure, secondary elements and less frequently applied elements (elements that are not often used in fertilizers). In this research, it is believed that manipulating the concentration of elements plays a major role in the alteration of the genetic makeup of the corn. The table 4.1 shows 4 categories in which elements are grouped as they are expected to appear on the identified results.

In this section, equations (1), (2) and (3) were used to calculate mean, standard deviation and standard error.

For mean: $\bar{X} = \frac{Sum\ of\ concentrations}{Number\ of\ concentrations}$ Equation (1)

where $\bar{x}$ is mean

For standard deviation: $\sigma = \sqrt{\frac{\sum(x_i - \bar{x})^2}{N-1}}$ Equation (2)

where: $N = number\ of\ elements$, $\bar{x} = mean\ value, x_i = value\ of\ a\ single\ element$ and $\sigma = standard\ deviation$

For standard error: $SE = \frac{\sigma}{\sqrt{n}}$ Equation (3)

Table 4.1: All elements found in organic (natural) grain of corn.

From air and water	From fertilizer and manure	Secondary elements	Less frequently applied elements
Carbon	Nitrogen	Sulphur	Chlorine (Cl)
Hydrogen	Phosphorus	Calcium	Iron (Fe)
Oxygen	Potassium	Magnesium	Manganese (Mn)
			Zinc (Zn)
			Copper (Cu)
			Boron (B)
			Silicon (Si)
			Aluminium (Al)

4.1 Organic samples

Identified elements and their concentration means and illustrated in figure 4.1a and 4.1b. Figure 4.1a is the plot of concentration means of different elements including their error bars. it shows how much nitrogen was present as compared to other elements. The amount of nitrogen scales was too high that other elements are barely visible on the graph. This high amount of nitrogen does not agree with the standard NPK ratio, which is approximately 2:1:2 (Farahani et al., 2017). Figure 4.1b shows the identified elements plotted without nitrogen. In this graph we can clearly see that potassium (K) and phosphorus (P) does not agree with the standard ratio and it also indicate clearly how other element's concentrations differed. In this case, and regardless of the mean concentration, the degree of uncertainty (error) was very small, this indicates the elemental consistence in all three trials. In this case, two elements, hydrogen and oxygen were not measured. The two elements that were not measured, are indicated on table 4.1 as elements from air and water, which makes sense in this case since the experiment takes place in the absence of water. All three expected elements under fertilizer and manure (nitrogen, potassium and phosphorus) were measured with nitrogen having a very high concentration as compared to all other elements detected. Calcium (Ca), sulphur (S) and magnesium (Mg) were all detected from the category of secondary elements.

Lastly, all elements from the less frequently applied elements were detected.

The earth's atmosphere is 78% nitrogen (N) and can also be found in water and air (Aczel, 2019). In this case, the higher level of nitrogen (N) indicates that a nitrogen rich compost or manure was used, which is the primary source of nutrients in organic plants. Furthermore, a high level of nitrogen (N) can be toxic to the soil and the plants themselves, the plants will have a dark green colour and a stunted growth (Osorio et al., 2016). There is no limited amount of nitrogen (N) in plants and soil since the concentration is often adjusted depending on the amount of nitrogen needed on that particular plant. Calcium (Ca), iron (Fe), aluminium (Al), manganese (Mn), zinc (Zn), copper (Cu) and boron (B) have very low concentration. Ca^{+2} uptake is inhibited by a high content of K^{+}, which affects the membrane integrity and plant's growth. Fe^{+2} deficiency affects the absorption of Mn, Cu and Zn and delays the plant's growth.

4.1.1 ICP-MS data: Golden bantam

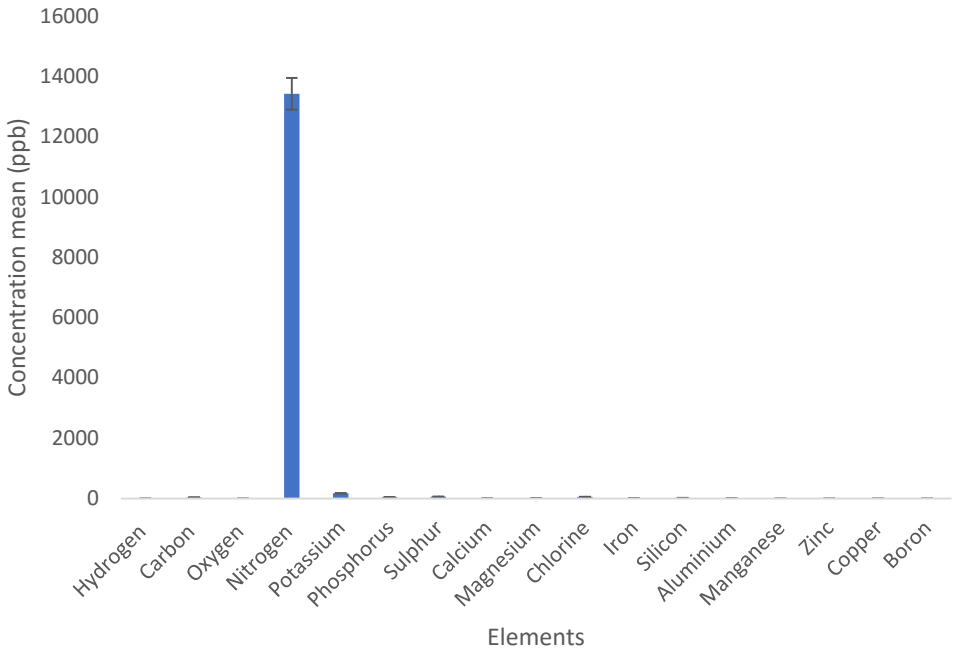

Figure 4.1a: The graph of concentration means with nitrogen.

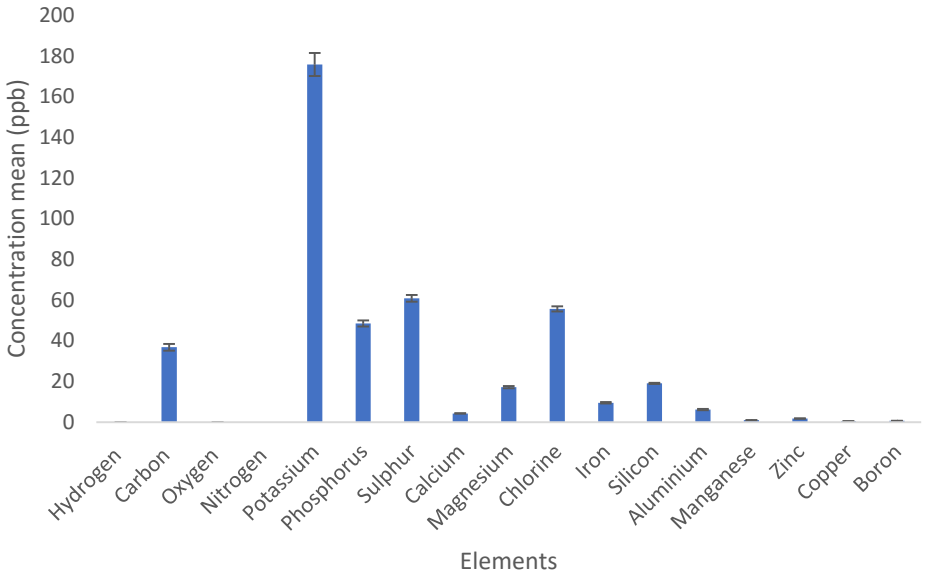

Figure 4.1b: The plot of detected concentration means without nitrogen.

4.1.2 LIBS data: Golden bantam

The software used to identify the elements (SPECLINE version 2.1, supplied by PLASUS) can identify more than 100 elements in one peak. In this case, only the element with higher wavelength (between 200 and 900) were selected per peak.

In the figures below (figure 4.3, 4.3 and 4.4) and tables (table 4, 5 and 6), only 5 elements were plotted in which oxygen was the only element from air and water category that was detected in all three trials. From the fertilizer and manure category, only potassium was detected but in very small quantity. No element was detected from the secondary elements. From the less frequently applied elements category, we had iron (Fe), manganese (Mn) and copper (Cu) of which Fe and Mn appeared to be the dominant elements. Since iron (Fe) was the dominant detected element with higher activity identified at more than one peak, this indicated that the type of soil is laterite soil. Laterite soil is a red-like type of soil rich in iron oxide, this type of soil is found in the coastal areas of KwaZulu Natal and Pretoria (Sithole et al., 2017).

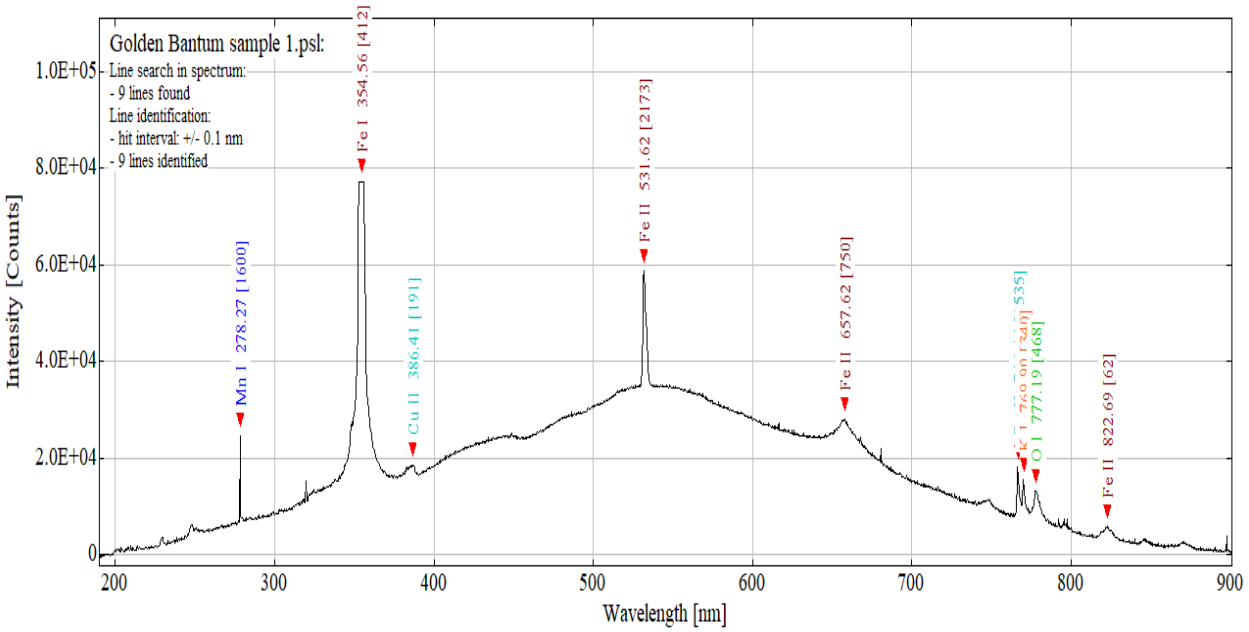

Figure 4.2: Emission spectra of sample Golden Bantam 1st trial.

Table 2.2: Golden Bantam 1st trial peak information.

Peak	Element	Wave length (nm)	Intensity	Energy Lower -upper	Transition Lower-upper	Quantum numbers
1	Mn I	278.27	1600	2.11 - 6.57	5D)4s a6D - 7S) s4f w6F	4½ - 5½
2	Fe I	354.56	412	6.35 - 2.85	6D)4d e7F - 5D) sp z7F	4 - 4
3	Cu II	386.42	191	14.96 - 18.17	5p ^{3}F - 6d ^{3}F	3 - 3
4	Fe II	531.62	2173	10.42 - 12.75	5D)4d e6G - 4)4f ^{2}2[6]]	6½ - 6½
5	Fe II	657.61	750	13.00 - 11.11	5D)5d 6D - 4P) sp 6P	2½ - 1½
6	Cu II	766.47	1535	14.96 - 16.58	5p ^{3}F - 6s ^{3}D	3 - 2
7	K I	769.90	340	0.00 - 1.61	4s ^{2}S - 4p ^{2}P°	½ - ½
8	O I	777.19	468	9.15 - 10.74	3s 5S° - 3p 5P	2 - 3
9	Fe II	822.69	62	9.94 - 11.45	5D)5s e4D - 4G) sp v4F	1½ - 2½

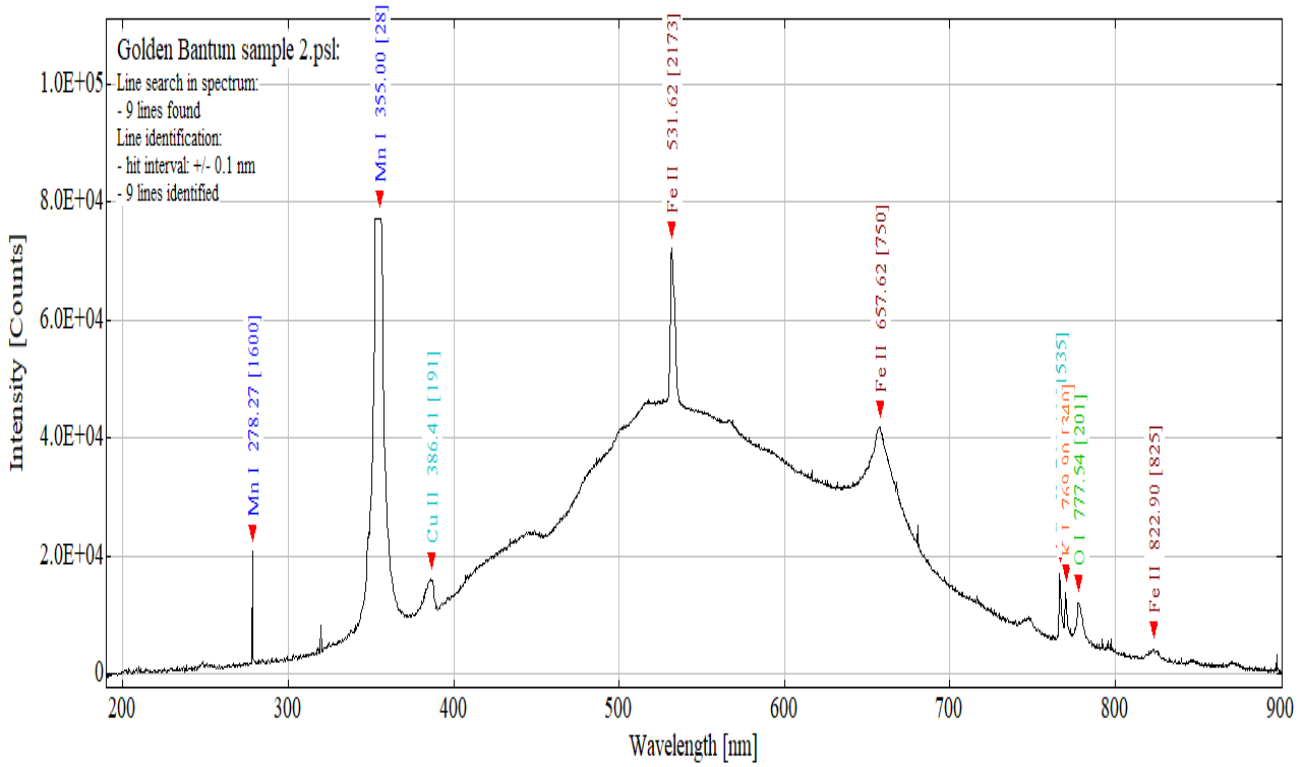

Figure 4.3: Emission spectra of sample Golden Bantam 2nd trial.

Table 4.3: Golden Bantam 2nd trial peak information.

Peak	Element	Wave length (nm)	Intensity	Energy Lower -upper	Transition Lower-upper	Quantum numbers
1	Mn I	278.27	1600	2.11 - 6.57	5D)4s a6D - 7S) s4f w6F	4½ - 5½
2	Mn I	354.10	28	4.26 - 7.75	3H)4s a4H - 3G)4p v4F	4½ - 3½
3	Cu II	386.41	191	14.96 - 18.17	5p ^{3}F - 6d ^{3}F	3 - 3
4	Fe II	531.62	2173	10.42 - 12.75	5D)4d e6G - 4)4f ^{2}2[6]]	6½ - 6½
5	Fe II	657.62	750	13.00 - 11.11	5D)5d 6D - 4P) sp 6P	2½ - 1½
6	Cu II	766.47	1535	14.96 - 16.58	5p ^{3}F - 6s ^{3}D	3 - 2
7	K I	769.90	340	0.00 - 1.61	4s ^{2}S - 4p ^{2}P°	½ - ½
8	O I	777.19	201	9.15 - 10.74	3s 5S° - 3p 5P	2 - 1
9	Fe II	822.69	825	9.70 - 11.21	5D)5s e6D - 5G) 5p 4F	3½ - 4½

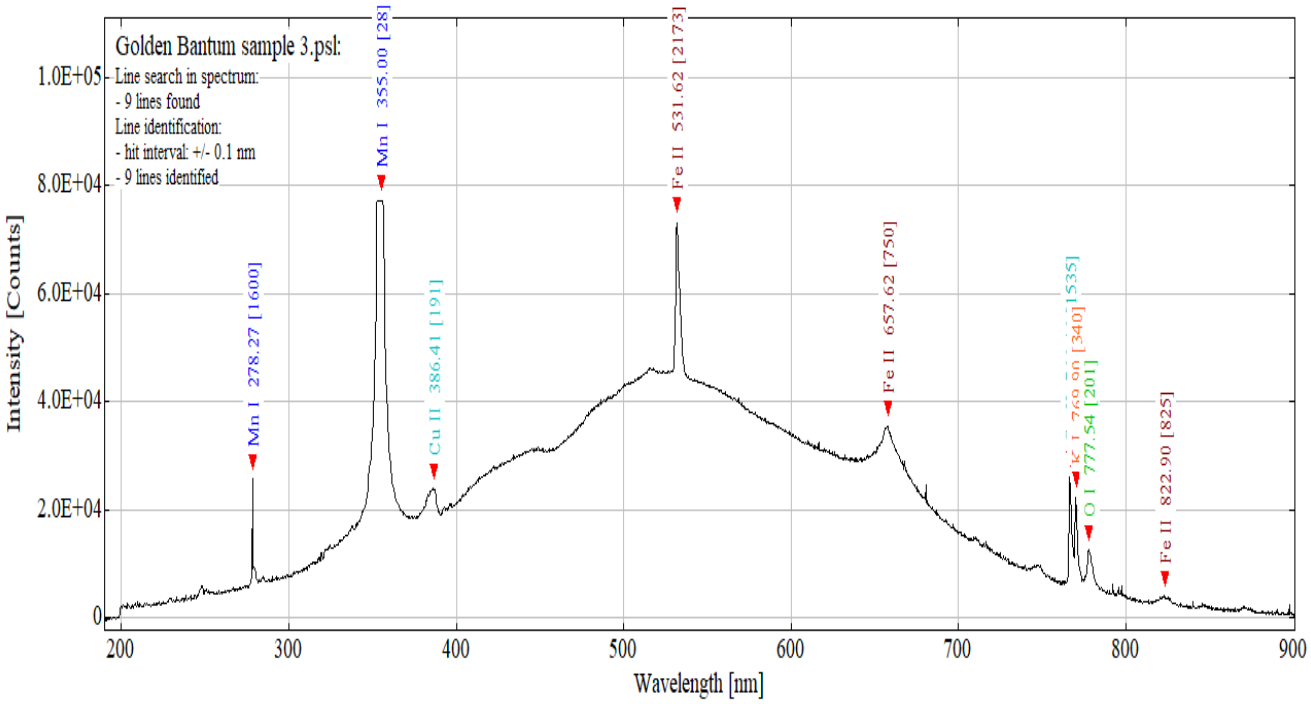

Figure 4.4: Emission spectra of sample Golden Bantam 3rd trial.

Table 4.4: Golden Bantam 3rd trial peak information.

Peak	Element	Wave length (nm)	Intensity	Energy Lower -upper	Transition Lower-upper	Quantum numbers
1	Mn I	278.27	1600	2.11 - 6.57	5D)4s a6D - 7S) s4f w6F	4½ - 5½
2	Mn I	354.90	28	4.26 - 7.75	3H)4s a4H - 3G)4p v4F	4½ - 3½
3	Cu II	386.41	191	14.96 - 18.17	5p ^{3}F - 6d ^{3}F	3 - 3
4	Fe II	531.62	2173	10.42 - 12.75	5D)4d e6G - 4)4f ^{2}2[6]]	6½ - 6½
5	Fe II	657.62	750	13.00 - 11.11	5D)5d 6D - 4P) sp 6P	2½ - 1½
6	Cu II	766.47	1535	14.96 - 16.58	5p ^{3}F - 6s ^{3}D	3 - 2
7	K I	769.90	340	0.00 - 1.61	4s ^{2}S - 4p ^{2}P°	½ - ½
8	O I	777.19	201	9.15 - 10.74	3s 5S° - 3p 5P	2 - 1
9	Fe II	822.69	825	9.70 - 11.21	5D)5s e6D - 5G) 5p 4F	3½ - 4½

4.1.3 Statistical analysis

There was a higher degree of error measured in O I than others due to the fact the measured intensity was slightly higher in the first trial and zero error was observed in those elements that were equally measured in all trial runs as indicated by figure 4.5.

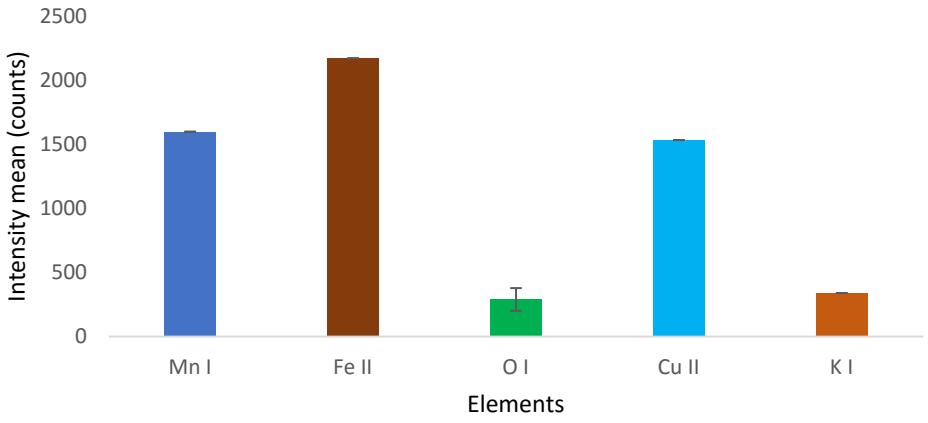

Figure 4.5: The graph of intensity means with standard errors.

4.1.4 ICP-MS data: Stowells evergreen

Figure 4.6a is the graph of elements that were averaged from all three trials. This graph was plotted just to indicate how the concentration of nitrogen overshadows other elements. It displays all expected elements that were previously categorized under table 4.1. In Figure 4.6b, the elements were plotted without nitrogen to show that these elements were not as little as they appeared in Figure 4.6b. In this plot, potassium was the one that had a higher concentration. The ratio between potassium and phosphorus is approximately 1:4, which is common in other fertilizers, it shows that even elements with a lower concentration mean can have a higher error, which is indicated on chlorine. Potassium had the highest mean concentration but its error was even smaller than that of sulphur. From the category of elements from air and water, only carbon was measured. Furthermore, all elements were measured from the category of fertilizer and manure, nitrogen with the highest concentration as compared to all other measured elements in the sample. A high concentration of nitrogen was basically due to atmospheric nitrogen and nitric acid (HNO_3) used as a reagent for sample digestion known as background signals (Wilschefski and Baxter, 2019).

All three elements from the secondary macronutrients were measured and detected in small quantity as they were supposed to be (Shergill-Bonner, 2017). The importance of these secondary macronutrients has been explained under section 4.1. In the category of less frequently applied elements, all eight elements were measured with Al, Mn, Zn Cu and B having extremely lower concentrations. The significance of these less frequently applied micronutrients was equal to those of macronutrients (N, P and K) but in small amount (Dhaliwal et al., 2019). Shortage of these less frequently applied micronutrients can always be supplemented by the NPK fertilizer, manure or organic compost, depending on the nutrient deficiency in soil or the farmers' desired traits.

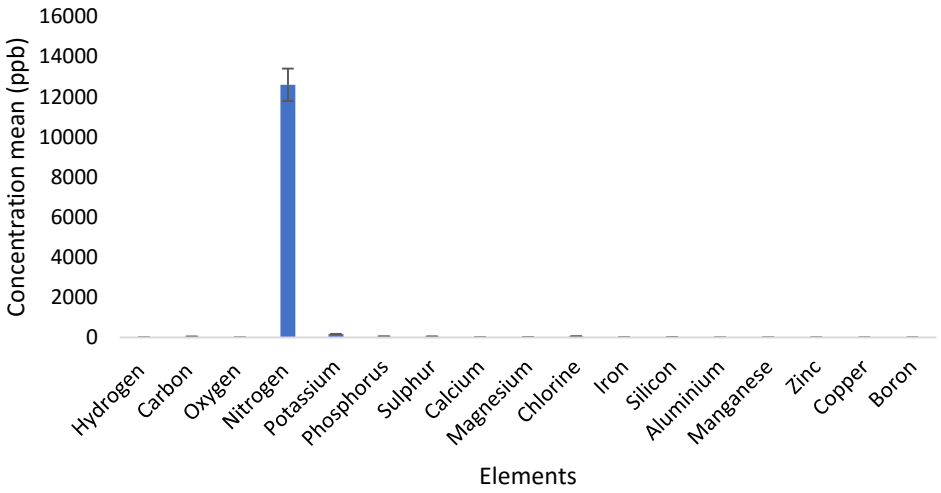

Figure 4.6a: The plot of mean concentration with nitrogen.

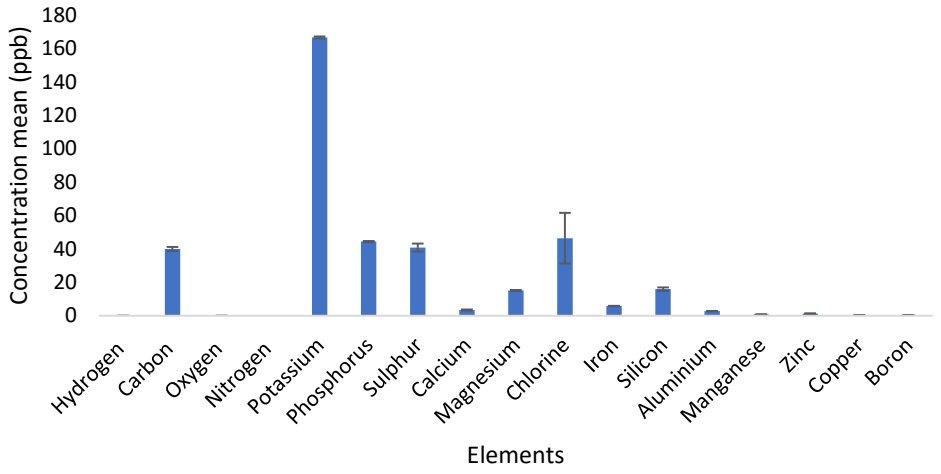

Figure 4.6b: The plot of mean concentration without nitrogen.

4.1.5 LIBS data: Stowells ever-green.

In figures below (Figure 4.7, 4.8 and 4.9) and tables (table 4.5, 4.6 and 3.7), the sample was run into three trials in order to get precise and accurate results. 9 elements were detected from the first trial, 11 elements from the second trial and 10 elements from the third trial. In all trials, it was evident that Fe and Mn were the dominant elements. This technique is different from the ICP-MS due to the fact that LIBS detected the excited elements. In this case, Fe was excited first and more rapidly as compared to the other elements. Only potassium from the category of manure and fertilizer was detected, from air and water, high intensity of oxygen was observed more than magnesium. Oxygen plays a major role in respiration and photosynthesis (Shi et al., 2012). None of the secondary elements was identified. Finally, we have Fe, Mn and Cu from the less frequently applied elements. Iron, being dominant, can only mean that corn was supplemented with Fe since it plays a key role or it is due to its geographical location as previously mentioned. In this case, potassium was available in small content. Since we had 9 to 11 elements detected on this sample, it means that the plant may suffer from deficiency of those nutrient elements missing.

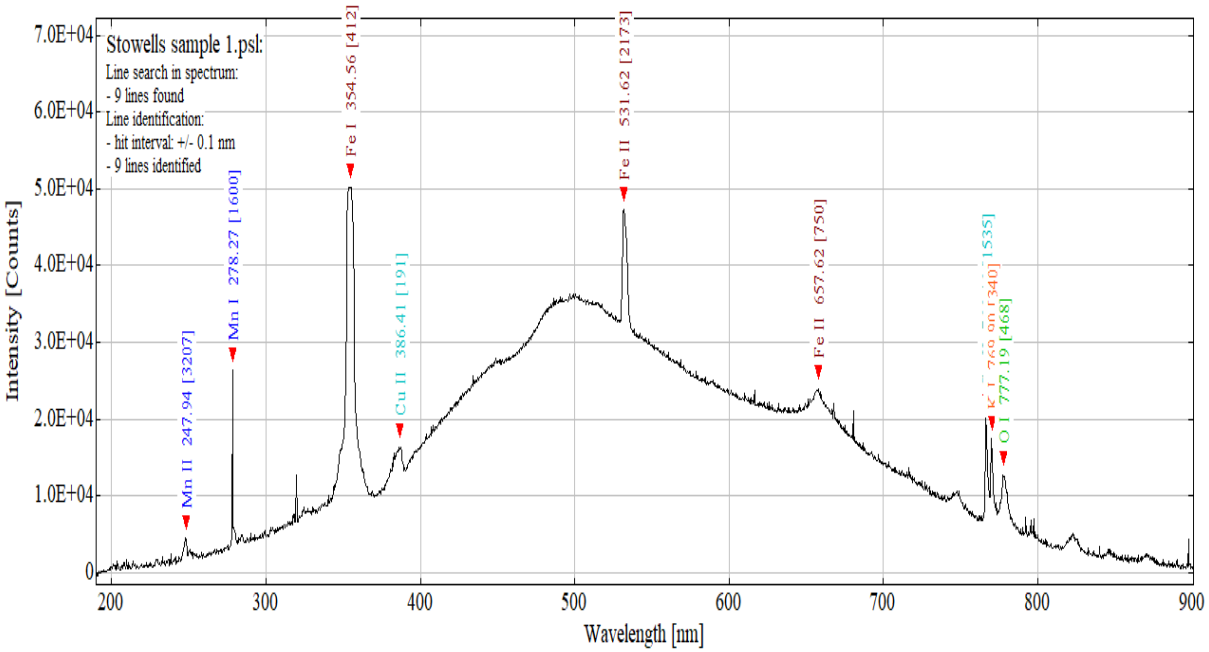

Figure 4.7: Emission spectra of sample stowells ever-green 1st trial.

Table 4.5: Stowells 1st trial peak information.

Peak	Element	Wave length (nm)	Intensity	Energy Lower -upper	Transition Lower-upper	Quantum numbers
1	Mn II	247.94	3207	13.16 – 8.16	4G)4d e5H - 4G)4p z5H	7 - 7
2	Mn I	278.27	1600	2.11 – 6.57	5D)4s a6D - 7S) s4f w6F	4½ - 5½
3	Fe I	354.56	412	6.35 – 2.85	6D)4d e7F - 5D) sp z7F	4 - 4
4	Cu II	386.43	191	14.96 – 18.17	5p ^{3}F - 6d ^{3}F	3 - 3
5	Fe II	531.62	2173	10.42 -12.75	5D)4d e6G - 4)4f ^{2}2[6]]	6½ - 6½
6	Fe II	657.63	750	13.00 - 11.11	5D)5d 6D - 4P) sp 6P	2½ - 1½
7	Cu II	766.47	1535	14.96 - 16.58	5p ^{3}F - 6s ^{3}D	3 - 2
8	Fe II	709.19	31	6.70 - 4.96	4F)4d e3G - 5D) sp x5D	4 - 3
9	K I	769.90	340	0.00 - 1.61	4s ^{2}S - 4p ^{2}P°	½ - ½
10	O I	777.19	468	9.15 - 10.74	3s 5S° - 3p 5P	2 - 3

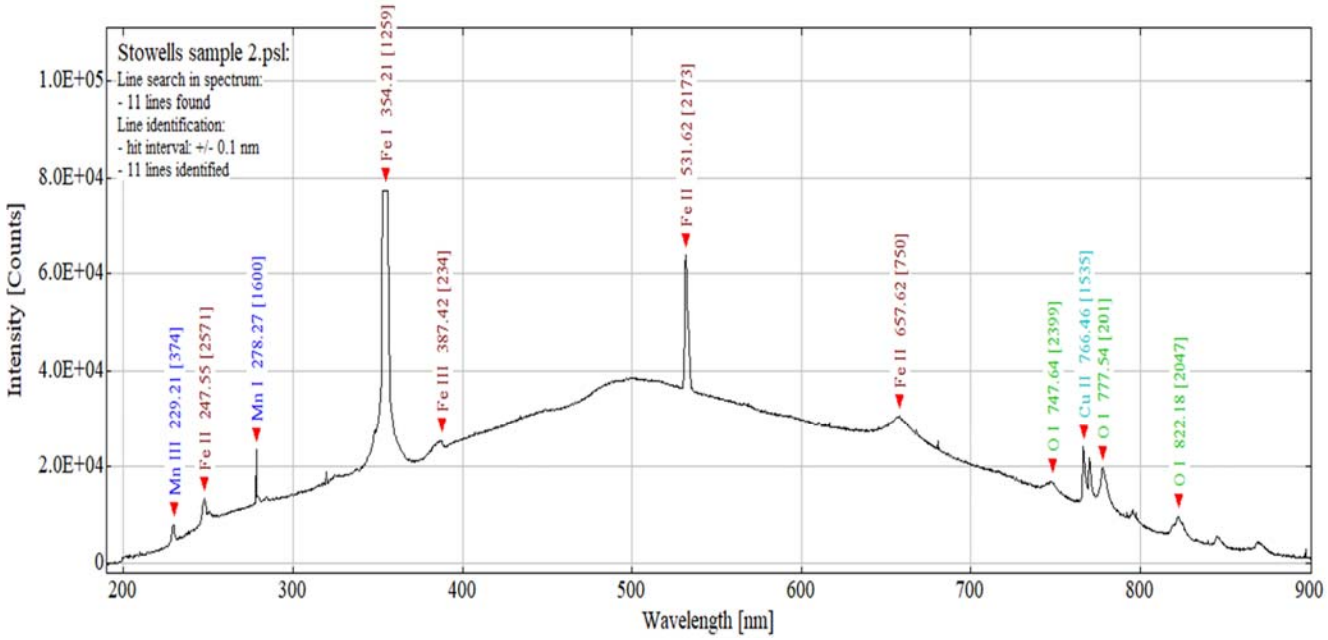

Figure 4.8: Emission spectra of sample Stowells ever-green 2nd trial.

Table 4.6: Stowells 2nd trial peak information.

Peak	Element	Wave length (nm)	Intensity	Energy Lower -upper	Transition Lower-upper	Quantum numbers
1	Mn II	229.21	374	11.74 - 17.15	3D)4s c4D - 3G)4p x4F	3½ - 4½
2	Fe II	247.55	2571	10.60 - 5.59	5D)4d e4G - 5D)4p z4F	3½ - 2½
3	Mn I	278.27	1600	2.11 – 6.57	5D)4s a6D - 7S) s4f w6F	4½ - 5½
4	Fe I	354.56	412	6.35 – 2.85	6D)4d e7F - 5D) sp z7F	4 - 4
5	Fe III	387.42	234	24.00 - 27.20	6S)5d 5D - 4F)5p 5F	4 - 5
6	Fe II	531.62	2173	10.42 -12.75	5D)4d e6G - 4)4f ^{2}2[6]]	6½ - 6½
7	Fe II	657.62	750	13.00 - 11.11	5D)5d 6D - 4P) sp 6P	2½ - 1½
8	O I	747.64	2399	14.12 - 15.78	3s" ^{3}P - 3p" ^{3}D	2 - 3
9	Cu II	766.47	1535	14.96 - 16.58	5p ^{3}F - 6s ^{3}D	3 - 2
10	O I	777.19	468	9.15 - 10.74	3s 5S° - 3p 5P	2 - 3
11	O I	822.18	2047	12.54 - 14.05	3s' ^{3}D - 3p' ^{3}D	3 -3

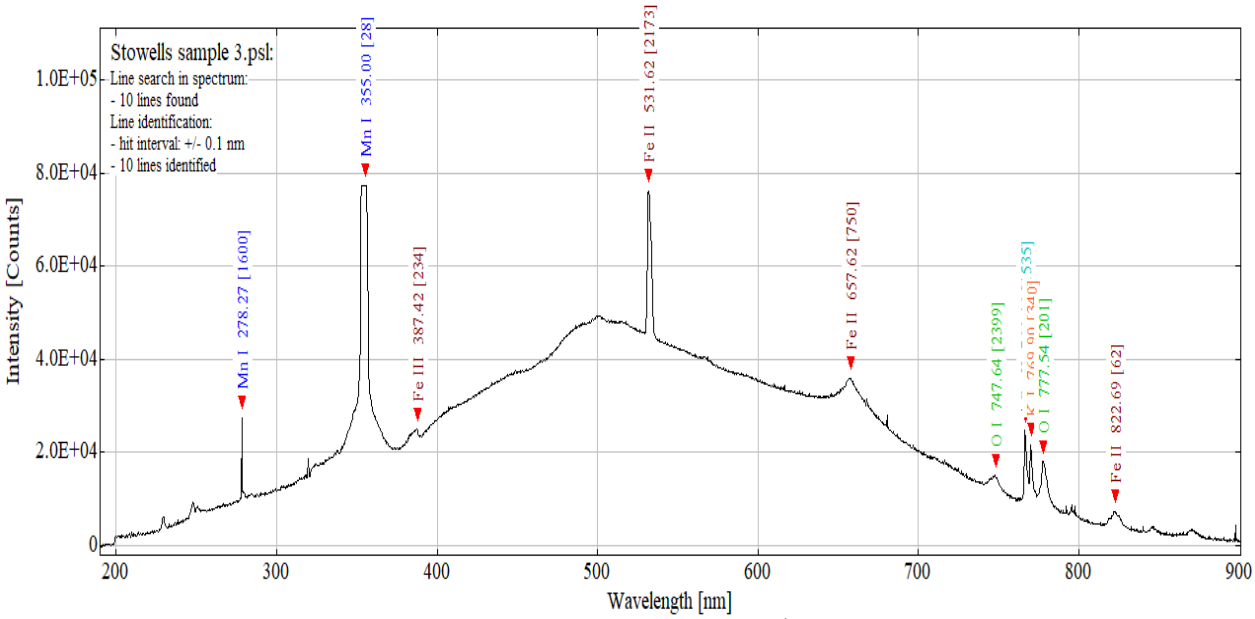

Figure 4.9: Emission spectra of sample Stowells ever-green 3rd trial.

Table 4.7: Stowells 3rd trial peak information.

Peak	Element	Wave length (nm)	Intensity	Energy Lower -upper	Transition Lower-upper	Quantum numbers
1	Mn I	278.27	1600	2.11 - 6.57	5D)4s a6D -7S) s4f w6F	4½ - 5½
2	Mn I	354.10	28	4.26 - 7.75	3H)4s a4H - 3G)4p v4F	4½ - 3½
3	Fe III	387.42	234	24.00 - 27.20	6S)5d 5D - 4F)5p 5F	4 - 5
4	Fe II	531.62	2173	10.42 -12.75	5D)4d e6G - 4)4f ²2[6]]	6½ - 6½
5	Fe II	657.62	750	13.00 - 11.11	5D)5d 6D - 4P) sp 6P	2½ - 1½
6	O I	747.64	2399	14.12 - 15.78	3s" ³P - 3p" ³D	2 - 3
7	Cu II	766.47	1535	14.96 - 16.58	5p ³F - 6s ³D	3 - 2
8	K I	769.90	340	0.00 - 1.61	4s ²S - 4p ²P°	½ - ½
9	O I	777.19	468	9.15 - 10.74	3s 5S° - 3p 5P	2 - 3
10	Fe II	822.69	62	9.94 - 11.45	5D)5s e4D - 4G) sp v4F	1½ - 2½

4.1.6 Statistical analysis

Figure 4.10 shows that there was a huge uncertainty or error for Mn II, O I, Fe I and K I. This was due to inconsistence of the instrument since some elements were not detected or detected at very small amount for some trials.

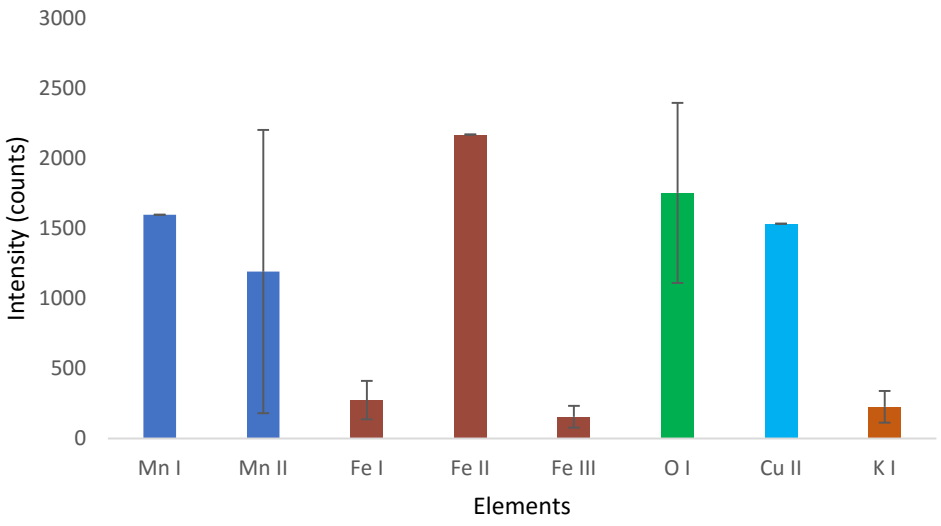

Figure 4.10: The plot of intensity means of different elements.

4.2 Genetically modified samples

In Figure 4.11, the concentration of nitrogen was too high that other elements were barely appearing on the graph, which is why Figure 4.11b was plotted. Plotting the average concentration without nitrogen helped us study the concentration ratios between other elements and it also showed that those elements were not as closer to zero as they appeared in the presence of nitrogen. In figure 4.11b, it is clear that not all elements with higher concentration had a huge error as compared to those plotted in the presence of nitrogen. This is an indication of inconsistence of the instrument since same samples were measured in three replicates. Two elements that were not measured are indicated under table 4.1 as elements from air and water, which makes sense in this case, since the experiment took place in the absence of water. Secondly, these three elements (H.C and O) are found in fertilizers.

For the secondary elements, we had sulphur with the higher concentration followed by magnesium. Both these secondary elements are essential in plants but in small amounts as indicated by the results, the deficiency of these elements may result into plant's health problems. There were a bit higher level of chlorine and iron from the last category of the less applied elements. The indicated amount was barely enough for plants since less than 5000 ppb is required in plants (Nibali, 2005). Lastly, 4 elements were present in very small amount like Mn, Cu, Al, and Zn, which plays a major role in plant's defence mechanism like the production of phenolic compounds by manganese and zinc. These elements helps in the plant's ability to trigger defence mechanism through its accumulation in the plant which is toxic to pests (Cabot et al., 2019). This agrees with the earlier mentioned statement that CRN 3505 is a dual trait version of *Bacillus thuringiensis* that combines two transgenes Cry1A.105 and Cry2Ab, which are responsible for toxin-production, this process is known as pyramiding, which is a way of replacing a single ineffectual transgene. This results in high yield and drought tolerance.

4.2.1 ICP-MS data: CRN 3505

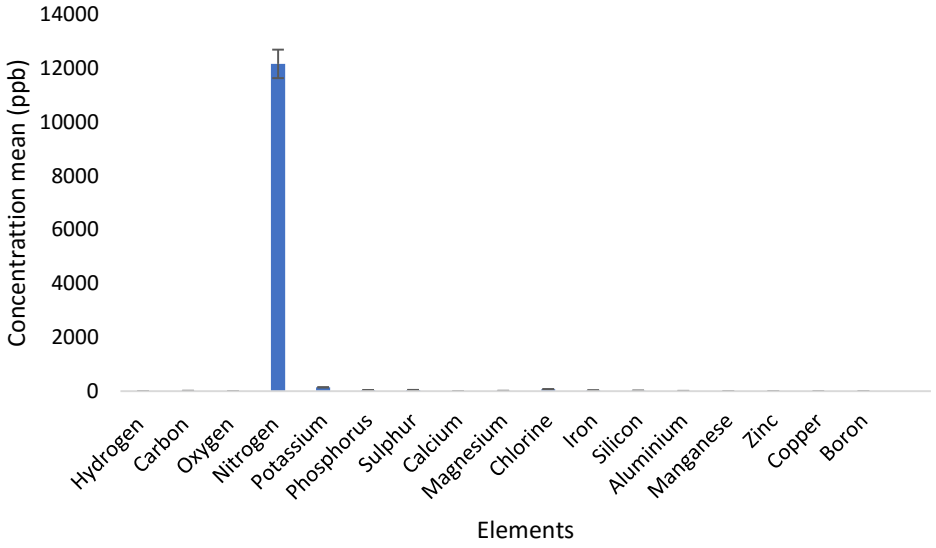

Figure 4.11a: The plot of concentration means with nitrogen.

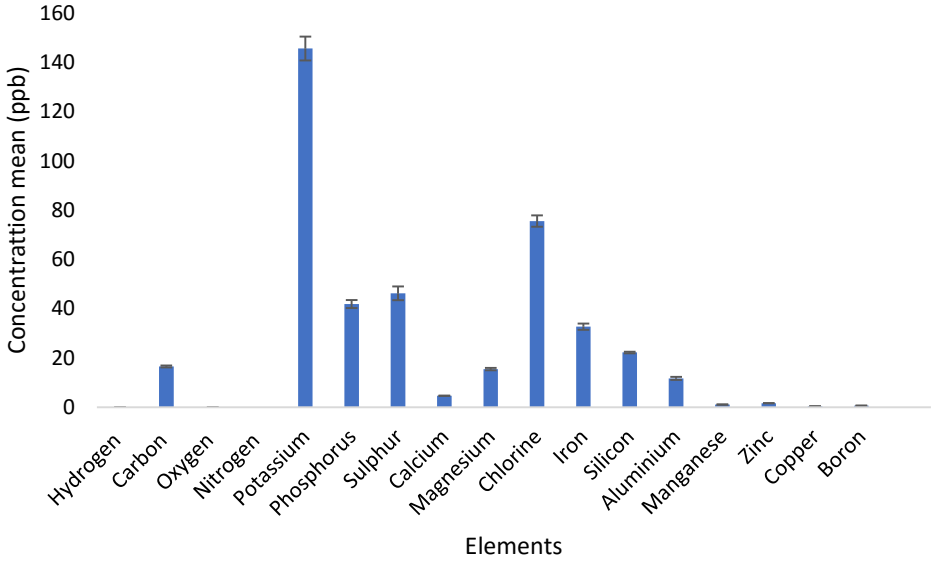

Figure 4.11b: The plot of concentration means without nitrogen.

4.2.2 LIBS data: CRN 3505

In figures (figure 4.12, 4.13 and 4.14) and tables (table 4.9, 4.10 and 4.11) below, only 7 elements were plotted in which oxygen and carbon were the only elements from the air and water category but carbon was not observed from the first trial, which is why it is important to run three trials. From the fertilizer and manure category, we had, nitrogen and potassium but in small quantities. Thirdly, a small quantity of calcium was detected from the secondary elements. Calcium deficiency is normally triggered if magnesium or potassium level is too high. From the less frequently applied elements category, we had iron (Fe) and manganese (Mn), which were appearing to be the dominant elements. The deficiency of any of these two elements is often mistaken for one another, like stunt and inhibition of plants growth. In terms of the plant's specific features, manganese and copper played the key role.

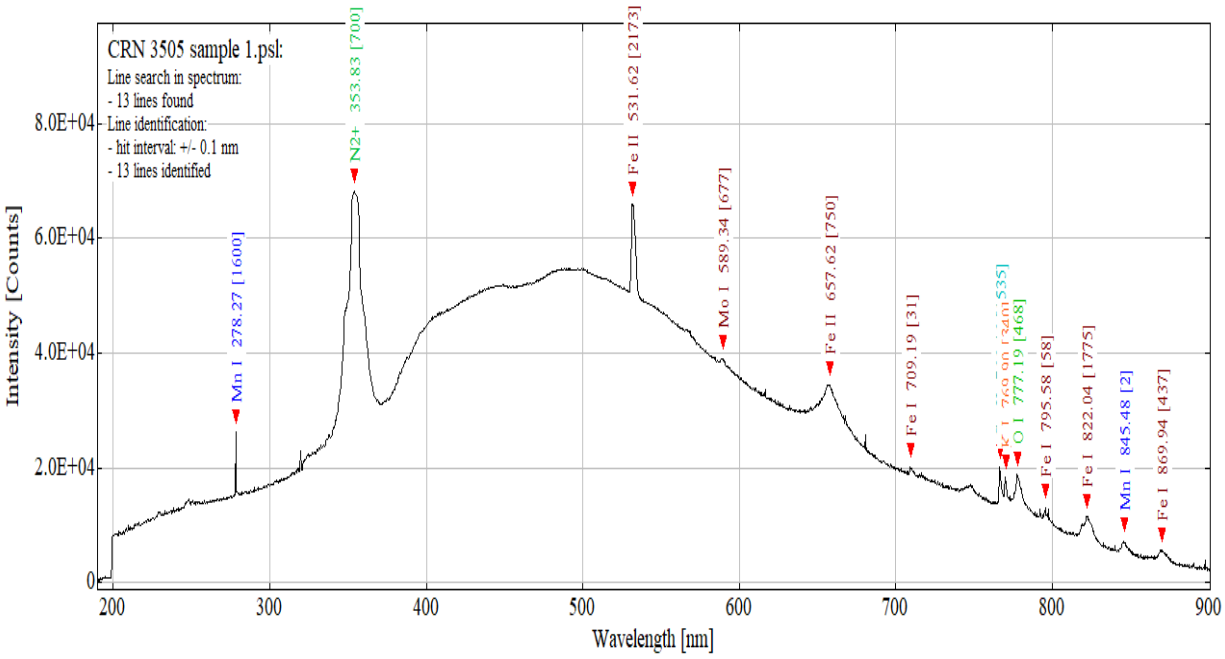

Figure 4.12: Emission spectra of sample CRN 3505 1st trial.

Table 4.8: CRN 3505 1st trial peak information.

Peak	Element	Wave length	Intensity	Energy Lower -upper	Transition Lower-upper	Quantum numbers
1	Mn I	278.27	1600	2.11 - 6.57	5D)4s a6D -7S) s4f w6F	4½ - 5½
2	N2+	353.83	700	0 - 3.16	X²Sig+u - B²Sig+u	3 - 4
3	Fe II	531.62	2173	10.42 -12.75	5D)4d e6G - 4)4f ²2[6]]	6½ - 6½
4	N II	589.2	2042	26.26 - 28.37	3s' ³P - 7f ²[3½]	2 - 3
5	Fe II	657.62	750	13.00 - 11.11	5D)5d 6D - 4P) sp 6P	2½ - 1½
6	Fe II	709.19	31	6.70 - 4.96	4F)4d e3G - 5D) sp x5D	4 - 3
7	Cu II	766.47	1535	14.96 - 16.58	5p ³F - 6s ³D	3 - 2
8	K I	769.90	340	- 1.61	4s ²S - 4p ²P°	½ - ½
9	O I	777.19	468	9.15 - 10.74	3s 5S° - 3p 5P	2 - 3
10	Fe I	795.58	58	6.59 - 5.03	4F)4d f5P - 5D) sp x5F	3 - 4
11	Fe I	822.04	1775	5.83 - 4.32	4F)5s e5F - 4F)4p z5G	5 - 6
12	Mn I	845.48	2	7.00 - 8.47	e4D - 4F) sp 4F	3½ - 4½
13	Fe I	869.95	437	6.38 - 4.96	6D)4d f5F - 5D) sp x5D	4 - 3

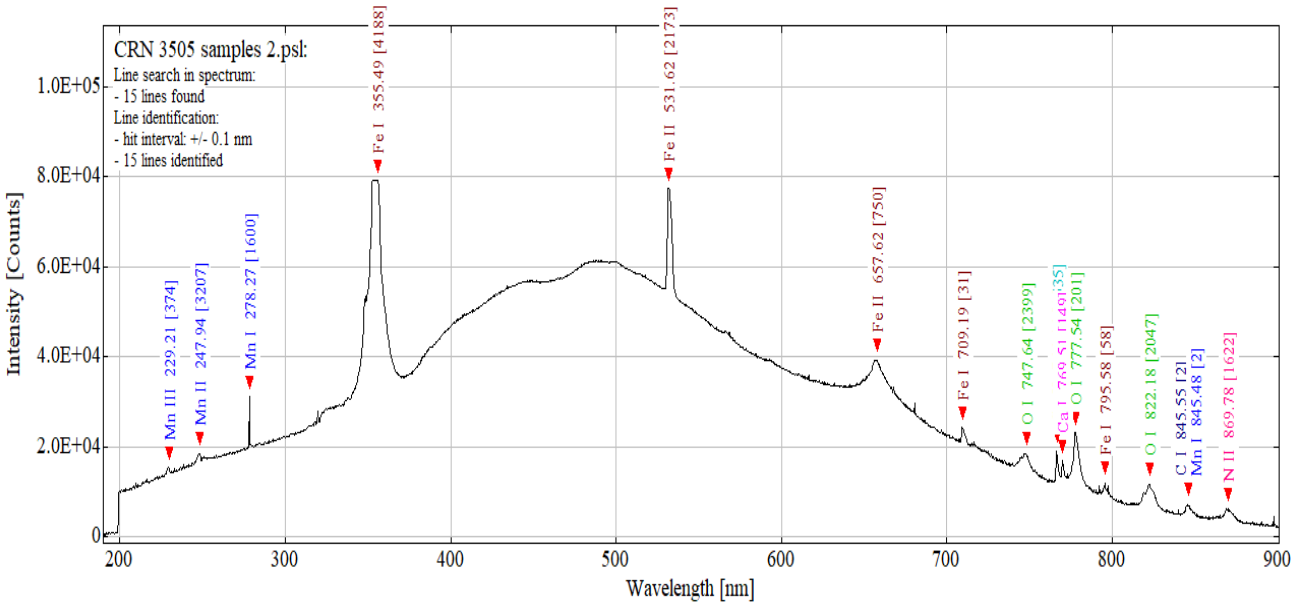

Figure 4.13: Emission spectra of sample CRN 3505 2nd trial.

Peak	Element	Wave length (nm)	Intensity	Energy Lower -upper	Transition Lower-upper	Quantum numbers
1	Mn III	229.21	374	11.74 - 17.15	3D)4s c4D - 3G)4p x4F	3½ - 4½
2	Mn II	247.94	3207	13.16 - 8.16	4G)4d e5H - 4G)4p z5H	7 - 7
3	Mn I	278.27	1600	2.11 - 6.57	5D)4s a6D -7S) s4f w6F	4½ - 5½
4	Fe I	355.49	4188	6.32 - 2.83	6D)4d e7G - 5D) sp z7F	6 - 5
5	Fe II	531.62	2173	10.42 -12.75	5D)4d e6G - 4)4f ²2[6]]	6½ - 6½
6	Fe II	657.62	750	13.00 - 11.11	5D)5d 6D - 4P) sp 6P	2½ - 1½
7	Fe II	709.19	31	6.70 - 4.96	4F)4d e3G - 5D) sp x5D	4 - 3
8	O I	747.64	2399	14.12 - 15.78	3s" ³P -3p" ³D	2 - 3
9	Cu II	766.47	1535	14.96 - 16.58	5p ³F - 6s ³D	3 - 2
10	Ca I	777.19	468	9.15 - 10.74	3s 5S° - 3p 5P	2 - 3
11	O I	777.54	201	9.15 - 10.74	3s 5S° - 3p 5P	2 - 1

12	Fe I	795.58	58	6.59 - 5.03	4F)4d f5P - 5D) sp x5F	5 - 6
13	Mn I	845.48	2	7.00 - 8.47	e4D - 4F) sp 4F	3½ - 4½
	C I	845.55	2	9.33 - 10.80	1s2p³ ³P - 6p ³P	1 - 0
14	N II	869.78	1622	26.00 - 27.43	4d ³F° - 5f' ²[3½]	3 - 4

Table 4.9: CRN 3505 2nd trial peak information.

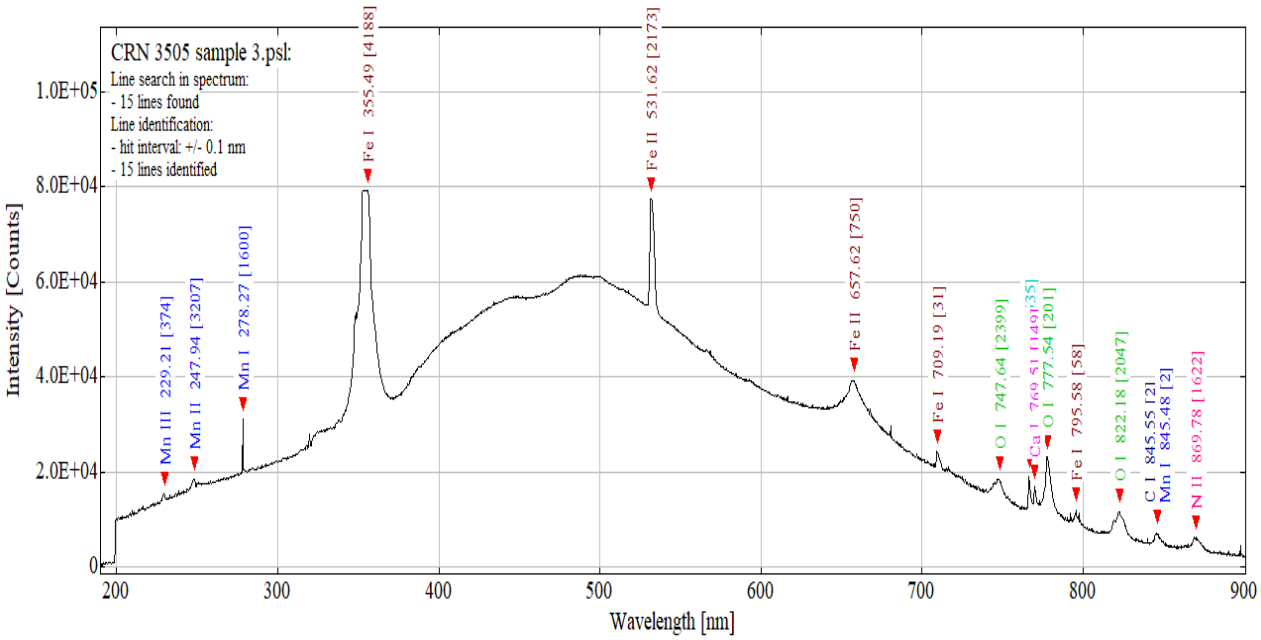

Figure 4.14: Emission spectra of sample CRN 3505 3rd trial.

Table 4.10: CRN 3505 3rd trial peak information.

Peak	Element	Wave length (nm)	Intensity	Energy Lower -upper	Transition Lower-upper	Quantum numbers
1	Mn III	229.21	374	11.74 – 17.15	3D)4s c4D – 3G)4p x4F	3½ - 4½
2	Mn II	247.94	3207	13.16 – 8.16	4G)4d e5H – 4G)4p z5H	7 – 7

3	Mn I	278.27	1600	2.11 – 6.57	5D)4s a6D -7S) s4f w6F	4½ - 5½
4	Fe I	355.49	4188	6.32 – 2.83	6D)4d e7G – 5D) sp z7F	6 – 5
5	Fe II	531.62	2173	10.42 -12.75	5D)4d e6G – 4)4f ²2[6]]	6½ - 6½
6	Fe II	657.62	750	13.00 – 11.11	5D)5d 6D – 4P) sp 6P	2½ - 1½
7	Fe II	709.19	31	6.70 – 4.96	4F)4d e3G – 5D) sp x5D	4 – 3
8	O I	747.64	2399	14.12 – 15.78	3s” ³P - 3p” ³D	2 – 3
9	Cu II	766.47	1535	14.96 – 16.58	5p ³F – 6s ³D	3 – 2
10	Ca I	777.19	468	9.15 – 10.74	3s 5S° - 3p 5P	2 – 3
11	O I	777.54	201	9.15 – 10.74	3s 5S° - 3p 5P	2 – 1
12	Fe I	795.58	58	6.59 – 5.03	4F)4d f5P – 5D) sp x5F	5 – 6
13	Mn I	845.48	2	7.00 – 8.47	e4D – 4F) sp 4F	3½ - 4½
	C I	845.55	2	9.33 – 10.80	1s2p³ ³P – 6p ³P	1 – 0
14	N II	869.78	1622	26.00 – 27.43	4d ³F° - 5f’ ²[3½]	3 – 4

4.2.3 Statistical analysis

There was high error in elements like Mn II, Fe I and O I due to the fact that there were not measured is some trials and zero error was observed in those elements that were equally measured in all trial runs as indicated in figure 4.15.

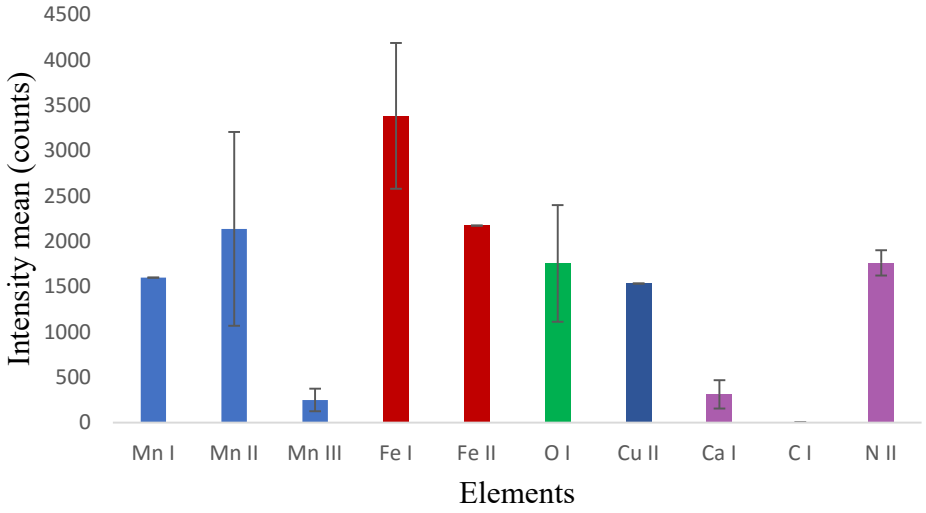

Figure 4.15: Bar-chart of mean intensity of elements found in GMO CRN3505 maize.

4.2.4 ICP-Ms data: Mon 89

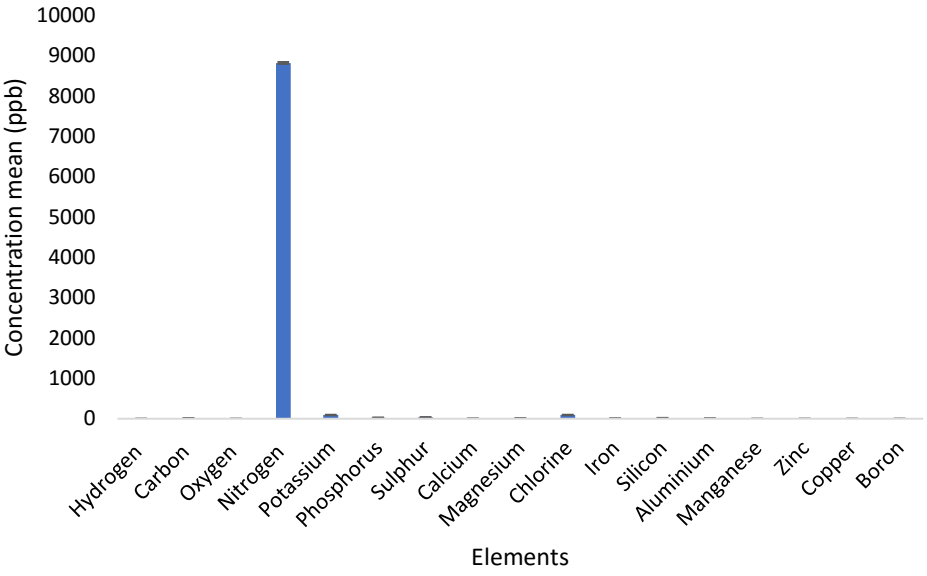

Figure 4.16a: The plot of concentration means with nitrogen.

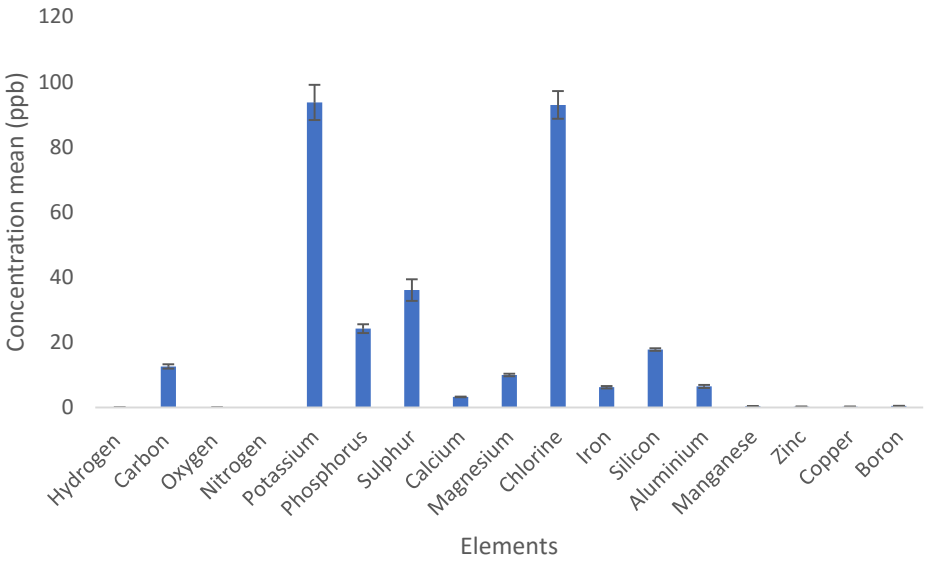

Figure 4.16b: The plot of concentration means without nitrogen.

Figures 4.16a and 4.16b illustrates that although the concentration of nitrogen had reduced by a factor of 10000 ppb but it was still very high. It was important to plot the figures with and without nitrogen in order to clearly observe how other elements has increased or decreased. In Figure 4.16b, the error was visible as compared to Figure 4.16a as one would conclude that the degree of uncertainity was zero. Figure 4.16b was very important because, for the first time, the observed concentration level of chlorine is approximately equal to potassium. These was evident that there was difference in elemental content for different samples and this marked the significance of the change in the elemental content. Like in previous samples, Figure 4.16a showed 15 expected elements and only two elements, hydrogen and oxygen are not measured. Two elements that were not measured are indicated under table 4.1 as elements from air and water, which make sense in this case since the experiment took place in the absence of water. Secondly, we had higher concentration of nitrogen, but in this case, nitrogen was not as higher as in other samples. Nitrogen is responsible for leaf growth (Kelly, 2018); Potassium is responsible for the overall plant's performance and phosphorus is responsible for the growth of roots (Yin et al., 2018b). These three elements are found in the fertilizers and manure category. For the secondary elements, we have sulphur, magnesium and chlorine. Both these secondary elements are essential in plants but in small amount as indicated by the results. In the category for less applied micronutrients, we had

Mn, Zn, Cu and B in very small amount, this was expected since these elements are required in small content.

4.2.5 LIBS data: Mon 89

Figure 4.17, 4.18 and 4.19 and table 4.11, 4.12 and 4.13 shows that Eight lines were identified in all three trials, there was only 5 elements detected with iron (Fe) being the dominant element in all trials. We had oxygen from the category of air and water, no hydrogen (H) and carbon (C) was detected. Plants need carbon and hydrogen for productive growth, the deficiency symptoms of these elements can not be determined (Behboudian et al., 2017). We had potassium from the category of manure and fertilizer, no nitrogen (N) and phosphorus (P) was detected. No elements from the category of secondary elements (Sulphor (S), alcium (Ca) and magnesium (Mg) was identified. Finally, we had Mn, Fe and Cu from the category of less frequently applied elements. The elements from the less frequently applied category were the dominant micronutrients in this case and there were supposed to be detected in small content under normal circumstances. Some elements were not identified only because of the working princles of the technique, meaning they were not neccesarily deficient.

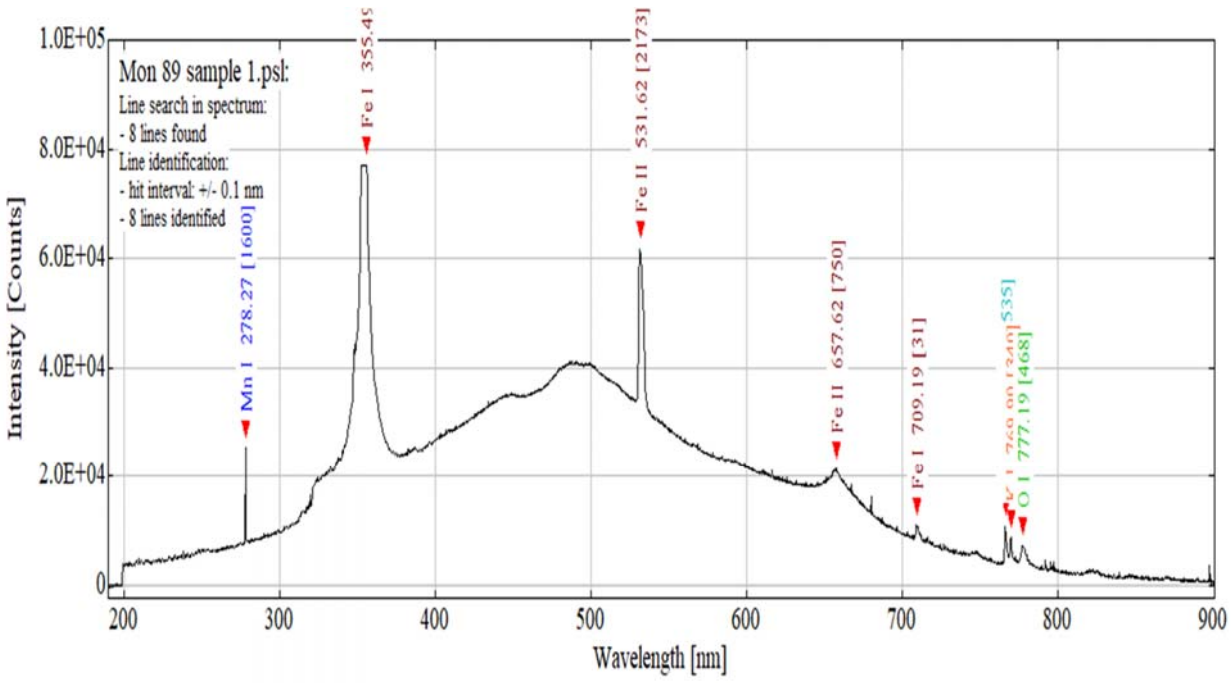

Figure 4.17: Emission spectra of sample Mon 89 1st trial.

Table 4.11: Mon 89 1st trial peak information.

Peak	Element	Wave length (nm)	Intensity	Energy Lower -upper	Transition Lower-upper	Quantum numbers
1	Mn I	278.27	1600	2.11 - 6.57	5D)4s a6D -7S) s4f w6F	4½ - 5½
2	Fe I	355.49	4188	6.32 - 2.83	6D)4d e7G - 5D) sp z7F	6 - 5
3	Fe II	531.62	2173	10.42 -12.75	5D)4d e6G - 4)4f ^{2}2[6]]	6½ - 6½
4	Fe II	657.62	750	13.00 - 11.11	5D)5d 6D - 4P) sp 6P	2½ - 1½
5	Fe I	709.19	31	6.70 - 4.96	4F)4d e3G - 5D) sp x5D	4 - 3
6	Cu II	766.47	1535	14.96 - 16.58	5p ^{3}F - 6s ^{3}D	3 - 2
7	K I	769.9-	340	0.00 - 1.61	4s ^{2}S - 4p ^{2}P°	½ - ½
8	O I	777.19	468	9.15 - 10.74	3s 5S° - 3p 5P	2 - 3

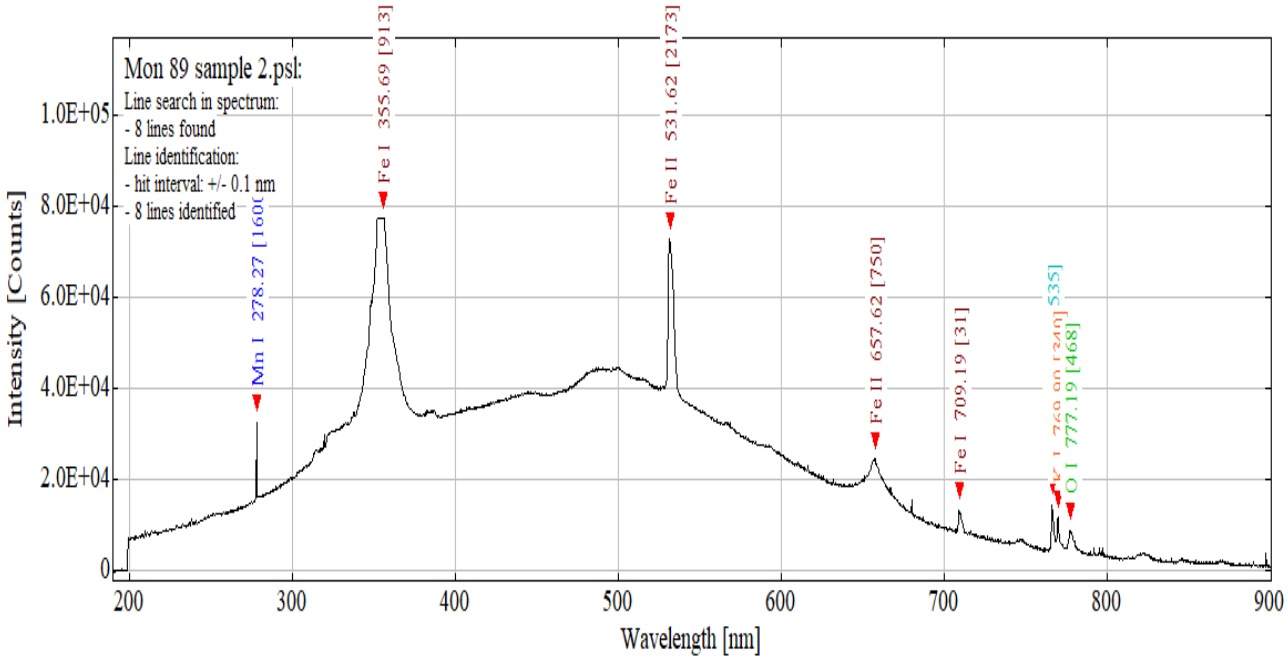

Figure 4.18: Emission spectra of sample Mon 89 2nd trial.

Table 4.12: Mon 89 2nd trial peak information.

Peak	Element	Wave length (nm)	Intensity	Energy Lower -upper	Transition Lower-upper	Quantum numbers
1	Mn I	278.27	1600	2.11 - 6.57	5D)4s a6D -7S) s4f w6F	4½ - 5½
2	Fe I	355.69	913	6.34 - 2.85	6D)4d f5F - 5D) sp z7F	5 - 4
3	Fe II	531.62	2173	10.42 -12.75	5D)4d e6G - 4)4f ²2[6]]	6½ - 6½
4	Fe II	657.62	750	13.00 - 11.11	5D)5d 6D - 4P) sp 6P	2½ - 1½
5	Fe I	709.1	31	6.70 - 4.96	4F)4d e3G - 5D) sp x5D	4 - 3
6	Cu II	766.47	1535	14.96 - 16.58	5p ³F - 6s ³D	3 - 2
7	K I	769.90	340	0.00 - 1.61	4s ²S - 4p ²P°	½ - ½
8	O I	777.19	468	9.15 - 10.74	3s 5S° - 3p 5P	2 - 3

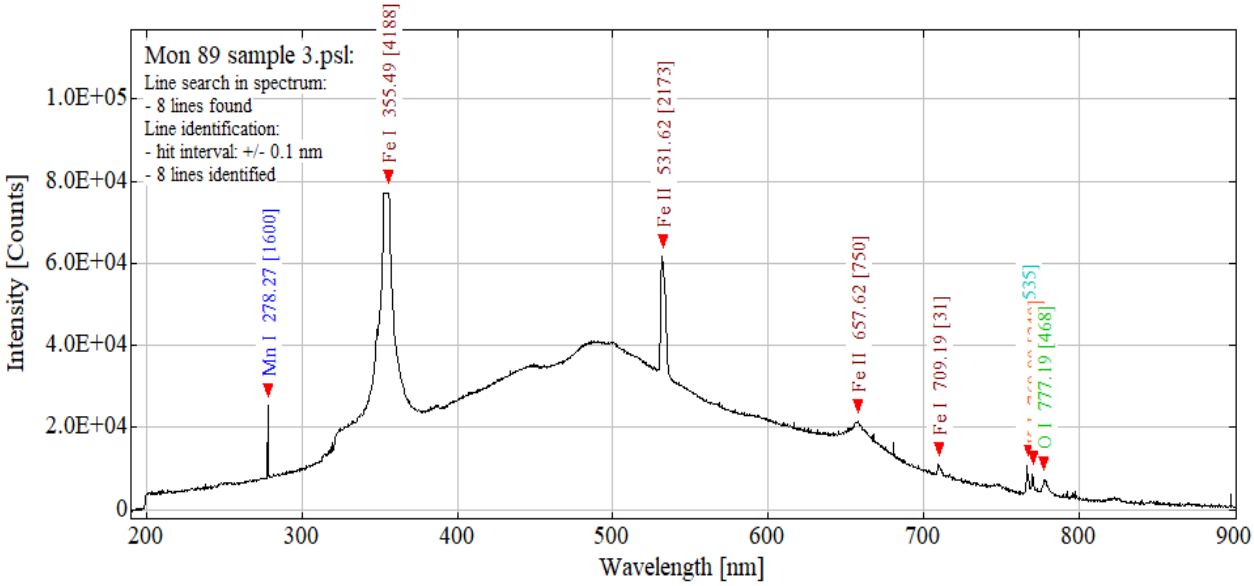

Figure 4.19: Emission spectra of sample Mon 89 3rd trial.

Table 4.13: Mon 89 3rd trial peak information.

Peak	Element	Wave length (nm)	Intensity	Energy Lower -upper	Transition Lower-upper	Quantum numbers
1	Mn I	278.27	1600	2.11 - 6.57	5D)4s a6D -7S) s4f w6F	4½ - 5½
2	Fe I	355.49	4188	6.32 - 2.83	6D)4d e7G - 5D) sp z7F	6 - 5
3	Fe II	531.62	2173	10.42 -12.75	5D)4d e6G - 4)4f ^{2}2[6]]	6½ - 6½
4	Fe II	657.62	750	13.00 - 11.11	5D)5d 6D - 4P) sp 6P	2½ - 1½
5	Fe I	709.19	31	6.70 - 4.96	4F)4d e3G - 5D) sp x5D	4 - 3
6	Cu II	766.47	1535	14.96 - 16.58	5p ^{3}F - 6s ^{3}D	3 - 2
7	K I	769.90	340	0.00 - 1.61	4s ^{2}S - 4p ^{2}P°	½ - ½
8	O I	777.19	468	9.15 - 10.74	3s 5S° - 3p 5P	2 - 3

4.2.6 Statistical analysis

In Figure 4.20, all elements had zero degree of uncertainity (error) except for Fe I, which had more error. Fe I had higher error due to the fact that it was not measured equally in all trials.

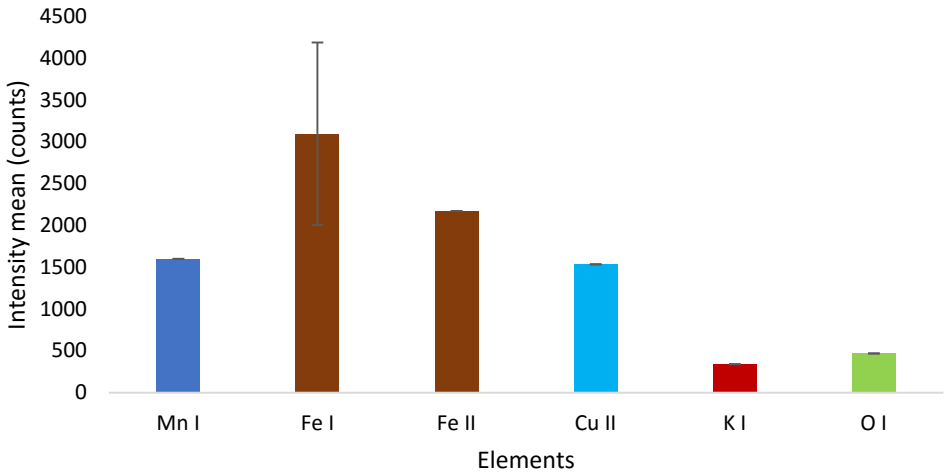

Figure 4.20: Bar-chart of mean intensity of elements found in GMO MON89 maize

4.2.7 ICP-MS data: Mon 810

In the above Figures 4.21a and 4.21b, it is shown that there was an increase in chlorine and a decrease in carbon concentration. These are very important figures, as they allowed us to trace the change in elemental content from sample to sample. In this figure, nitrogen and potassium had a larger error as compared to iron (Fe), silicon (Si), etc. Figure 4.21b shows that 15 out of 17 elements were detected. Only carbon was detected from the first category (air and water). Secondly, all elements from the second category (fertilizer and manure) were detected with nitrogen (N) having the highest concentration. We have all three elements identified from the secondary elements (S, Ca and Mg).

Finally, all elements from the less applied elements were identified but in small quantities. The concentration of nitrogen had decreased from 14000 ppb (Golden bantam) to 7500 ppb as compared to this sample samples. In this research, There was a decrease in carbon and an increase in chlorine concentration as compared to the first two organic samples (Golden Bantam and Stowells). These changes are what is believed to be the change in elemental composition since the sample is geneticall modified. nitrogen has always been too high, this can be due to the fact that nitrogen fertilizer was used on the plant or nitrogen was detected from the atmosphere. Hence, the content of available N, P and K does not agree with the standard NPK ratio (3:2:1) in fertilizers (Shiling et al.).These elements, Mn, Cu, Al, and Zn played a major role in plant's defence mechanism just like the production of phenolic compounds by manganese and zinc, with the ability to trigger defence mechanism through its accumulation in the plant, which is toxic to pests (Cabot et al., 2019).

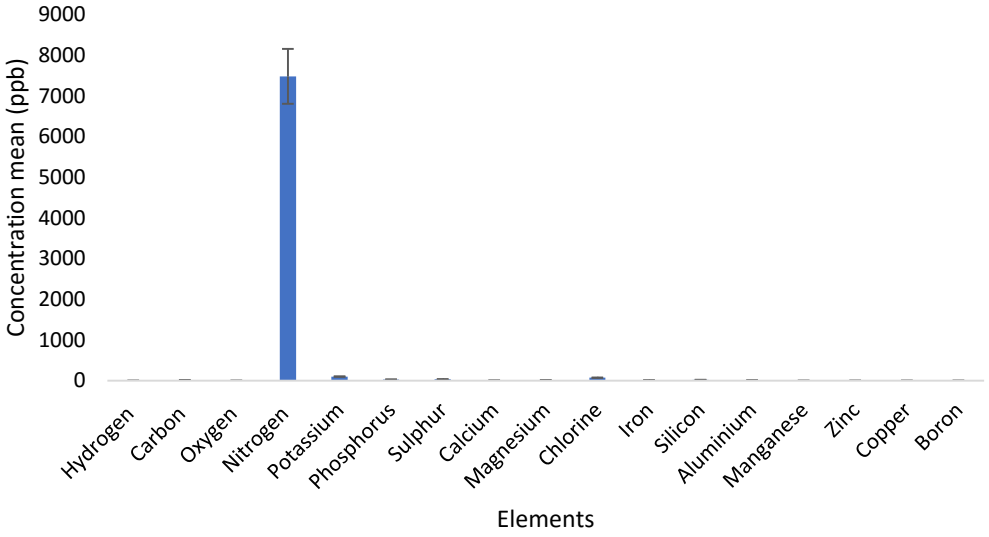

Figure 4.21a: The plot of mean concentration with nitrogen.

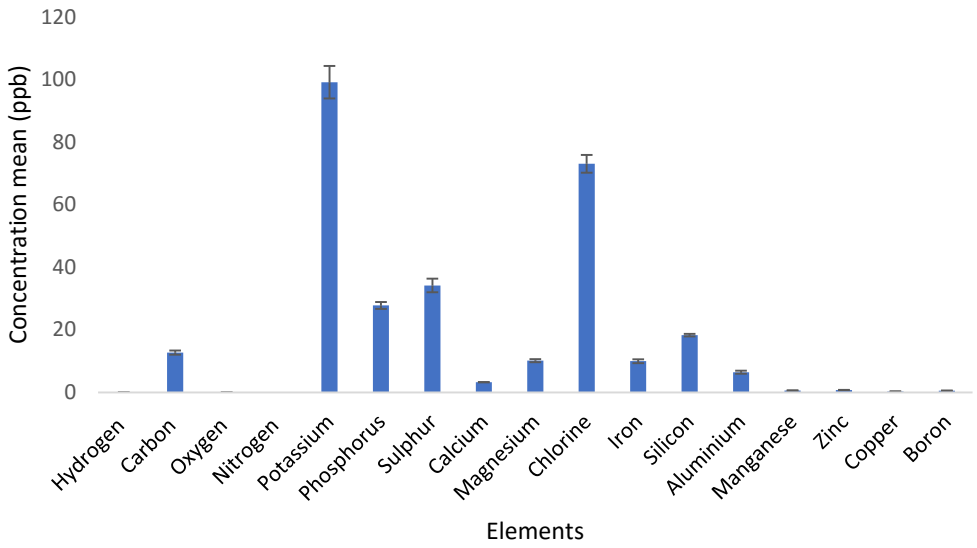

Figure 4.21b: The plot of mean concentration without nitrogen.

4.2.7 LIBS data: Mon 810

Figure 4.12 shows that 7 elements detected and figure 4.13 and 4.14 detected 9 elements from the sample; Mon 810. From the detected samples, only oxygen (O) from the first category (air and water), nitrogen (N) from the second category (fertilizer and manure), calcium (Ca) from the third category (secondary elements) and finally, 3 elements (Mn, Fe and Cu) from the last category (less applied elements). manganese was identified as the first elements in all samples. Nitrogen was (N) detected only in the first trial, this element is mostly supplemented through fertilizers and manure (Gojon, 2017). Iron (Fe), which was the dominant elements, indicated that the type of soil is laterite soil.

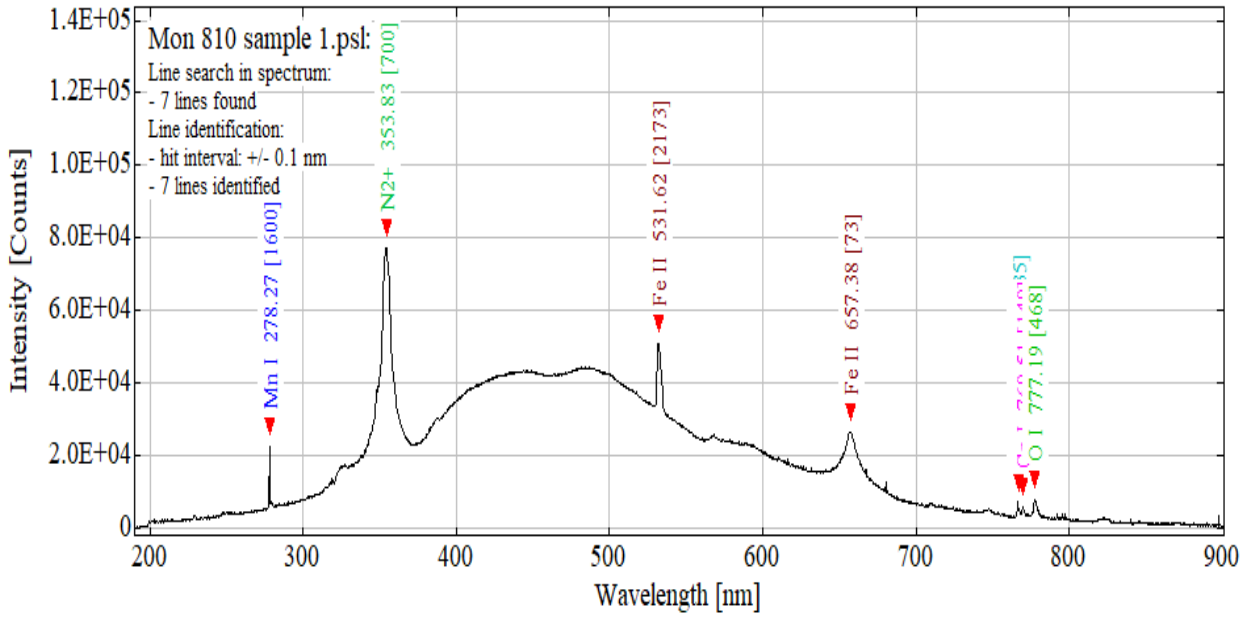

Figure 4.22: Emission spectra of sample Mon 810 1st trial.

Table 4.14: Mon 810 1st trial peak information.

Peak	Element	Wave length (nm)	Intensity	Energy Lower -upper	Transition Lower-upper	Quantum numbers
1	Mn I	278.27	1600	2.11 - 6.57	5D)4s a6D -7S) s4f w6F	4½ - 5½
2	N2+	353.83	700	0 - 3.16	X^2Sig+u - B^2Sig+u	3 – 4
3	Fe II	531.62	2173	10.42 -12.75	5D)4d e6G - 4)4f ^{2}2[6]]	6½ - 6½

4	Fe II	657.62	750	13.00 - 11.11	5D)5d 6D - 4P) sp 6P	2½ - 1½
5	Cu II	766.47	1535	14.96 - 16.58	5p ^{3}F - 6s ^{3}D	3 - 2
6	Ca I	769.51	149	6.05 - 4.44	4s16d ^{1}D - 3d4p ^{1}D	2- 2
7	O I	777.19	468	9.15 - 10.74	3s 5S° - 3p 5P	2 - 3

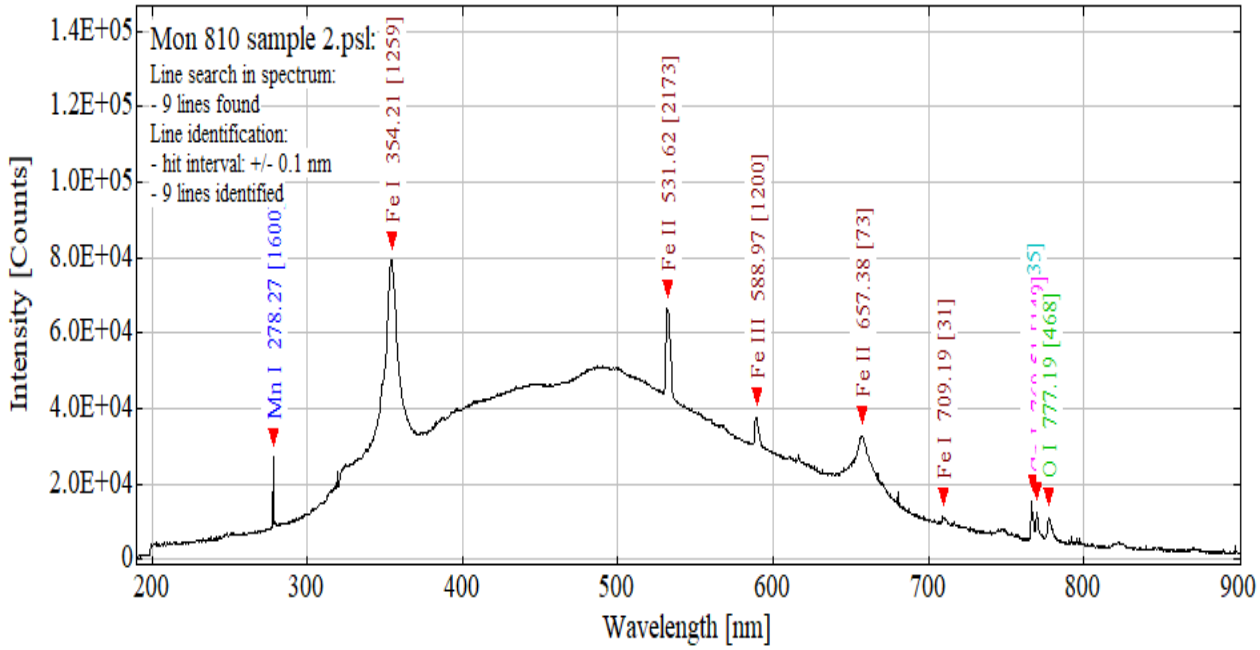

Figure 4.23: Emission spectra of sample Mon 810 2nd trial.

Table 4.15: Mon 810 2nd trial peak information.

Peak	Element	Wave length (nm)	Intensity	Energy Lower -upper	Transition Lower-upper	Quantum numbers
1	Mn I	278.27	1600	2.11 - 6.57	5D)4s a6D -7S) s4f w6F	4½ - 5½
2	Fe I	354.21	1259	6.36 - 2.87	6D)4d e7G - 5D) sp z7F	4 - 3
3	Fe II	531.62	2173	10.42 -12.75	5D)4d e6G - 4)4f ^{2}2[6]]	6½ - 6½

4	Fe II	588.97	1200	25.05 - 27.15	4F)5s 5F - 4F)5p 5G	3 - 4
5	Fe II	657.38	73	10.93 - 12.82	5D)4d 4P - 3)4f ^{2}2[3]]	1½ - 2½
6	Fe I	709.19	31	6.70 - 4.96	4F)4d e3G - 5D) sp x5D	4 - 3
7	Cu II	766.47	1535	14.96 - 16.58	5p ^{3}F - 6s ^{3}D	3 - 2
8	Ca I	769.51	149	6.05 - 4.44	4s16d ^{1}D - 3d4p ^{1}D	2- 2
9	O I	777.19	468	9.15 - 10.74	3s 5S° - 3p 5P	2 - 3

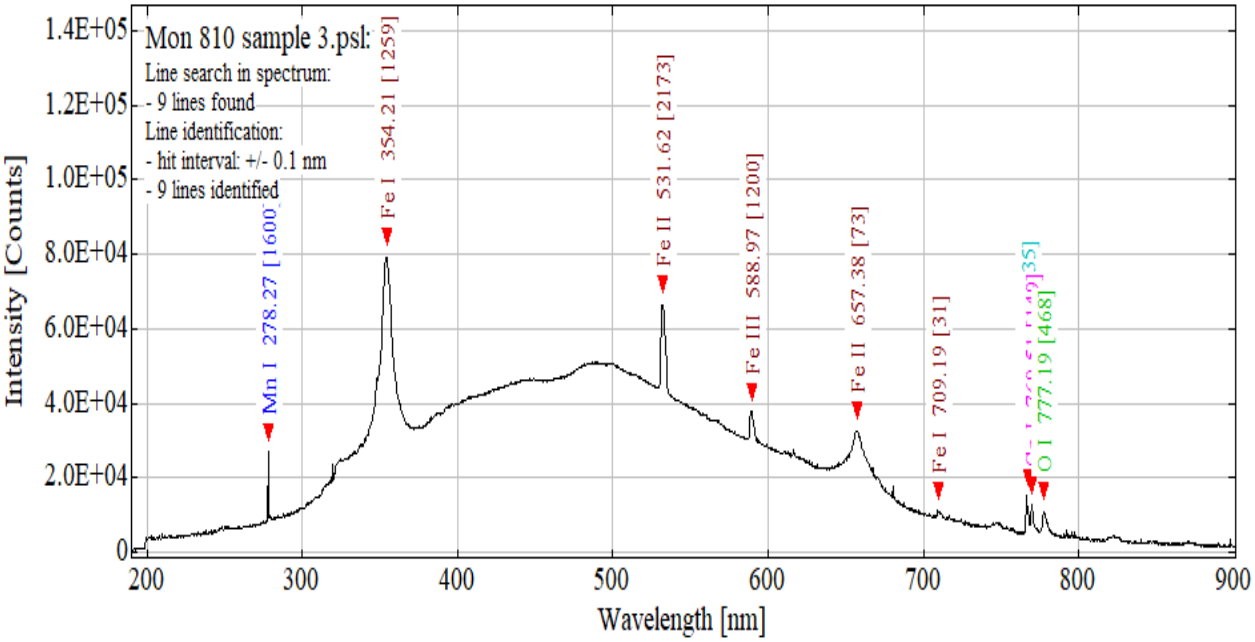

Figure 4.24: Emission spectra of sample Mon 810 3rd trial.

Table 4.16: Mon 810 3rd trial peak information.

Peak	Element	Wave length (nm)	Intensity	Energy Lower -upper	Transition Lower-upper	Quantum numbers
1	Mn I	278.27	1600	2.11 - 6.57	5D)4s a6D -7S) s4f w6F	4½ - 5½
2	Fe I	354.21	1259	6.36 - 2.87	6D)4d e7G - 5D) sp z7F	4 - 3
3	Fe II	531.62	2173	10.42 -12.75	5D)4d e6G - 4)4f ^{2}2[6]]	6½ - 6½

4	Fe II	588.97	1200	25.05 - 27.15	4F)5s 5F - 4F)5p 5G	3 - 4
5	Fe II	657.38	73	10.93 - 12.82	5D)4d 4P - 3)4f ^{2}2[3]]	1½ - 2½
6	Fe I	709.19	31	6.70 - 4.96	4F)4d e3G - 5D) sp x5D	4 - 3
7	Cu II	766.47	1535	14.96 - 16.58	5p ^{3}F - 6s ^{3}D	3 - 2
8	Ca I	769.51	149	6.05 - 4.44	4s16d ^{1}D - 3d4p ^{1}D	2- 2
9	O I	777.19	468	9.15 - 10.74	3s 5S° - 3p 5P	2 - 3

4.2.9 Statistical analysis

In figure 4.25, there is high error on N^{2+} and Fe I due to the fact that they were not measured in some trials and zero error was observed in those elements that were equally measured in all trial runs.

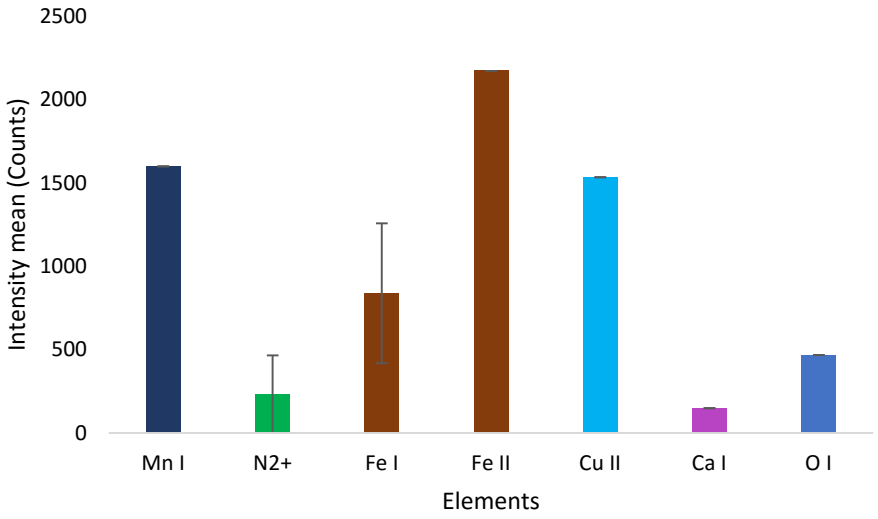

Figure 4.25: Bar-chart of mean intensity of elements found in GMO MON810 maize.

4.3. Discussion

4.3.1 ICP-MS results

In this research project, LIBS and ICP-MS are the two techniques that were used to study the difference in elemental composition between organic and genetically modified plants. Due to some complications in finding genetically modified plants in South Africa, five different types of corn grains were used in which, Mon 89, Mon 810 and CRN 3505 are GMO samples whilst Stowells and Golden Bantam are organic maize samples. The grains were grinded into powder using Polymix (PX-MCF 90 D), the idea was for the sample to have a uniform phase during the analysis. The grinded powder was digested into liquid using Titan microwave digester (full steps are described under methodology, Chapter 3). The created sample solution was then used for LIBS and ICP-MS.

All expected elements were identified even those with very small concentration. Oxygen and hydrogen were not measured in all samples, this is because ICP-MS is limited to part per-billion (ppb) (Wilschefski and Baxter, 2019). For all samples (organic and GMOs), the concentration of nitrogen (N) has always been very high, which can be toxic to the soil and the plants itself, the plants will have a dark green colour and stunt growth (Osorio et al., 2016). There is no limited amount of nitrogen (N) in plants and soil since the concentration I often adjusted depending on the amount of nitrogen needed on that particular plant. In this project, another possibility of high nitrogen level is due to nitrogen background and nitric acid (HNO_3) used as a reagent. Calcium (Ca), iron (Fe), aluminum (Al), manganese (Mn), zinc (Zn), Copper (Cu) and boron (B) has very low concentration. Iron is responsible for chlorophyll synthesis and chloroplast structure maintenance, copper is essential for plant's growth and development (Shabbir et al., 2020). The deficiency of any of these elements is often mistaken for one another, like stunt and inhibition of plants growth. Corn needs potassium (K) for water and nutrient transport, starch synthesis, photosynthesis, enzyme activation and crop quality control (Prajapati, 2012).

Manganese is responsible for plant's defense mechanism like the production of phenolic compounds whilst copper plays role in lignin synthesis as an enzyme co-factor (Tang et al., 2020a). Ca^{+2} uptake is inhibited by high content of K^{+}, which affects the membrane integrity and plant's growth. Fe^{+2} deficiency affects the absorption of Mn, Cu and Zn and delays the plant's growth.

Boron is understandably in very low content since it is responsible for the development of flowers which is unnecessary in this case (Urban and Restrepo-Diaz, 2017).

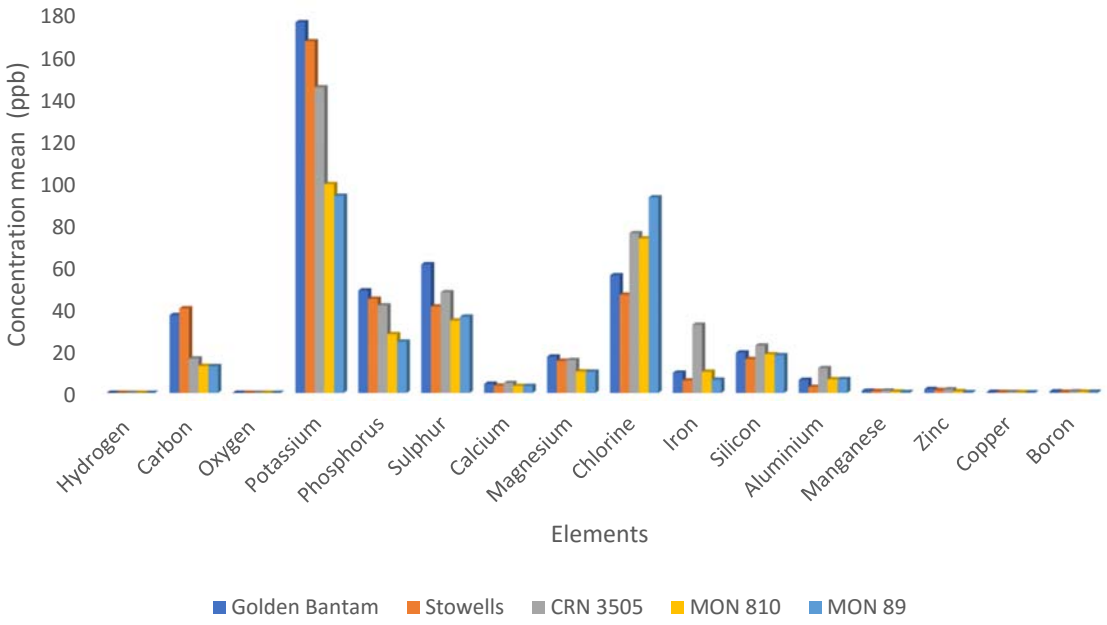

Figure 4.26: The graph of all sample concentration means without nitrogen using ICP-MS.

Figure 38 shows how the elemental concentrations differs in all five samples (from organic to GMOs). Golden Bantam, Stowells and CRN 3505 has higher concentration of carbon, potassium, phosphorus and sulphur than MON 89 and MON 810, while MON 89 and MON 810 has higher concentration of chlorine. From all the samples, Mn, Zn, Cu and B has very smaller concentration. From elemental display in figure 4.26, Golden Bantam and Stowels are expected to share similar traits, MON 89 and MON 810 are expected to share some few similar traits whilst CRN 3505 have combined traits (from organic and GMOs). Meanwhile, the difference in elemental composition can only be due to the measured concentrations. Different micronutrients in plants are required at different concentrations, manipulating the elemental content eventually alter the plant's genetic traits.

4.3.2. LIBS results

Laser induced breakdown spectroscopy (LIBS) is known for its ability to perform multi-elemental analysis with a little or no sample preparation (Zhang et al., 2020b). There are six elements, Mn I, Fe I, Fe II, Cu II, K I and O I that are found in all organic samples, but with different intensities,

For GMOs we have the previously mentioned elements plus Ca II, C I, N II and Ca I. This sums to ten out of 17 expected elements. The difference between these two technques is due to their working principles. LIBS does not detect all the elements in a sample since it is focused on sample surface (Wang et al., 2018) and sample exicitation states. The elements will always appear in ionic form, because the ablated laser atomises and excites the sample in order for the characteristic light to be emitted then captured via optic fiber (François et al., 2020). Using LIBS, we are able to determine the element's excitation energies, transition states and quantum numbers. This allows us to understand how much energy is required to change an electron from one energy state to another.

There is no tracable relationsip between sample type (organic or GMO) and transition energies since the specific element have the same quantum number and the same transtion state for any sample type. Under peak information; we have energy level (principal quantum numbers), orbital type, specific orbital and spin quantum number. These transition states reveals information about electron configuration. Orbital quantum number describes the orbital shape, size and location and can be calculated using the equation 1 that is indicated below:

$$l^2 = \hbar^2 l(l + l) \quad \text{.....Equation (4.1).}$$

Spin quantum number is the the fraction $\left(\frac{1}{2}\right)$ that we seen in the quantum numbers. Knowing the quantum numbers we can calculate the energy of an electron within the atom using the following formula (equation 2):

$$E_n = \frac{E_0}{n^2} \text{.....Equation (4.2).}$$

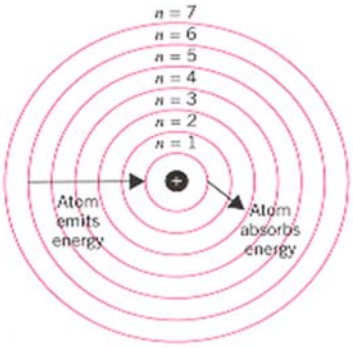

Figure 4.27: Neil Bohr's Model (Bohr, 1925)

Using the above model, the quantum number in this study give us more information about how closer to the surface the electrons are and the amount of energy needed for excitation. There is a

huge noisy hump (spectral contamination) in all LIBS results obtained, this is due to the presence of matrix effect, which is an overlap of spectral features (when multiple elements are excited at the same time) (Chen et al., 2020a). The matrix effect is dependent on the composition of the material, the physical (graine size, thermal conductivity and surface roughness) and chemical (element concentration and type of element) properties of the sample. Therefore, this results to high intensity spectral line suffering from self-absoption (Zhang et al., 2020a).

At first, the liquid sample was run under LIBS. LIBS require little or no sample preparation, in this case, prepared sample was utilised because it was believed to be uniform but no peaks were identified. According to (Gaubeur et al., 2015), it is not easy to run liquid sample due to the fact that most plasma energy is lost in the process to cavitation and vaporization of liquid during laser ablation, no excitation is reached. Secondly, the powder sample was used. Peaks were identified on powder sample, but with lower intensity. To increase the intensity, the experiment was carried out at night to avoid light interference, there was an unexpected difficulty which was due to the geometry of the setup. The laser kept on blowing the sample off and scatter the sample, there was no enough time for laser – matter (sample) interaction on sample surface. To fix this, the solid sample (grain of maize) was used. Using a grain of maize, no sample preparation was involved and the results were a bit improved as compared to those of liquid and powder. To get a better peak intensity, boxcar, scans and integration time were increased. The acquired data does not show which element belong to which peak., For peak-element identification, the Software SPECLINE, from Spectra-Suite (by Ocean Optics) was further used. SPECLINE can identify more than 100 elements per peak, in this case, only elements with high intensity (in the range 30 – 4500) were selected and the ones with lower intensity were removed. Spectra-suite gives a graph that shows, wavelength, intensity and elements. Furthermore, it allows one to study more about excitation energies, excitation states, quantum numbers and angular momentum.

4.3.3 Summary

In this project, ICP-MS was used to validate LIBS results. Because of the working prinple of these techniques, ICP-MS can be used more as a competitive techinique than a verifying one. This project aimed to study the difference in elemental composition between the organic and genetically modified plants. The research purpose was driven by the hypothesis that *genetic modification leads*

to the change in elemental composition. To achieve this, two techniques (LIBS and ICP-MS) had to be used. LIBS is a non-destructive elemental analysis technique based on laser ablation and elemental excitation (Zhang et al., 2020b) whilst ICP-MS is elemental quantification technque based on high temperature ionisation (Yu et al., 2020). This research was focused to achieve four objectives which are written in chapter 1.

The results obtained from the two techniques, showed that, different samples (organic and GMO) have different elements since GMO is believed to have altered genetic make (elemental composition). Same elements were determined but in different concentrations, this means that genetic modification alters the plants elemental concentration without necessarily eliminating other essential elements.

Chapter 5: Conclusion

In this research, two techniques (which are LIBS and ICP-MS) were used to analyse and differentiate the elemental composition between organic and genetically modified maize. Since genetic modification is believed to result in elemental alteration, this dissertation is mainly focused on studying the elemental compositions of these two maize categories, differentiate them according to their trace elements and also differentiate the two techniques based on their working principles. In this case, Mon89, Mon810 and CRN 3505 are the genetically modified maize samples that were analyzed whilst Stowells evergreen and Golden Bantams are the organic maize samples analyzed. From the analyzed results, all expected seventeen elements were detected from both organic and GMP by ICP-MS, including those with a very low concentration. The difference in elemental compositions between the two categories was due to the difference in element concentrations, meaning genetic modification manipulated the plant's elemental concentrations of the same elements. LIBS was able to detect six elements, Mn I, Fe I, Fe II, Cu II, K I and O I that are found in all organic samples, but with different intensities for GMO, the previously mentioned elements plus Ca II, C I, N II and Ca I, this summed up to ten elements. The absence of other elements on LIBS was due to its working limitation, which is the surface analysis. LIBS provides the results in ionic form and this is due to the fact that LIBS technique is based on excitation and de-excitation of elements through laser ablation. For future studies, LIBS results enable you to study the transition energy, excitation energy quantum states and quantum numbers of different elements especial for fields like material sciences, nuclear physics and quantum physics.

Since this study was focused on the nutrient elements (micro and macro-nutrients), no harmful elements were detected on both samples, meaning there will not be any negative impact on humans and the environment. The two techniques were reliable and each carried different advantage over the other. LIBS is best for in-situ analysis, which allows you to get the results on the same day. No sample preparation is needed for LIBS, though the laser ablation takes place at the surface of the sample. LIBS works best on solid samples and this was accurately proven in this research since the practical was tested for all sample form (liquid, powder and solid). ICP-MS requires a rigorous sample preparation, treatment and analysis, which can take hours to get accurate and reliable results. For future use, since there were no possible harmful elements detected, farmers can use genetically modified maize plants since it carried numerous benefits as compared to organic plants. Labelling the GMO package is very important since they contain modified elemental

concentrations. LIBS technique suffers from matrix effect and self-absorption that sometimes weakens the absorption peak, this caused by laser ablation then radiates outwards energy (Tang et al., 2020b), therefore, this technique can be carried out in the presence of argon gas to improve the detection sensitivity and eliminate self-absorption. The practical can also produce best results when performed in the dark to avoid light interference. For commercial uses, there is a new LIBS equipment that is small, portable and can be carried especially for forensic and environmental analysis. It is highly recommended for future researchers to run the same experiment following the above recommendations and compare the results.

Reference

ACZEL, M. R. 2019. What Is the Nitrogen Cycle and Why Is It Key to Life? *Front. Young Minds*.

AHMED, N., LIAQAT, U., RAFIQUE, M., BAIG, M. A. & TAWFIK, W. 2020. Detection of toxicity in some oral antidiabetic drugs using LIBS and LA-TOF-MS. *Microchemical Journal,* 155**,** 104679.

AMAIS, R. S., DONATI, G. L. & ZEZZI ARRUDA, M. A. 2020. ICP-MS and trace element analysis as tools for better understanding medical conditions. *TrAC Trends in Analytical Chemistry,* 133**,** 116094.

ANDERSEN, M.-B. S., FRYDENVANG, J., HENCKEL, P. & RINNAN, Å. 2016. The potential of laser-induced breakdown spectroscopy for industrial at-line monitoring of calcium content in comminuted poultry meat. *Food Control,* 64**,** 226-233.

AR1, A., AR1, P. E. & GAGA, E. O. 2020. Chemical characterization of size-segregated particulate matter (PM) by inductively coupled plasma – Tandem mass spectrometry (ICP-MS/MS). *Talanta,* 208**,** 120350.

AWASTHI, S., KUMAR, R., RAI, G. K. & RAI, A. K. 2016. Study of archaeological coins of different dynasties using libs coupled with multivariate analysis. *Optics and Lasers in Engineering,* 79**,** 29-38.

BAI, X., ALLÈGRE, H., GOSSELIN, M., DILLMANN, P., LOPEZ, M., TÉREYGEOL, F. & DETALLE, V. 2020. Impact of laser-induced breakdown spectroscopy implementation for the quantification of carbon content distribution in archaeological ferrous metals. *Spectrochimica Acta Part B: Atomic Spectroscopy,* 172**,** 105964.

BAIN, C. & SELFA, T. 2017. Non-GMO vs organic labels: purity or process guarantees in a GMO contaminated landscape. *Agriculture and human values,* 34**,** 805-818.

BEAUCHEMIN, D. 2017. Inductively Coupled Plasma Mass Spectrometry Methods. *In:* LINDON, J. C., TRANTER, G. E. & KOPPENAAL, D. W. (eds.) *Encyclopedia of Spectroscopy and Spectrometry (Third Edition).* Oxford: Academic Press.

BEHBOUDIAN, M. H., PICKERING, A. H. & DAYAN, E. 2017. Deficiency Diseases, Principles. *In:* THOMAS, B., MURRAY, B. G. & MURPHY, D. J. (eds.) *Encyclopedia of Applied Plant Sciences (Second Edition).* Oxford: Academic Press.

BHATT, C. R., GOUEGUEL, C. L., JAIN, J. C., MCINTYRE, D. L. & SINGH, J. P. 2020. Chapter 9 - LIBS application to liquid samples. *In:* SINGH, J. P. & THAKUR, S. N. (eds.) *Laser-Induced Breakdown Spectroscopy (Second Edition).* Amsterdam: Elsevier.

BISSON, R., MARKELJ, S., MOUREY, O., GHIORGHIU, F., ACHKASOV, K., LAYET, J.-M., ROUBIN, P., CARTRY, G., GRISOLIA, C. & ANGOT, T. 2015. Dynamic fuel retention in tokamak wall materials: an in situ laboratory study of deuterium release from polycrystalline tungsten at room temperature. *Journal of Nuclear Materials,* 467**,** 432-438.

BLAKEY, L. S., SHARPLES, G. P., CHANA, K. & BIRKETT, J. W. 2018. Fate and behavior of gunshot residue—a review. *Journal of forensic sciences,* 63**,** 9-19.

BOHR, N. 1925. Atomic Theory and Mechanics 1. *Nature,* 116**,** 845-852.

BRARA, Z., COSTA, J., VILLA, C., GRAZINA, L., BITAM, A. & MAFRA, I. 2020. Surveying genetically modified maize in foods marketed in Algeria. *Food Control,* 109**,** 106928.

BRIDGE, C. M., POWELL, J., STEELE, K. L., WILLIAMS, M., MACINNIS, J. M. & SIGMAN, M. E. 2006. Characterization of automobile float glass with laser-induced

breakdown spectroscopy and laser ablation inductively coupled plasma mass spectrometry. *Applied spectroscopy,* 60**,** 1181-1187.
BULSKA, E. & WAGNER, B. 2016. Quantitative aspects of inductively coupled plasma mass spectrometry. *Philosophical Transactions of the Royal Society A: Mathematical, Physical and Engineering Sciences,* 374**,** 20150369.
CABOT, C., MARTOS, S., LLUGANY, M., GALLEGO, B., TOLRÀ, R. & POSCHENRIEDER, C. 2019. A Role for Zinc in Plant Defense Against Pathogens and Herbivores. *Frontiers in Plant Science,* 10.
CHEN, D., WANG, T., MA, Y., WANG, G., KONG, Q., ZHANG, P. & LI, R. 2020a. Rapid characterization of heavy metals in single microplastics by laser induced breakdown spectroscopy. *Science of The Total Environment,* 743**,** 140850.
CHEN, T., ZHANG, T. & LI, H. 2020b. Applications of laser-induced breakdown spectroscopy (LIBS) combined with machine learning in geochemical and environmental resources exploration. *TrAC Trends in Analytical Chemistry***,** 116113.
CHEN, Z. C., PENG, W. T., LI, J. & LIAO, H. 2018. Functional dissection and transport mechanism of magnesium in plants. *Seminars in Cell & Developmental Biology,* 74**,** 142-152.
CONTESSI, S., CALGARO, L., DALCONI, M. C., BONETTO, A., BELLOTTO, M. P., FERRARI, G., MARCOMINI, A. & ARTIOLI, G. 2020. Stabilization of lead contaminated soil with traditional and alternative binders. *Journal of Hazardous Materials,* 382**,** 120990.
DE CASTRO, M. D. L. & JURADO-LÓPEZ, A. 2019. The role of analytical chemists in the research on the cultural heritage. *Talanta,* 205**,** 120106.
DE LA CÁMARA, C. M.-F., SALOM, D., SEQUEDO, M. D., HERVAS, D., MARÍN-LAMBÍES, C., ALLER, E., JAIJO, T., DÍAZ-LLOPIS, M., MILLÁN, J. M. & RODRIGO, R. 2013. Altered antioxidant-oxidant status in the aqueous humor and peripheral blood of patients with retinitis pigmentosa. *PLoS One,* 8**,** e74223.
DEELSTRA, H., BURNS, D. T. & WALKER, M. 2014. The adulteration of food, lessons from the past, with reference to butter, margarine and fraud. *European Food Research and Technology,* 239**,** 725-744.
DELL'AGLIO, M., ALRIFAI, R. & DE GIACOMO, A. 2018. Nanoparticle enhanced laser induced breakdown spectroscopy (NELIBS), a first review. *Spectrochimica Acta Part B: Atomic Spectroscopy,* 148**,** 105-112.
DHALIWAL, S. S., NARESH, R. K., MANDAL, A., SINGH, R. & DHALIWAL, M. K. 2019. Dynamics and transformations of micronutrients in agricultural soils as influenced by organic matter build-up: A review. *Environmental and Sustainability Indicators,* 1-2**,** 100007.
DÍAZ PACE, D. M., GABRIELE, N. A., GARCIMUÑO, M., D'ANGELO, C. A., BERTUCCELLI, G. & BERTUCCELLI, D. 2011. Analysis of minerals and rocks by laser-induced breakdown spectroscopy. *Spectroscopy Letters,* 44**,** 399-411.
DOÑA-FERNÁNDEZ, A., DE ANDRES-GIMENO, I., SANTIAGO-TORIBIO, P., VALTUILLE-FERNÁNDEZ, E., ALLER-SANCHEZ, F. & HERAS-GONZÁLEZ, A. 2018. Real-time detection of GSR particles from crime scene: A comparative study of SEM/EDX and portable LIBS system. *Forensic Science International,* 292**,** 167-175.
EGLINE J., B. A. 2016. How to Differentiate GMO Tomatoes from Organic Ones in These Two Simple Steps. *Food and nutrion*.

EL-DEFTAR, M. M., SPEERS, N., EGGINS, S., FOSTER, S., ROBERTSON, J. & LENNARD, C. 2014. Assessment and forensic application of laser-induced breakdown spectroscopy (LIBS) for the discrimination of Australian window glass. *Forensic Science International,* 241**,** 46-54.

FABRE, C. 2020. Advances in Laser-Induced Breakdown Spectroscopy analysis for geology: A critical review. *Spectrochimica Acta Part B: Atomic Spectroscopy,* 166**,** 105799.

FARAHANI, S. S., RAJABIPOUR, A., KEYHANI, A. & SHARIFI, M. 2017. Energy use and economic analysis of NPK-15:8:15 fertilizer granulation process in Iran. *Journal of the Saudi Society of Agricultural Sciences,* 16**,** 265-269.

FORMAN, J. & SILVERSTEIN, J. 2012. Organic foods: health and environmental advantages and disadvantages. *Pediatrics,* 130**,** e1406-15.

FRANÇOIS, E., GAZELI, O., COURIS, S., ANGELOPOULOS, G. N., BLANPAIN, B. & MALFLIET, A. 2020. Laser-induced breakdown spectroscopy analysis of the free surface of liquid secondary copper slag. *Spectrochimica Acta Part B: Atomic Spectroscopy,* 170**,** 105921.

FRENCH, J. & MORGAN, R. 2015. An experimental investigation of the indirect transfer and deposition of gunshot residue: Further studies carried out with SEM–EDX analysis. *Forensic science international,* 247**,** 14-17.

FURIO, R. N., MARTÍNEZ-ZAMORA, G. M., SALAZAR, S. M., COLL, Y., PERATO, S. M., MARTOS, G. G. & DÍAZ RICCI, J. C. 2020. Role of calcium in the defense response induced by brassinosteroids in strawberry plants. *Scientia Horticulturae,* 261**,** 109010.

GAUBEUR, I., AGUIRRE, M., KOVACHEV, N., HIDALGO, M. & CANALS, A. 2015. Dispersive liquid–liquid microextraction combined with laser-induced breakdown spectrometry and inductively coupled plasma optical emission spectrometry to elemental analysis. *Microchemical Journal,* 121**,** 219-226.

GODED, S., EKROOS, J., AZCÁRATE, J. G., GUITIÁN, J. A. & SMITH, H. G. 2019. Effects of organic farming on plant and butterfly functional diversity in mosaic landscapes. *Agriculture, Ecosystems & Environment,* 284**,** 106600.

GOJON, A. 2017. Nitrogen nutrition in plants: rapid progress and new challenges. *Journal of Experimental Botany,* 68**,** 2457-2462.

GOUEGUEL, C., LAVILLE, S., VIDAL, F., SABSABI, M. & CHAKER, M. 2010. Investigation of resonance-enhanced laser-induced breakdown spectroscopy for analysis of aluminium alloys. *Journal of Analytical Atomic Spectrometry,* 25**,** 635-644.

GUIRADO, S., FORTES, F. J., LAZIC, V. & LASERNA, J. J. 2012. Chemical analysis of archeological materials in submarine environments using laser-induced breakdown spectroscopy. On-site trials in the Mediterranean Sea. *Spectrochimica Acta Part B: Atomic Spectroscopy,* 74-75**,** 137-143.

GUO, L., ZHANG, B., HE, X., LI, C., ZHOU, Y., WU, T., PARK, J., ZENG, X. & LU, Y. 2012. Optimally enhanced optical emission in laser-induced breakdown spectroscopy by combining spatial confinement and dual-pulse irradiation. *Optics express,* 20**,** 1436-1443.

GUPTA, A., CURRAN, J. M., COULSON, S. & TRIGGS, C. M. 2017. Comparison of intra-day and inter-day variation in LIBS spectra. *Forensic Chemistry,* 3**,** 36-40.

GURĂU, C. & RANCHHOD, A. 2016. The futures of genetically-modified foods: Global threat or panacea? *Futures,* 83**,** 24-36.

HAHN, D. W. & OMENETTO, N. 2010. Laser-induced breakdown spectroscopy (LIBS), part I: review of basic diagnostics and plasma–particle interactions: still-challenging issues within the analytical plasma community. *Applied spectroscopy,* 64**,** 335A-366A.
HARMON, R. S., THROCKMORTON, C. S., HARK, R. R., GOTTFRIED, J. L., WÖRNER, G., HARPP, K. & COLLINS, L. 2018. Discriminating volcanic centers with handheld laser-induced breakdown spectroscopy (LIBS). *Journal of Archaeological Science,* 98**,** 112-127.
HEIRLOOM, O. S. A. 2012. Organic seeds: Stowell evergreen and GOLDEN BANTAM SWEETCORN.
HILBECK, A., BINIMELIS, R., DEFARGE, N., STEINBRECHER, R., SZÉKÁCS, A., WICKSON, F., ANTONIOU, M., BEREANO, P. L., CLARK, E. A. & HANSEN, M. 2015. No scientific consensus on GMO safety. *Environmental Sciences Europe,* 27**,** 4.
HUBERT, J., KUDLÍKOVÁ-KŘÍŽKOVÁ, I. & STEJSKAL, V. 2008. Effect of MON 810 Bt transgenic maize diet on stored-product moths (Lepidoptera: Pyralidae). *Crop protection,* 27**,** 489-496.
HUSSAIN SHAH, S. K., IQBAL, J., AHMAD, P., KHANDAKER, M. U., HAQ, S. & NAEEM, M. 2020. Laser induced breakdown spectroscopy methods and applications: A comprehensive review. *Radiation Physics and Chemistry,* 170**,** 108666.
ISAAA 2020. Crop: Zea mays L. - Maize, Corn. *International Service for the Acquisition of Agri-biotech Applications (ISAAA)*.
JAHAN, S., WAHOCHO, N., LAGHARI, G., LAGHARI, A., BHABHAN, G., HUSSAINTALPUR, K., AHMED, T., WAHOCHO, S. & LASHARI, A. 2016. Role of Nitrogen for Plant Growth and Development: A review. *Advances in Environmental Biology,* 10**,** 209-218.
JUNJURI, R., ZHANG, C., BARMAN, I. & GUNDAWAR, M. K. 2019. Identification of post-consumer plastics using laser-induced breakdown spectroscopy. *Polymer Testing,* 76**,** 101-108.
KELLY, S. 2018. The Amount of Nitrogen Used for Photosynthesis Modulates Molecular Evolution in Plants. *Molecular biology and evolution,* 35**,** 1616-1625.
KHEDR, A. & HARITH, M. 2013. In-depth micro-spectrochemical analysis of archaeological Egyptian pottery shards. *Applied Physics A,* 113**,** 835-842.
KIM, G., YOON, Y.-J., KIM, H.-A., CHO, H.-J. & PARK, K. 2017. Elemental composition of Arctic soils and aerosols in Ny-Ålesund measured using laser-induced breakdown spectroscopy. *Spectrochimica Acta Part B: Atomic Spectroscopy,* 134**,** 17-24.
KOBAYASHI, T., NOZOYE, T. & NISHIZAWA, N. K. 2019. Iron transport and its regulation in plants. *Free Radical Biology and Medicine,* 133**,** 11-20.
KRASHENINNIKOV, S., KUKUSHKIN, A. & PSHENOV, A. 2016. Divertor plasma detachment. *Physics of Plasmas,* 23**,** 055602.
KUBITZA, S., SCHRÖDER, S., DIETZ, E., FROHMANN, S., HANSEN, P. B., RAMMELKAMP, K., VOGT, D. S., GENSCH, M. & HÜBERS, H.-W. 2020. Detecting sulfur on the Moon: The potential of vacuum ultraviolet laser-induced breakdown spectroscopy. *Spectrochimica Acta Part B: Atomic Spectroscopy,* 174**,** 105990.
LEGNAIOLI, S., CAMPANELLA, B., PAGNOTTA, S., POGGIALINI, F. & PALLESCHI, V. 2019. Determination of Ash Content of coal by Laser-Induced Breakdown Spectroscopy. *Spectrochimica Acta Part B: Atomic Spectroscopy*.

LEWEN, N. 2011. The use of atomic spectroscopy in the pharmaceutical industry for the determination of trace elements in pharmaceuticals. *Journal of Pharmaceutical and Biomedical Analysis,* 55**,** 653-661.
LIN, J., LIN, X. & GUO, L. 2019. Enhancement effects of different elements by argon shield in laser induced breakdown spectroscopy. *Optik*.
LOHMAN, T., WANG, Z. & GOING, S. B. 2005. *Human body composition*, Human Kinetics.
LÓPEZ-CLAROS, M., FORTES, F. J. & LASERNA, J. J. 2018. Subsea spectral identification of shipwreck objects using laser-induced breakdown spectroscopy and linear discriminant analysis. *Journal of Cultural Heritage,* 29**,** 75-81.
LUCENA, P., DONA, A., TOBARIA, L. & LASERNA, J. J. 2011. New challenges and insights in the detection and spectral identification of organic explosives by laser induced breakdown spectroscopy. *Spectrochimica Acta Part B: Atomic Spectroscopy,* 66**,** 12-20.
MACARTHUR, A., ROBINSON, I., ROSSINI, M., DAVIS, N. & MACDONALD, K. A dual-field-of-view spectrometer system for reflectance and fluorescence measurements (Piccolo Doppio) and correction of etaloning. 2014 2014. 22-24.
MACHADO, A. S., SILVA, A. S. S., CAMPOS, G. N., GOMES, C. S., OLIVEIRA, D. F. & LOPES, R. T. 2019. Analysis of metallic archaeological artifacts by x-ray computed microtomography technique. *Applied Radiation and Isotopes,* 151**,** 274-279.
MAI, H.-J. & BAUER, P. 2016. From the proteomic point of view: Integration of adaptive changes to iron deficiency in plants. *Current Plant Biology,* 5**,** 45-56.
MARKIEWICZ-KESZYCKA, M., CAMA-MONCUNILL, R., PIETAT CASADO-GAVALDA, M., SULLIVAN, C. & CULLEN, P. J. 2019. Laser-induced breakdown spectroscopy for food authentication. *Current Opinion in Food Science,* 28**,** 96-103.
MATEO, M., BECERRA, J., ZADERENKO, A. P., ORTIZ, P. & NICOLÁS, G. 2019. Laser-induced breakdown spectroscopy applied to the evaluation of penetration depth of bactericidal treatments based on silver nanoparticles in limestones. *Spectrochimica Acta Part B: Atomic Spectroscopy,* 152**,** 44-51.
MAURYA, G. S., MARÍN-ROLDÁN, A., VEIS, P., PATHAK, A. K. & SEN, P. 2020. A review of the LIBS analysis for the plasma-facing components diagnostics. *Journal of Nuclear Materials,* 541**,** 152417.
MENG, D., ZHAO, N., WANG, Y., MA, M., FANG, L., GU, Y., JIA, Y. & LIU, J. 2017. On-line/on-site analysis of heavy metals in water and soils by laser induced breakdown spectroscopy. *Spectrochimica Acta Part B: Atomic Spectroscopy,* 137**,** 39-45.
MIŠKOVIČOVÁ, J., ANGUŠ, M., VAN DER MEIDEN, H. & VEIS, P. 2020. Selection of molybdenum lines by quantitative analysis of molybdenum- zirconium-titanium alloy by CF-LIBS for future fusion applications. *Fusion Engineering and Design,* 153**,** 111488.
MYAKALWAR, A. K., SREEDHAR, S., BARMAN, I., DINGARI, N. C., VENUGOPAL RAO, S., PREM KIRAN, P., TEWARI, S. P. & MANOJ KUMAR, G. 2011. Laser-induced breakdown spectroscopy-based investigation and classification of pharmaceutical tablets using multivariate chemometric analysis. *Talanta,* 87**,** 53-59.
NAWAZ, M. A., TSATSAKIS, A. M., ERCISLI, S. & CHUNG, G. 2018. Genetically Modified Plants: Risks to Environment. *Reference Module in Earth Systems and Environmental Sciences.* Elsevier.
NAWAZ, M. A., TSATSAKIS, A. M., ERCISLI, S. & CHUNG, G. 2019. Genetically Modified Plants: Risks to Environment. *In:* NRIAGU, J. (ed.) *Encyclopedia of Environmental Health (Second Edition).* Oxford: Elsevier.

NIBALI, J. T. A. E. 2005. Excessive chlorine bothers plants; smaller trees are more cost-effective. *THE BALTIMORE SUN*.
NISAR, S., DASTGEER, G., SHAFIQ, M. & USMAN, M. 2019. Qualitative and semi-quantitative analysis of health-care pharmaceutical products using laser-induced breakdown spectroscopy. *Journal of Pharmaceutical Analysis,* 9**,** 20-24.
NOLL, R. 2012. Laser-induced breakdown spectroscopy. *Laser-Induced Breakdown Spectroscopy.* Springer.
ORELLANA, F. A., GÁLVEZ, C. G., ORELLANA, F. A., GÁLVEZ, C. G., ROLDÁN, M. T., GARCÍA-RUIZ, C., ROLDÁN, M. T. & GARCÍA-RUIZ, C. 2013. Applications of laser-ablation-inductively-coupled plasma-mass spectrometry in chemical analysis of forensic evidence. *TrAC Trends in Analytical Chemistry,* 42**,** 1-34.
OSORIO, V., SANCHÍS, J., ABAD, J. L., GINEBREDA, A., FARRÉ, M., PÉREZ, S. & BARCELÓ, D. 2016. Investigating the formation and toxicity of nitrogen transformation products of diclofenac and sulfamethoxazole in wastewater treatment plants. *Journal of Hazardous Materials,* 309**,** 157-164.
PETER, R., MOJCA, J. & PRIMOŽ, P. 2011. Genetically Modified Organisms (GMOs). *In:* NRIAGU, J. (ed.) *Encyclopedia of Environmental Health (Second Edition).* Oxford: Elsevier.
PRAJAPATI, K. 2012. THE IMPORTANCE OF POTASSIUM IN PLANT GROWTH – A REVIEW. *Indian Journal of Plant Sciences,* 1**,** 177-186.
REHAN, I., GONDAL, M. A. & REHAN, K. 2018. Determination of lead content in drilling fueled soil using laser induced spectral analysis and its cross validation using ICP/OES method. *Talanta,* 182**,** 443-449.
REHSE, S. J. 2019. A review of the use of laser-induced breakdown spectroscopy for bacterial classification, quantification, and identification. *Spectrochimica Acta Part B: Atomic Spectroscopy,* 154**,** 50-69.
RICROCH, A., BERGÉ, J. B. & KUNTZ, M. 2010. Is the German suspension of MON810 maize cultivation scientifically justified? *Transgenic research,* 19**,** 1-12.
RINKE-KNEAPLER, C. N. & SIGMAN, M. E. 2014. 15 - Applications of laser spectroscopy in forensic science. *In:* BAUDELET, M. (ed.) *Laser Spectroscopy for Sensing.* Woodhead Publishing.
RIZWAN, M., ALI, S., UR REHMAN, M. Z. & MAQBOOL, A. 2019. A critical review on the effects of zinc at toxic levels of cadmium in plants. *Environmental Science and Pollution Research,* 26**,** 6279-6289.
RUSAK, D. A., MARSICO, R. M. & TAROLI, B. L. 2011. Using laser-induced breakdown spectroscopy to assess preservation quality of archaeological bones by measurement of calcium-to-fluorine ratios. *Applied spectroscopy,* 65**,** 1193-1196.
SÁNCHEZ-AKÉ, C., GARCÍA-FERNÁNDEZ, T., BENÍTEZ, J. L., DE LA MORA, M. B. & VILLAGRÁN-MUNIZ, M. 2018. Intensity enhancement of LIBS of glass by using Au thin films and nanoparticles. *Spectrochimica Acta Part B: Atomic Spectroscopy,* 146**,** 77-83.
SATOH, R. & TESHIMA, R. 2016. Chapter 40 - Allergen Analysis in Plants and Use in the Assessment of Genetically Modified Plants. *In:* WATSON, R. R. & PREEDY, V. R. (eds.) *Genetically Modified Organisms in Food.* San Diego: Academic Press.
SCHNURR, M. 2019. *Africa's Gene Revolution: Genetically Modified Crops and the Future of African Agriculture*.

ŠEBESTOVÁ, A., BARON, D., PECHANCOVÁ, R., PLUHÁČEK, T. & PETR, J. 2019. Determination of oxaliplatin enantiomers at attomolar levels by capillary electrophoresis connected with inductively coupled plasma mass spectrometry. *Talanta,* 205**,** 120151.
SHAAYA, E., KOSTYUKOVSKY, M. & QUINN, E. 2016. Chapter 12 - Improving the Control of Insects in Food Processing. *In:* LELIEVELD, H., HOLAH, J. & GABRIĆ, D. (eds.) *Handbook of Hygiene Control in the Food Industry (Second Edition).* San Diego: Woodhead Publishing.
SHABBIR, Z., SARDAR, A., SHABBIR, A., ABBAS, G., SHAMSHAD, S., KHALID, S., NATASHA, MURTAZA, G., DUMAT, C. & SHAHID, M. 2020. Copper uptake, essentiality, toxicity, detoxification and risk assessment in soil-plant environment. *Chemosphere,* 259**,** 127436.
SHARMA, A., PATNI, B., SHANKHDHAR, D. & SHANKHDHAR, S. C. 2013. Zinc - an indispensable micronutrient. *Physiology and molecular biology of plants : an international journal of functional plant biology,* 19**,** 11-20.
SHERGILL-BONNER, R. 2017. Micronutrients. *Paediatrics and Child Health,* 27**,** 357-362.
SHI, K., FU, L.-J., ZHANG, S., LI, X., DONG, D.-K., JIANG, Y.-P., ZHOU, Y.-H., XIA, X.-J., LIANG, W.-S. & YU, J.-Q. 2012. The reduction of reactive oxygen species formation by mitochondrial alternative respiration in tomato basal defense against TMV infection. *Planta,* 235**,** 225-238.
SHILING, L., LIN, C., BAOGUO, Y., HONGYAN, J., SHENGJIANG, P., PEI, Z. & HUI, W. Effects of nitrogen and phosphorus fertilization on biomass allocation and root morphology in Betula alnoides clones.
SINGH, P., MAL, E., KHARE, A. & SHARMA, S. 2018. A study of archaeological pottery of Northeast India using laser induced breakdown spectroscopy (LIBS). *Journal of Cultural Heritage,* 33**,** 71-82.
SIOZOS, P., PHILIPPIDIS, A. & ANGLOS, D. 2017. Portable laser-induced breakdown spectroscopy/diffuse reflectance hybrid spectrometer for analysis of inorganic pigments. *Spectrochimica Acta Part B: Atomic Spectroscopy,* 137**,** 93-100.
SITHOLE, S. C., MUGIVHISA, L. L., AMOO, S. O. & OLOWOYO, J. O. 2017. Pattern and concentrations of trace metals in mushrooms harvested from trace metal-polluted soils in Pretoria, South Africa. *South African Journal of Botany,* 108**,** 315-320.
SNOECK, C., JONES, C., POUNCETT, J., GODERIS, S., CLAEYS, P., MATTIELLI, N., ZAZZO, A., REIMER, P. J., LEE-THORP, J. A. & SCHULTING, R. J. 2020. Isotopic evidence for changing mobility and landscape use patterns between the Neolithic and Early Bronze Age in western Ireland. *Journal of Archaeological Science: Reports,* 30**,** 102214.
SOETAN, K., OLAIYA, C. & OYEWOLE, O. 2010. The importance of mineral elements for humans, domestic animals and plants: A review. *African journal of food science,* 4**,** 200-222.
SOMEKAWA, T., OTSUKA, M., KUZE, H., MAEDA, Y., KAWANAKA, J. & FUJITA, M. 2020. Laser-fluence dependence of signal enhancement in femtosecond double-pulse laser induced breakdown spectroscopy. *Spectrochimica Acta Part B: Atomic Spectroscopy,* 164**,** 105755.
SONG, E. K., MOSER, D. K. & LENNIE, T. A. 2013. Less Than 2g of Daily Sodium Intake Independently Predict Higher Micronutrient Deficiency in Patients with Heart Failure. *Journal of Cardiac Failure,* 19**,** S41.

STONEY, D. A. & STONEY, P. L. 2015. Critical review of forensic trace evidence analysis and the need for a new approach. *Forensic science international,* 251**,** 159-170.
SYVILAY, D., GUEZENOC, J. & BOUSQUET, B. 2019. Guideline for increasing the analysis quality in laser-induced breakdown spectroscopy. *Spectrochimica Acta Part B: Atomic Spectroscopy,* 161**,** 105696.
TANG, R.-J. & LUAN, S. 2017. Regulation of calcium and magnesium homeostasis in plants: from transporters to signaling network. *Current Opinion in Plant Biology,* 39**,** 97-105.
TANG, Y., KANG, H., QIN, Z., ZHANG, K., ZHONG, Y., LI, H. & MO, L. 2020a. Significance of manganese resistant bacillus cereus strain WSE01 as a bioinoculant for promotion of plant growth and manganese accumulation in Myriophyllum verticillatum. *Science of The Total Environment,* 707**,** 135867.
TANG, Y., MA, S., YUAN, R., MA, Y., SHENG, W., ZHAN, S., WANG, J. & GUO, L. 2020b. Spectral interference elimination and self-absorption reduction in laser-induced breakdown spectroscopy assisted with laser-stimulated absorption. *Optics and Lasers in Engineering,* 134**,** 106254.
TEMIZ, H. T., SEZER, B., BERKKAN, A., TAMER, U. & BOYACI, I. H. 2018. Assessment of laser induced breakdown spectroscopy as a tool for analysis of butter adulteration. *Journal of Food Composition and Analysis,* 67**,** 48-54.
TOGNONI, E. & CRISTOFORETTI, G. 2016. Signal and noise in laser induced breakdown spectroscopy: an introductory review. *Optics & Laser Technology,* 79**,** 164-172.
TOLIAS, P., KOMM, M., RATYNSKAIA, S. & PODOLNIK, A. 2020. Origin and nature of the emissive sheath surrounding hot tungsten tokamak surfaces. *Nuclear Materials and Energy,* 25**,** 100818.
TSATSAKIS, A. M., NAWAZ, M. A., KOURETAS, D., BALIAS, G., SAVOLAINEN, K., TUTELYAN, V. A., GOLOKHVAST, K. S., LEE, J. D., YANG, S. H. & CHUNG, G. 2017. Environmental impacts of genetically modified plants: A review. *Environmental Research,* 156**,** 818-833.
URBAN, L. & RESTREPO-DIAZ, H. 2017. Influences of Abiotic Factors in Growth and Development☆. *Reference Module in Life Sciences.* Elsevier.
VANHAECKE, F., RESANO, M. & MOENS, L. 2002. Electrothermal vaporisation ICP-mass spectrometry (ETV-ICP-MS) for the determination and speciation of trace elements in solid samples – A review of real-life applications from the author's lab. *Analytical and Bioanalytical Chemistry,* 374**,** 188-195.
VERTKOV, A., LYUBLINSKI, I., ZHARKOV, M., MAZZITELLI, G., APICELLA, M. L. & IAFRATI, M. 2017. Liquid tin limiter for FTU tokamak. *Fusion Engineering and Design,* 117**,** 130-134.
WANG, J., LI, X., WANG, C., ZHANG, L. & LI, X. 2018. Effect of laser wavelength and energy on the detecting of trace elements in steel alloy. *Optik,* 166**,** 199-206.
WANG, M., ZHENG, Q., SHEN, Q. & GUO, S. 2013. The critical role of potassium in plant stress response. *International journal of molecular sciences,* 14**,** 7370-7390.
WASFI, A., AWWAD, F. & AYESH, A. I. 2018. Graphene-based nanopore approaches for DNA sequencing: A literature review. *Biosensors and Bioelectronics,* 119**,** 191-203.
WILLIAMSON, A. P. & KIEFER, J. 2018. Strategies for suppressing elastically scattered laser light in ungated laser-induced breakdown spectroscopy. *Spectrochimica Acta Part B: Atomic Spectroscopy,* 149**,** 267-270.

WILSCHEFSKI, S. C. & BAXTER, M. R. 2019. Inductively Coupled Plasma Mass Spectrometry: Introduction to Analytical Aspects. *The Clinical biochemist. Reviews,* 40**,** 115-133.

WONG, D. M., BOL'SHAKOV, A. A. & RUSSO, R. E. 2017. Laser Induced Breakdown Spectroscopy. *In:* LINDON, J. C., TRANTER, G. E. & KOPPENAAL, D. W. (eds.) *Encyclopedia of Spectroscopy and Spectrometry (Third Edition).* Oxford: Academic Press.

YANG, S., JIANG, S., HU, K. & WEN, X. 2020. Investigation of dispersive solid-phase extraction combined with slurry sampling thermospray flame furnace atomic absorption spectrometry for the determination of cadmium. *Microchemical Journal,* 154**,** 104542.

YIN, W., LIU, Y., ZHOU, F., ZHU, R., ZHANG, Q. & JIN, F. 2018a. Rapid analysis of heavy metals in the coal ash with laser-induced breakdown spectroscopy. *Optik,* 174**,** 550-557.

YIN, Z., GUO, W., XIAO, H., LIANG, J., HAO, X., DONG, N., LENG, T., WANG, Y., WANG, Q. & YIN, F. 2018b. Nitrogen, phosphorus, and potassium fertilization to achieve expected yield and improve yield components of mung bean. *PloS one,* 13**,** e0206285-e0206285.

YTSMA, C. R. & DYAR, M. D. 2018. Effects of univariate and multivariate regression on the accuracy of hydrogen quantification with laser-induced breakdown spectroscopy. *Spectrochimica Acta Part B: Atomic Spectroscopy,* 139**,** 27-37.

YU, X., HE, M., CHEN, B. & HU, B. 2020. Recent advances in single-cell analysis by inductively coupled plasma-mass spectrometry: A review. *Analytica Chimica Acta*.

YUAN, R., TANG, Y., ZHU, Z., HAO, Z., LI, J., YU, H., YU, Y., GUO, L., ZENG, X. & LU, Y. 2019. Accuracy improvement of quantitative analysis for major elements in laser-induced breakdown spectroscopy using single-sample calibration. *Analytica Chimica Acta*.

ZHANG, D., CHU, Y., MA, S., ZHANG, S., CUI, H., HU, Z., CHEN, F., SHENG, Z., GUO, L. & LU, Y. 2020a. A plasma-image-assisted method for matrix effect correction in laser-induced breakdown spectroscopy. *Analytica Chimica Acta,* 1107**,** 14-22.

ZHANG, G., SONG, H., JIN, Y., MA, J., LI, S. & REN, Z. 2019a. Correction of self-absorption effect for quantitative analysis of laser-induced breakdown spectroscopy. *Optik,* 183**,** 375-380.

ZHANG, L. & YANG, Y. 2020. Simultaneous quantitative analysis of non-metallic elements in coal by laser-induced breakdown spectroscopy assisted with machine learning. *Optik,* 222**,** 165449.

ZHANG, P., XU, C., WANG, H., XU, Z., YANG, Y., WU, Y. & WANG, Q. 2020b. Relationships of mineral elements in rice plant based on collinear double pulses laser-induced breakdown spectroscopy. *Optik,* 218**,** 164979.

ZHANG, W., ZHOU, R., YANG, P., LIU, K., YAN, J., GAO, P., TANG, Z., LI, X., LU, Y. & ZENG, X. 2019b. Determination of chlorine with radical emission using laser-induced breakdown spectroscopy coupled with partial least square regression. *Talanta,* 198**,** 93-96.

ZORBA, V., GONZALEZ, J. J., CHAN, G. C. Y., MAO, X. & RUSSO, R. E. 2017. Laser-Induced Breakdown Spectroscopy (LIBS), Applications of. *In:* LINDON, J. C., TRANTER, G. E. & KOPPENAAL, D. W. (eds.) *Encyclopedia of Spectroscopy and Spectrometry (Third Edition).* Oxford: Academic Press.

Appendix

Organic samples

ICP-MS: Golden bantam

Table 3: ICP-MS, Golden Bantam sample concentration (ppb).

Analyte	1 trial	2nd trial	3rd trial	Std Mean	Std deviation	Std error
Hydrogen	-	-	-	-	0	0
Carbon	33.51	38.27	38.70	36.83	2.88	1.66
Oxygen	-	-	-	-	0	0
Nitrogen	12372.61	13871.81	14012.67	13419.03	908.96	524.79
Potassium	164.52	182.32	180.55	175.79	9.80	5.66
Phosphorus	45.57	49.64	50.38	48.53	2.59	1.50
Sulphur	57.54	62.19	62.89	60.87	2.91	1.68
Calcium	4.14	4.42	4.28	4.28	0.14	0.08
Magnesium	16.09	17.70	17.77	17.19	0.95	0.55
Chlorine	53.18	56.97	56.91	55.68	2.17	1.25
Iron	8.86	9.99	9.83	9.56	0.61	0.35
Silicon	18.49	19.30	19.40	19.06	0.50	0.29
Aluminium	5.57	6.62	6.36	6.18	0.54	0.31
Manganese	0.93	1.05	1.03	1.00	0.06	0.04
Zinc	1.61	1.89	1.80	1.77	0.15	0.08
Copper	0.43	0.47	0.46	0.45	0.02	0.01
Boron	0.63	0.66	0.67	0.66	0.02	0.01

LIBS data: Golden bantam

Statistical analysis

Table 4: Calculated mean, standard deviation and error.

Element	1st trial	2nd trial	3rd trial	Mean	Std dev	Std error
Mn I	1600	1600	1600	1600	0	0
Fe II	2173	2173	2173	2173	0	0
O I	468	201	201	290	154.15	89
Cu II	1535	1535	1535	1535	0	0
K I	340	340	340	340	0	0

ICP-MS data: Stowells evergreen

Table 5: ICP-MS, Stowells evergreen sample concentration (ppb).

Analyte	1 trial	2nd trial	3rd trial	Mean	Std dev	Std error
Hydrogen	-	-	-	-	0	0.
Carbon	40.934	41.459	37.531	39.97	2.13	1.23
Oxygen	-	-	-	-	0	0
Nitrogen	11756.655	14219.787	11844.325	12606.90	1397.47	806.83
Potassium	167.764	165.743	166.668	166.73	1.01	0.58
Phosphorus	44.551	43.863	45.018	44.48	0.58	0.34
Sulphur	44.421	36.328	41.852	40.87	4.14	2.39
Calcium	3.616	2.834	3.859	3.44	0.54	0.31
Magnesium	15.661	14.695	15.131	15.16	0.48	0.28
Chlorine	62.923	16.082	60.304	46.44	26.32	15.20
Iron	5.944	5.648	5.966	5.85	0.18	0.10
Silicon	17.027	13.958	16.983	15.99	1.76	1.02
Aluminium	2.905	2.781	2.735	2.81	0.09	0.05
Manganese	0.820	0.808	0.823	0.82	0.01	0.00
Zinc	1.233	1.113	1.598	1.31	0.25	0.15
Copper	0.362	0.341	0.372	0.36	0.02	0.01
Boron	0.524	0.428	0,648	0.48	0.07	0.04

LIBS data: Stowells ever-green

Statistical analysis

Table 6: LIBS, Stowells ever-green sample Intensity (counts).

Element	1st trial	2nd trial	3rd trial	Mean	Std dev	Std error
Mn I	1600	1600	1600	1600	0	0
Mn II	3207	374	0	1193.67	1753.60	1012.44
Fe I	412	412	0	274.67	237.87	137.33
Fe II	2173	2173	2173	2173	0	0
Fe III	0	234	234	156	135.10	78.00
O I	468	2399	2399	1755	1114.86	643.67
Cu II	1535	1535	1535	1535	0	0
K I	340	0	340	226.67	196.30	113.33

Genetically modified samples

ICP-Ms data: CRN 3505

Table 7: ICP-Ms, CRN 3505 sample concentration (ppb).

Analyte	1 trial	2nd trial	3rd trial	Mean	Std deviation	Std error
Hydrogen	-	-	-	0	0	0
Carbon	16.06	17.08	15.77	16.30	0.68	0.40
Oxygen	-	-	-	0	0.00	0.00
Nitrogen	11251.69	13077.13	12060.72	12129.85	914.68	528.09
Potassium	137.40	154.03	143.28	144.90	8.43	4.87
Phosphorus	39.27	44.58	40.36	41.40	2.81	1.62
Sulphur	41.99	50.55	50.28	47.61	4.87	2.81
Calcium	4.56	4.82	4.57	4.65	0.15	0.09
Magnesium	14.68	16.31	15.55	15.51	0.82	0.47
Chlorine	71.63	79.67	75.45	75.58	4.03	2.32
Iron	30.71	34.78	31.29	32.26	2.20	1.27
Silicon	21.71	22.77	22.14	22.40	0.53	0.31
Aluminium	10.65	12.77	11.76	11.73	1.06	0.61
Manganese	1.02	1.18	1.06	1.08	0.08	0.05
Zinc	1.58	1.71	1.60	1.63	0.07	0.04
Copper	0.35	0.38	0.36	0.36	0.02	0.01
Boron	0.65	0.65	0.65	0.65	0.00	0.00

LIBS data: CRN 3505

Statistical analysis

Table 8: Calculated mean, standard deviation and error.

Element	1st trial	2nd trial	3rd trial	Mean	Std dev	Std error
Mn I	1600	1600	1600	1600	0	0
Mn II	0	3207	3207	1069	1851.56	1069
Mn III	0	374	374	124.67	215.93	124.67
Fe I	1775	4188	4188	5075.5	1393.15	804.33
Fe II	2173	2173	2173	2173	0	0
O I	468	2399	2399	1755	1114.86	643.67
Cu II	1535	1535	1535	1535	0	0
Ca I	0	468	468	312	270.20	156
C I	0	2	2	1.33	1.15	0.67
N II	2042	1622	1622	1762	242.49	140

ICP-Ms data: Mon 89

Table 9: ICP-MS, Mon 89 sample concentration (ppb).

Analyte	1 trial	2nd trial	3rd trial	Mean	Std dev	Std error
Hydrogen	-	-	-	0	0	0
Carbon	13.96	12.06	11.90	12.64	1.15	0.66
Oxygen	-	-	-	0	0	0
Nitrogen	8845.64	8847.95	8773.98	8822.52	42.06	24.28
Potassium	104.49	87.92	88.67	93.69	9.36	5.40
Phosphorus	26.91	22.93	22.86	24.23	2.32	1.34
Sulphur	42.73	33.06	32.47	36.09	5.76	3.33
Calcium	3.44	3.16	3.19	3.26	0.15	0.09
Magnesium	10.78	9.67	9.55	10.00	0.68	0.39
Chlorine	101.42	89.12	88.24	92.93	7.37	4.25
Iron	6.95	5.85	5.93	6.24	0.61	0.35
Silicon	18.58	17.49	17.38	17.82	0.66	0.38
Aluminium	7.41	6.01	6.05	6.49	0.80	0.46
Manganese	0.48	0.40	0.39	0.42	0.05	0.03
Zinc	0.35	0.24	0.24	0.28	0.06	0.04
Copper	0.28	0.26	0.26	0.27	0.01	0.01
Boron	0.52	0.51	0.51	0.51	0.01	0.00

LIBS data: Mon 89

Statistical analysis

Table 10: Calculated mean, standard deviation and error.

Element	1st trial	2nd trial	3rd trial	Mean	Std dev	Std error
Mn I	1600	1600	1600	1600	0	0
Fe I	4188	913	4188	3096.33	1890.82	1091.67
Fe II	2173	2173	2173	2173	0	0
Cu II	1535	1535	1535	1535	0	0
K I	340	340	340	340	0	0
O I	468	468	468	468	0	0

ICP-Ms data: Mon 810

Table 11: ICP-MS, Mon 810 sample concentration (ppb).

Analyte	1 trial	2nd trial	3rd trial	Mean	Std deviation	Std error
Hydrogen	-	-	-	0	0	0
Carbon	12.98	11.45	13.71	12.71	1.15	0.67
Oxygen	-	-	-	0	0	0
Nitrogen	8016.37	6144.09	8296.42	7485.63	1170.21	675.62
Potassium	105.23	88.84	103.54	99.20	9.01	5.20
Phosphorus	28.97	25.60	28.84	27.80	1.91	1.10
Sulphur	36.24	29.87	36.52	34.21	3.76	2.17
Calcium	3.32	3.14	3.33	3.26	0.11	0.06
Magnesium	10.75	9.21	10.50	10.15	0.83	0.48
Chlorine	76.46	67.42	75.40	73.09	4.94	2.85
Iron	10.72	8.74	10.47	9.98	1.08	0.62
Silicon	18.67	17.49	18.72	18.29	0.70	0.40
Aluminium	7.01	5.47	6.83	6.44	0.84	0.49
Manganese	0.64	0.52	0.61	0.59	0.06	0.04
Zinc	0.79	0.64	0.78	0.74	0.08	0.05
Copper	0.31	0.28	0.30	0.30	0.02	0.01
Boron	0.54	0.54	0.54	0.54	0	0.00

LIBS data: Mon 810

Statistical analysis

Table 12: Calculated mean, standard deviation and error.

Element	1st trial	2nd trial	3rd trial	Mean	Std dev	Std error
Mn I	1600	1600	1600	1600	0	0
N2+	700	0	0	233.33	404.15	233.33
Fe I	0	1259	1259	839.33	726.88	419.67
Fe II	2173	2173	2173	2173	0	0
Cu II	1535	1535	1535	1535	0	0
Ca I	149	149	149	149	0	0
O I	468	468	468	468	0	0

Calculations

For mean: $$\bar{X} = \frac{Sum\ of\ concentrations}{Number\ of\ concentrations}$$ Equation 3

where $\bar{x}$ is mean

For standard deviation: $\sigma = \sqrt{\frac{\sum(x_i - \bar{x})^2}{N-1}}$ Equation 4

where: $N = number\ of\ elements$, $\bar{x} = mean\ value, x_i = value\ of\ a\ single\ element$ and $\sigma = standard\ deviation$

For standard error: $SE = \frac{\sigma}{\sqrt{n}}$ Equation 5

where: $SE = Standard\ error\ of\ sample$, σ = *standard deviation and n = number of elements*

Equations 1, 2 and 3 were used to calculate mean, standard deviation and standard error.

All samples concentrations means comparison

Table 13: All samples concentration means.

Analyte	**Golden Bantam**	**Stowells**	**CRN 3505**	**MON 810**	**MON 89**
Hydrogen	0	0	0	0	0
Carbon	36.827	39.97	16.30	12.71	12.64
Oxygen	0	0	0	0	0
Nitrogen	13419.03	12606.90	12129.85	7485.63	8822.52
Potassium	175.794	166.73	144.90	99.20	93.69
Phosphorus	48.529	44.48	41.40	27.80	24.23
Sulphur	60.870	40.87	47.61	34.21	36.09
Calcium	4.281	3.44	4.65	3.26	3.26
Magnesium	17.187	15.16	15.51	10.15	10.00
Chlorine	55.683	46.44	75.58	73.09	92.93
Iron	9.559	5.85	32.26	9.98	6.24
Silicon	19.062	15.99	22.40	18.29	17.82
Aluminium	6.184	2.81	11.73	6.44	6.49
Manganese	1.004	0.82	1.08	0.59	0.42
Zinc	1.769	1.31	1.63	0.74	0.28
Copper	0.451	0.36	0.36	0.30	0.27
Boron	0.655	0.48	0.65	0.54	0.51